THE
PHYSICAL REVIEW
A journal of experimental and theoretical physics established by E. L. Nichols in 1893

SECOND SERIES, VOL. 71, No. 4 FEBRUARY 15, 1947

The Scattering of Slow Neutrons by Bound Protons

I. Methods of Calculation

G. BREIT*
University of Wisconsin, Madison, Wisconsin
(Received November 29, 1946)

The mathematical problem of the scattering of slow neutrons by chemically bound protons is stated in terms of a boundary condition and its equivalent integral equation. By means of the latter it is possible to calculate corrections to the results of Fermi which can be considered as the first approximation to the more accurate equations. The method is applied to free protons, and it is shown how the well-known results for this case are obtained from the more general equations. This special case allows also an estimate (10^{-3}) of the order of the corrections in the case of chemically bound protons in agreement with general estimates in connection with Eq. (8.4) of Section 7 of the present paper and the application to harmonic oscillator binding made in the succeeding paper jointly with P. R. Zilsel. The corrections discussed are greater than the inaccuracies of the boundary condition formulation which are of the order 10^{-4}.

1. INTRODUCTION

FERMI[1] has given a theory of the effect of chemical binding of protons on their scattering cross section for slow neutrons. At the time of Fermi's work there was no necessity of great accuracy, and his answer was generally considered to be good enough. The advance in experimental methods that has taken place since makes it desirable to be able to estimate theoretical effects more accurately than previously. The whole effect dealt with is of the order of a factor 4, and it is natural, therefore, to inquire into the accuracy of its estimates. Its knowledge is needed in the interpretation of experimental material on neutron-proton scattering in terms of effective neutron proton potentials, and the comparison of such potentials with corresponding quantities for other pairs of nuclear particles. As is well known, such a comparison is essential for the field theories of nuclear particles, and it has indicated in the past that the specifically nuclear interactions are essentially independent of the charge. It appeared advisable to be reasonably sure of the accuracy of the Fermi correction factor in this connection on account of its bearing on the fundamental problem of forces between nuclear particles. An additional incentive has been the large accumulation[2] of experimental material on the scattering of slow neutrons by solids which presents very similar mathematical problems. In this case, just as in the scattering of neutrons by protons, the nuclear properties can be described by quantities a which have the significance of intercepts on the axis

* Now at Yale University.
[1] Enrico Fermi, Ricerca Scient. VII–II, 13 (1936). See Eqs. (71)–(103).
[2] Herbert L. Anderson, Enrico Fermi, Leona Marschall, paper E 1, Proc. Amer. Phys. Soc. Meeting at Chicago, June 20–22 (1946); W. H. Zinn, *idem*, paper E 2, Phys. Rev. 70, 102 (1946).

referring to the neutron-scattering nucleus distance in a graph of the product of this distance by the radial wave function. The quantity a has the significance of the amplitude of the scattered wave per unit intensity of the incident wave in a suitable normalization. The interactions of the scattered neutron with individual nuclear particles, matter in the problem of scattering of slow neutrons only insofar as they affect the intercepts a which are therefore important nuclear parameters. The close relationship of the present paper to the mathematical problem of determining these parameters added to the desirability of finding a systematic way for the calculation presented below.

The method consists of two steps: (a) the replacement of the wave equation in the region of the nuclear potential by a boundary condition Eq. (3); (b) the formulation of the boundary condition in terms of an integral equation, Eq. (5). The physical justification for the boundary condition is made in Section 3, and it is found that the errors caused by this replacement are negligible in comparison with all effects considered here. The conversion of the problem to an integral equation is made in Section 4. Fermi's approximation is discussed in Sections 5 and 6, and the reasons for undertaking the present calculation are gone into in these sections. In Section 7 the expressions for the "background" are transformed into forms more suitable for applications than the original. In Section 8, the method is illustrated by considering free protons and seeing how the well-known answer is verified consistently with the approximations made.

2. NOTATION

$\mathbf{r}_\pi=(x_\pi, y_\pi, z_\pi)$ = proton coordinates.

$\mathbf{r}_\nu=(x_\nu, y_\nu, z_\nu)$ = neutron coordinates.

$U=U(x_\pi, y_\pi, z_\pi)$ = potential energy of proton caused by molecular binding.

$\mathbf{r}=\mathbf{r}_\nu-\mathbf{r}_\pi=(x, y, z)$ = relative coordinates.

E_n = energy of proton in a molecule in nth excited state.

$u_n(\mathbf{r}_\pi)$ = characteristic function of proton in state E_n.

$\Delta_\nu=\partial^2/\partial x_\nu^2+\partial^2/\partial y_\nu^2+\partial^2/\partial z_\nu^2$.

$\Delta_\pi=\partial^2/\partial x_\pi^2+\partial^2/\partial y_\pi^2+\partial^2/\partial z_\pi^2$.

$\Delta=\partial^2/\partial x^2+\partial^2/\partial y^2+\partial^2/\partial z^2$.

ψ = wave function of proton and neutron.

$g(r)$ = potential energy of proton in the field of the neutron; assumed to be a function of the distance $r=|\mathbf{r}|$ only.

E = energy of system.

M = proton mass; the mass of the neutron is assumed to be equal to the mass of the proton.

∇ = vector operator (gradient) with components $\partial/\partial x$, $\partial/\partial y$, $\partial/\partial z$. This is distinguished by suffixes ν, π to indicate replacement of relative by neutron or proton coordinates.

ρ = distance of the order of 3×10^{-13} cm beyond which the function g may be assumed to be zero.

a = intercept of tangent to graph of r times radial function for proton-neutron motion plotted against an axis of r. The intercept is by definition positive if tangent cuts axis of r to the left of origin.

$d\mathbf{r}=dxdydz$ = volume element in space x, y, z.

$d\mathbf{r}_\pi=dx_\pi dy_\pi dz_\pi$.

$d\mathbf{r}_\nu=dx_\nu dy_\nu dz_\nu$.

$\mathbf{R}=(X, Y, Z)=(1/2)(x_\pi+x_\nu, y_\pi+y_\nu, z_\pi+z_\nu)$ = center of mass coordinates.

$\langle A\rangle$ = angular average of any quantity A over directions of the vector $\mathbf{r}$. Equal weights to all solid angles are given in the average.

3. THE BOUNDARY CONDITION REPLACING THE PROTON-NEUTRON INTERACTION

The wave equation will be taken to be

$$E\psi=[-(\hbar^2/2M)(\Delta_\nu+\Delta_\pi)+U+g(r)]\psi \quad (1)$$

in the notation just explained. It is assumed that it is good enough to use one function $g(r)$ so that the discussion is applicable only to slow neutrons since otherwise one would have to bring in phase shifts for p and d waves which may correspond in general to other interaction potentials. The wave function ψ in the above equation is supposed to correspond to a definite value of the total spin. Different values of $g(r)$ are supposed to be used for the triplet and singlet interactions. This means, of course, that the representation of an ordinary experimental situation involves an analysis into wave functions ψ such as those dealt with in Eq. (1) with different values of $g(r)$. Such an analysis is well known and is described in most books concerned with

the theory of nuclear physics. It will not be gone into, therefore, at this stage.

The eigenfunctions u_n describing the stable states of a proton in a molecule satisfy the equation

$$E_n u_n = (-(\hbar^2/2M)\Delta_r + U)u_n. \qquad (1.1)$$

The wave function ψ can be analyzed into a linear combination of the functions $u_n(\mathbf{r}_r)$ with coefficients which are functions of the proton-neutron distance vector $\mathbf{r}$:

$$\psi = \sum_n a_n u_n(\mathbf{r}_r)\chi_n(\mathbf{r}). \qquad (1.2)$$

The quantities a_n occurring in the above formula are taken to be constant while the functions χ_n depend only on the relative rather than the absolute position of the neutron with respect to the proton.

It will be shown next by means of a few estimates through substitution of this form of ψ into Eq. (1), that for small values of the proton-neutron distance r, the difference in the space character of different functions χ_n is negligible. This means that in a good approximation one will be able to describe the function ψ as a product of a function of $\mathbf{r}$ multiplied by a function of $\mathbf{r}_r$. This approximation will be used only for values of r of the order of nuclear dimensions. The argument for the separability of ψ into two factors in this range of values of r follows.

Substitution of (1.2) into (1) gives

$$\sum_n (E-E_n)a_n\chi_n u_n = \sum_m a_m\left[-\frac{\hbar^2}{M}u_m\Delta\chi_m + \frac{\hbar^2}{M}\nabla\chi_m\cdot\nabla_r u_m + g\chi_m u_m\right]. \qquad (2)$$

It is understood here that the χ occur only with relative neutron-proton and the u only with proton coordinates. For a fixed value of $\mathbf{r}$, integration of the last equation over the proton coordinates after multiplication by u_n^* gives

$$\left[(E-E_n)\chi_n + \frac{\hbar^2}{M}\Delta\chi_n - g\chi_n\right]a_n = -\frac{1}{M}\sum_m(\mathbf{p}_{nm}^{(r)}\mathbf{p}\chi_m)a_m, \qquad (2.1)$$

where the operators $\mathbf{p}$ stand for $(\hbar/i)\nabla$ and correspond to the usual representation of the momentum. It is now clear that if the right side of (2.1) were absent, then inside the range of action of the nuclear potential g, one would be dealing with separate equations for each χ_n, and that there would exist solutions in which only one of the a_n is distinct from zero. The states $u_n\chi_n$ can be considered as being uncoupled in this approximation. Further, it is readily seen that if one were to set all the E_n in these equations equal to zero, the results of calculations on scattering would be unaffected provided the left side of Eq. (2.1) is *never* used for values of r greater than the range of nuclear forces. Within these small distances the effect of the very slight change in the value of the effective kinetic energy $E-E_n-g$ is small, and the change in the logarithmic derivative of χ_n caused by E_n is negligible at $r=\rho$. The truth of this point of view may be seen by noting that the effective kinetic energy is affected by E_n to the extent of, say, 10 ev while its total magnitude is of the order of 10^7 ev. The effect on the logarithmic derivative $rd(r\chi)/(r\chi)dr$ at $r=\rho$ is[3] of the order

$$\frac{\partial}{\partial E}\left[\frac{\partial F}{F\partial r}\right]_{r=\rho}\cdot\delta E_{\text{kin}} = -\frac{M}{\hbar^2 F^2}\int_0^\rho F^2 dr\cdot\delta E_{\text{kin}}. \qquad (2.2)$$

$$F = r\chi, \qquad (2.3)$$

where δE_{kin} is the change in the effective kinetic energy. This change in the logarithmic derivative corresponds to a change in the intercept a in accordance with

$$\rho+a = \left[\frac{\partial F}{F\partial r}\right]^{-1}_{r=\rho}; \quad \frac{\delta a}{\rho+a} = -(\rho+a)\delta\left[\frac{\partial F}{F\partial r}\right]_{r=\rho}.$$

[3] G. Breit and E. Wigner, Phys. Rev. **49**, 519 (1936). See Eq. (29).

By means of (2.2) one can transform the right side of the above equation and obtain

$$\frac{\delta a}{\rho+a}=\frac{\rho+a}{\rho}\frac{\delta E}{E_{\text{kin}}}\cdot\frac{\rho^2p^2}{\hbar^2}\cdot\frac{1}{\rho F^2}\int_0^\rho F^2dr, \tag{2.4}$$

where

$$p^2/M=E_{\text{kin}}. \tag{2.5}$$

The factor $(1/\rho F^2)\int_0^\rho F^2dr$ in (2.4) is of the order of $\frac{1}{2}$ since this is the value of this factor for an interaction potential $g(r)$ in the form of a square well. The quantity $\rho^2p^2/\hbar^2$ is of the order $(2\pi)^2(\lambda/4)^2/\lambda^2=(\pi/2)^2=2.5$. Here λ is the wave-length of relative proton-neutron motion inside the potential well. With these approximate values one obtains by means of (2.4)

$$\frac{\delta a}{a}\cong 1.2\frac{(\rho+a)^2}{\rho a}\frac{\delta E}{E_{\text{kin}}}.$$

For $a=20\times10^{-13}$ cm, $\rho=3\times10^{-13}$ cm, this relation becomes

$$\delta a/a=10\delta E/E_{\text{kin}},$$

and for $\delta E=10$ ev, $E_{\text{kin}}=10$ Mev

$$\delta a/a\cong10^{-5}.$$

The corresponding change in the scattering cross section is 0.002 percent and is negligible in most problems. The magnitudes of the quantities used in the estimates just made have been such as to give a too large rather than a too small value for the effect of δE, and it may be considered justifiable, therefore, to neglect its effect.

So far it has been shown that one has a negligible error if one neglects the difference between E and $E-E_n$ on the left side of Eq. (2.1). It is seen also that the coupling between different a_n caused by the occurrence of non-vanishing right-hand members in this equation is similarly of little consequence. These terms are of the same order of magnitude as the terms just discussed and contribute approximately the same amount to $\Delta\chi_n$. They may usually be neglected, therefore. An exception to this general situation occurs if one of the a_n is very small compared with some other a_m, or with at least one of them. If this is the case, the right side of Eq. (2.1) cannot be neglected because it may contribute an important part of $\Delta\chi_n$. In order that this should take place the ratio a_n/a_m has to be of the order of 10^{-5}, and this means that one is dealing with an unimportant part of the wave function in the expansion (1.2). It is thus seen that for ranges of nuclear forces that are customarily assumed it is legitimate to neglect the coupling between the a_n as well as the differences between the χ_n, provided, of course, one stays in the part of configuration space $r<\rho$.

This situation suggests a reformulation of the problem in terms of a boundary condition at $r=0$. The quantity ρ is made to approach zero. Simultaneously $g(r)$ is varied in such a way as to keep a at its experimental value. As the limit of $\rho=0$ is approached, the errors in the cross section assume values much smaller than the above estimate of 0.002 percent and finally approach zero. In view of the fact that the difference between this idealized and the more realistic original picture is negligible for most practical purposes, the limit of very deep and narrow potential wells will be used in what follows. This means that as $r\to0$ the limiting form of any χ will be taken to be

$$(1+a/r)b,$$

where b is a constant. Accordingly the limiting form of $\psi(\mathbf{r}_p,\mathbf{r}_n)$ for $|\mathbf{r}_p-\mathbf{r}_n|=r\to0$ will be taken to be

$$\lim_{r\to0}\psi(\mathbf{r}_p,\mathbf{r}_n)=(1+a/r)f(\mathbf{r}_n). \tag{3}$$

In this equation, the function f is a three-dimensional function of the proton coordinates. It is so far an unknown function and has to be determined through the requirement that ψ behave properly in other regions than those corresponding to near coincidence of the proton and neutron.

4. CONVERSION TO AN INTEGRAL EQUATION

By means of the boundary condition (3) the problem is simplified through the fact that through all of the configuration space with the exception of the three-dimensional region $r=0$, one may require instead of (1) the more manageable equation

$$H_0\psi = E\psi, \tag{4}$$

where

$$H_0 = -(\hbar^2/2M)(\Delta_\tau+\Delta_\nu)+U(\mathbf{r}_\nu). \tag{4.1}$$

One has to find solutions of this equation subject to the following requirements:

(a) Validity of boundary condition (3).
(b) The correct behavior of ψ in regions of configuration space corresponding to large values of $|\mathbf{r}_\nu|$. In these regions one should require that the wave function be representable as the sum of a plane neutron wave with a proton in a definite bound state plus diverging neutron waves with the proton in different bound states.

An explicit construction of such a wave function can be made by means of the quantity

$$K(\mathbf{r}_\tau, \mathbf{r}_\nu; \mathbf{r}_\tau', \mathbf{r}_\nu') = \frac{2\pi M}{\hbar^2}\sum_s u_s(\mathbf{r}_\tau)u_s^*(\mathbf{r}_\tau')\frac{e^{i\kappa_s|\mathbf{r}_\nu-\mathbf{r}_\nu'|}}{|\mathbf{r}_\nu-\mathbf{r}_\nu'|}, \tag{4.2}$$

where

$$\kappa_s^2 = (2M/\hbar^2)(E-E_s) \tag{4.3}$$

with the understanding that for real κ_s one makes $\kappa_s>0$, and for pure imaginary κ_s, $i\kappa_s$ is negative. This choice of the signs for κ_s has as a consequence that, in Eq. (4.2), the separate terms contributing to K are either diverging waves as is the case for real κ_s, or else they are attenuated waves which vanish exponentially as $|\mathbf{r}_\nu-\mathbf{r}_\nu'|\to\infty$. The construction of the kernel K is very similar to that employed[4] in the discussion of resonances in nuclear reactions. The especially useful property of K is expressed by the equation

$$(H_0-E)\int K(\mathbf{r}_\tau, \mathbf{r}_\nu; \mathbf{r}_\tau', \mathbf{r}_\nu')D(\mathbf{r}_\tau', \mathbf{r}_\nu')d\mathbf{r}_\tau'd\mathbf{r}_\nu' = D(\mathbf{r}_\tau, \mathbf{r}_\nu), \tag{4.4}$$

where D is a so far arbitrary density function. It will be convenient from now on to employ the abbreviation

$$K(\mathbf{r}_\tau, \mathbf{r}_\nu; \mathbf{r}_\tau', \mathbf{r}_\nu') = K(\ ,\ ') \tag{4.5}$$

and to express the wave function ψ as

$$\psi = \psi_0(\mathbf{r}_\tau, \mathbf{r}_\nu)+\int K(\ ,\ ')D(\mathbf{r}_\tau', \mathbf{r}_\nu')d\mathbf{r}_\tau'd\mathbf{r}_\nu' \tag{4.6}$$

where $\psi_0(\mathbf{r}_\tau, \mathbf{r}_\nu)$ is the incident wave

$$\psi_0 = u_i(\mathbf{r}_\tau)e^{i(\mathbf{p}_i\mathbf{r}_\nu)/\hbar}. \tag{4.6'}$$

Here u_i is the eigenfunction of the proton in its "initial" state, and $\mathbf{p}_i$ is the momentum of the neutron in its incident condition. The form (4.6) assures the correct behavior of ψ for large $|\mathbf{r}_\nu|$. The density function D has to be determined next so as to satisfy the requirements at small r. Substitution into (1) with the aid of (4.4) shows that

$$g\psi = -D(\mathbf{r}_\tau, \mathbf{r}_\nu). \tag{4.7}$$

One obtains on substitution into (4.6)

$$\psi(\mathbf{r}_\tau, \mathbf{r}_\nu) = \psi_0-\int K(\ ,\ ')g(r')\psi(\mathbf{r}_\tau', \mathbf{r}_\nu')d\mathbf{r}_\tau'd\mathbf{r}_\nu'. \tag{4.8}$$

[4] G. Breit, Phys. Rev. 58, 506 (1940). See Eq. (13.4).

This integral equation has been obtained without approximations from the original differential equation. It does not involve the approximations of the shortness of the range of nuclear forces or any of the specializations made in connection with the introduction of the boundary condition for small r of the preceding paragraph. One could employ this integral equation if it were necessary to take into account a finite range of nuclear forces. Since the arguments of the preceding paragraph have shown that the error caused by neglecting the finite range is negligible for ordinary problems, the integral equation (4.8) will now be modified so as to eliminate $g(r)$ and to bring in instead the intercept a.

The transformations involved in this process are described in Appendix I. It is shown there that in the limit of a very short range of nuclear forces

$$\int K(\ ,\ ')g(r')\psi(\ ')d\tau_\tau' d\tau_\nu' = -2a\sum_s u_s(\tau_\tau)\int u_s^*(\tau_\tau')f(\tau_\tau')\frac{e^{ik_0|\tau_\tau'-\tau_\nu|}}{|\tau_\tau'-\tau_\nu|}d\tau_\tau', \tag{4.9}$$

where f is that of Eq. (3). Substitution into (4.8) gives now

$$(1+a/r)f(\tau_\tau)=\psi_0(\tau_\tau,\tau_\nu)+2a\left\langle\sum_s u_s(\tau_\tau)\int u_s^*(\tau_\tau')f(\tau_\tau')\frac{e^{ik_0|\tau_\tau'-\tau_\nu|}}{|\tau_\tau'-\tau_\nu|}\right\rangle d\tau_\tau', \quad (r\to 0). \tag{4.95}$$

This equation has been averaged over the directions of the small vector τ because otherwise one does not obtain a limit independent of the direction in which the point $r=0$ is approached. The reason for averaging over directions is apparent also in the discussion of Eqs. (5.3) to (5.7). The boundary condition at $r\to 0$ is expressed directly by Eq. (4.95). It is inconvenient to leave the condition in this form, however, because for $r=0$, the left and the right sides become infinite. Substitution for $f(\tau_\tau)/|\tau_\tau-\tau_\nu|$ of its expansion in terms of the $u_s(\tau_\tau)$ gives a neater result, *viz.*

$$f(\tau_\tau)-a\langle B(\tau_\tau,\tau_\tau)\rangle=\psi_0(\tau_\tau,\tau_\tau) \tag{5}$$

with

$$B(\tau_\tau,\tau_\nu)=\sum u_s(\tau_\tau)\int u_s^*(\tau')\frac{2e^{ik_0|\tau'-\tau_\nu|}-1}{|\tau'-\tau_\nu|}f(\tau')d\tau'. \tag{5'}$$

In this form every term approaches a finite limit as $r=|\tau_\tau-\tau_\nu|\to 0$. Equations (4.95), (5) amount to three-dimensional integral equations on the function $f(\tau_\tau)$, and the problem is now reduced to the solution of an integral equation.

It follows from the way in which Eq. (5) has been derived that the coefficient of a on its left side should be finite. Otherwise the equation could not hold because all other terms in it are obviously finite. This fact may be verified as follows. One finds by direct calculation

$$(H_0-E)\sum_s u_s(\tau_\tau)\int u_s^*(\tau')f(\tau')\frac{e^{ik_0|\tau'-\tau_\nu|}}{|\tau'-\tau_\nu|}d\tau'=\frac{\hbar^2}{2\pi M}f(\tau_\tau)\delta(\tau_\tau-\tau_\nu). \tag{5.1}$$

It will now be noted that the multiplication by U which is contained in H_0-E on $\sum_s$ on the left side of Eq. (5.1) cannot introduce a δ function unless the δ function should be a part of the $\sum_s$. It is clear, however, that for a regular f the δ function is not a factor in f. The δ function on the right side of Eq. (5.1) has to arise therefore through the application of the Laplacian operators in H_0. The combination of these that occurs is

$$-\frac{\hbar^2}{2M}(\Delta_\tau+\Delta_\nu)=-\frac{\hbar^2}{M}\Delta-\frac{\hbar^2}{4M}\Delta_{\tau+\nu} \tag{5.2}$$

where the last term represents the Laplacian with respect to the center of mass coordinates of the proton and neutron. Only the first term on the right side of Eq. (5.2) has anything to do with the

right side of Eq. (5.1) so that the coefficient of $1/r$ in $\sum_s$ can be readily ascertained. It is thus found that

$$\sum_s \text{ of } (5.1) = 1/2r + \cdots,$$

where the remaining terms indicated by dots do not give rise to the singularity. Comparison with Eqs. (4.95), (5), (5.1) shows now that the coefficient 2 in the numerator under the integral sign in Eq. (5′) is just right to cancel the singularity in $1/r$. That this is the case will also be verified in the course of applications of the integral equation.

The integral equation (5) will now be derived without the use of the contraction of range procedure. The employment of the interaction potential $g(r)$ will be replaced by the requirement that the s part of the wave function is of the form $(1+a/r)f$ everywhere except at $r=0$. The wave function ψ can be analyzed in spherical harmonics Y_L of the angular coordinates of $\mathbf{r}$ as follows:

$$\psi(\mathbf{r}_s, \mathbf{r}_t) = \Phi_0(\mathbf{R}, r) + \sum_{L=1}^{\infty} \varphi_L(\mathbf{R}, r)\, Y_L. \tag{5.3}$$

Here $\mathbf{r}$, $\mathbf{R}$ are the relative coordinates and the coordinates of the center of mass, the functions φ_L are regular everywhere, while Φ_0 is not regular at $r=0$. There is no assumption involved in expressing ψ in the form (5.3). For any fixed $\mathbf{R}$, ψ is a function of $\mathbf{r}$ only, and if r is fixed in addition, then one has a function of the angular coordinates of $\mathbf{r}$ which can be expanded in terms of the spherical harmonics Y_L. Averaging Eq. (5.3) over angles one finds, of course,

$$\langle \psi(\mathbf{R}-\mathbf{r}/2, \mathbf{R}+\mathbf{r}/2)\rangle = \Phi_0(\mathbf{R}, r). \tag{5.31}$$

It has been assumed that the functions φ_L $(L=1, 2, \cdots)$ are regular everywhere so that as $\mathbf{r}$ is made to go to zero, the limit of any φ_L is the same independently of the direction from which the point $r=0$ is approached. The function Φ_0, on the other hand, is assumed to be such that

$$\lim_{r=0}[\Phi_0(\mathbf{R}, r) - \Phi(\mathbf{R})(1+a/r)] = 0. \tag{5.32}$$

The assumptions just made about Φ_0 and φ are what replaces the employment of $g(r)$ in the original wave equation (1). In Eq. (5.32) the function $\Phi(R)$ is independent of r as is indicated by the notation used.

It must now be explained that to a sufficient approximation for small values of r,

$$\langle \psi(\mathbf{R}-\mathbf{r}/2, \mathbf{R}+\mathbf{r}/2)\rangle = \langle \psi(\mathbf{r}_s-\mathbf{r}, \mathbf{r}_t)\rangle = \langle \psi(\mathbf{r}_s, \mathbf{r}_s+\mathbf{r})\rangle. \tag{5.33}$$

In fact, according to Eq. (5.3),

$$\psi(\mathbf{r}_s-\mathbf{r}, \mathbf{r}_t) = \Phi_0(\mathbf{r}_s-\mathbf{r}/2, r) + \sum_{L=1}^{\infty} \varphi_L(\mathbf{r}_s-\mathbf{r}/2, r)\, Y_L. \tag{5.34}$$

Since there is only s scattering, the functions φ_L for small r vanish as r^L or faster. The occurrence of $r/2$ in the combination $\mathbf{r}_s-\mathbf{r}/2$ in φ_L brings in a dependence on the direction of $\mathbf{r}$ in addition to that included in Y_L. Expanding the φ_L in Taylor's series, one obtains terms vanishing at least as fast as r^2. Such terms will not matter in the statement of a boundary condition such as (5.32) because they disappear from ψ as r approaches zero. One is concerned, therefore, only with

$$\begin{aligned}\langle \Phi_0(\mathbf{r}_s-\mathbf{r}/2, r)\rangle &= (1+a/r)\langle \Phi(|\mathbf{r}_s-\mathbf{r}/2|)\rangle \\ &= (1+a/r)\langle \Phi(\mathbf{r}_s) + (x^2/8)(\partial^2\Phi/\partial x_s^2) + \cdots\rangle \\ &= (1+a/r)[\Phi(\mathbf{r}_s) + (r^2/24)\Delta\Phi(\mathbf{r}_s) + \cdots].\end{aligned} \tag{5.35}$$

In the condition expressed by Eq. (5.32), it does not matter, therefore, whether one averages over angles with fixed center of mass coordinates or whether one keeps the neutron coordinates fixed,

averages over angles of $\mathbf{r}$, and then makes $\mathbf{r}_\tau$ approach $\mathbf{R}$. The same holds for $\mathbf{r}_\tau$. Combining this result with the consideration of the φ_L which was mentioned right after Eq. (5.34), one may restate Eq. (5.32) in the form

$$\lim_{r\to 0}[\langle\psi(\mathbf{r}_\tau, \mathbf{r}_\tau+\mathbf{r})\rangle-(1+a/r)\Phi(\mathbf{r}_\tau)]=0. \tag{5.4}$$

If now ψ is defined by

$$\psi(\mathbf{r}_\tau, \mathbf{r}_\nu)=\psi_0(\mathbf{r}_\tau, \mathbf{r}_\nu)+2a\sum_s, \tag{5.5}$$

where $\sum_s$ is as in Eq. (4.9), then simply as a matter of rearranging terms

$$\psi=\psi_0+B+af(\mathbf{r}_\tau)/r, \tag{5.51}$$

with B given by Eq. (5′). Averaging (5.51) over angles in order to substitute into Eq. (5.4) one has to consider first of all the term ψ_0. One has for it

$$\langle\psi_0(\mathbf{r}_\tau, \mathbf{r}_\tau+\mathbf{r})\rangle=\psi_0(\mathbf{r}_\tau, \mathbf{r}_\tau)+(r^2/6)[\Delta_\nu\psi(\mathbf{r}_\tau, \mathbf{r}_\nu)]_{\mathbf{r}_\nu=\mathbf{r}_\tau}+\cdots, \tag{5.52}$$

so that in (5.4) one may replace this term by $\psi_0(\mathbf{r}_\tau, \mathbf{r}_\tau)$. Substituting all terms that matter into (5.4) one has finally

$$(1+a/r)\Phi(\mathbf{r}_\tau)=\psi_0(\mathbf{r}_\tau, \mathbf{r}_\tau)+a\langle B\rangle_{r\to 0}+af(\mathbf{r}_\tau)/r+O(r), \tag{5.6}$$

where $O(r)$ designates terms of order r. Identifying coefficients of equal powers of r in Eq. (5.6) one has

$$\Phi=f;\ \Phi(\mathbf{r}_\tau)=\psi_0(\mathbf{r}_\tau, \mathbf{r}_\tau)+a\langle B\rangle_{r\to 0}. \tag{5.7}$$

These two equations are equivalent to Eq. (5).

It has thus been shown that the boundary condition statements of Eqs. (5.32), (5.4) require the validity of the integral equation (5) if it is assumed that ψ can be expressed in the form obtained by substituting for the integral on the right side of Eq. (4.8) its limiting form as in Eq. (4.9). The limiting contraction process has dropped out of the picture. Its only remnant is the suggestion of a possible form for ψ, and this suggestion is not necessary since one can show that $\langle B\rangle_{r\to 0}$ is a well defined quantity as will be seen in connection with Eq. (6.1).

5. COMPARISON WITH FERMI'S EQUATION

In the present paragraph a comparison with Fermi's equation[1] will be made from the point of view of expressing the quantities occurring in one in terms of those occurring in the other. The numerical comparison is postponed until formulas for the evaluation of quantities occurring in Eq. (5.1) are worked out.

Combining Eqs. (4.8), (4.9) one obtains

$$\psi=\psi_0+2a\sum_s u_s(\mathbf{r}_\tau)\int u_s^*(\mathbf{r}_\tau')f(\mathbf{r}_\tau')\frac{e^{iu_s|\mathbf{r}_\tau'-\mathbf{r}_\nu|}}{|\mathbf{r}_\tau'-\mathbf{r}_\nu|}d\mathbf{r}_\tau'. \tag{6}$$

It follows from this and Eq. (5.1) that

$$(H_0-E)\psi=(ah^2/\pi M)f(\mathbf{r}_\tau)\delta(\mathbf{r}_\tau-\mathbf{r}_\nu). \tag{6.1}$$

This relation has some similarity to Fermi's equation:

$$(H_0-E)\bar{\psi}=(ah^2/\pi M)\bar{\psi}\delta_R(\mathbf{r}_\tau-\mathbf{r}_\nu), \tag{6.2}$$

where $\bar{\psi}$ is the average of ψ over positions of the neutron within a sphere of radius R for fixed proton positions. The radius R is supposed to be large in comparison with nuclear dimensions and small in comparison with the size of the molecule. The delta function on the right side of Eq. (6.2) is first introduced by Fermi in such a way as to have a constant value within the sphere of radius R and so that its integral through the spherical volume is unity. In the applications of the equation Fermi

replaces the function δ_R by Dirac's δ function, and the function $\bar{\psi}$ on the right side of his equation he replaces by the incident wave in the spirit of Born's approximation.

Comparison of the exact equation (6.1) with Fermi's approximation (6.2) shows some points of similarity and also an obvious difference. Eq. (3) shows that $f(\mathbf{r}_\nu)$ is approximately Fermi's $\bar{\psi}$:

$$f(\mathbf{r}_\nu)\cong\bar{\psi}. \tag{6.3}$$

It follows, therefore, that if one is interested only in the scattering, then, to within the limits of validity of (6.3), the Eqs. (6.1) and (6.2) are nearly equivalent because for the calculation of the scattering the distinction between ψ and $\bar{\psi}$ on the left side of the two equations is immaterial. One may look, therefore, at Eq. (6.1) as a substantiation of the approximate validity of Fermi's method of calculation. One sees further that if Fermi's equation is used not exactly but in Born's first approximation and with the replacement of δ_R by Dirac's δ, then the only error involved is that of approximating $f(\mathbf{r}_\nu)$ by the incident wave. Equation (5) shows that $f(\mathbf{r}_\nu)$ is only approximately equal to ψ_0 and that more accurately one should add to ψ_0 the term in a on the left side of (5). This term will be referred to as the "background" for the following reason. It arose as the difference between the term in $2a$ on the right side of Eq. (4.95) and the quantity af/r. The term in $2a$ is, according to Eqs. (4.8), (4.9), equal to $\psi-\psi_0$ and represents, therefore, the effect of the diverging waves emanating from the source density f in the vicinity of $r=0$. A part of this term represents af/r. The excess over this is the "background" term.

Disregarding the "background" term there is no difference between the results obtained here and Fermi's method in Born's first approximation. The validity of Fermi's result is, on the other hand, no better than that of Born's first approximation as may be seen by noting that

$$\bar{\psi}(\mathbf{r}_\nu,\mathbf{r}_\nu)\cong\frac{3}{4\pi R^3}\int_0^R\left(1+\frac{a}{r}\right)f(\mathbf{r}_\nu)d\mathbf{r}_\nu=\left(1+\frac{3a}{2R}\right)f, \tag{6.4}$$

and that calculation with Fermi's Eq. (6.2) in the second Born's approximation would bring in terms having an order of magnitude relative to the zeroth of a divided by the linear molecular dimensions.

6. SIMPLIFIED EXPLANATION OF FERMI'S EQUATION

The end result of Fermi's averaging of the wave equation is the replacement of the nuclear interaction potential $g(r)$ by an interaction energy

$$V_F=-\frac{ah^2}{\pi M}\delta_R(\mathbf{r}_\nu-\mathbf{r}_\nu)=\frac{3a}{R}\frac{h^2}{MR^2}\quad(r<R). \tag{7}$$

$$V_F=0\quad(r>R)$$

For R slightly greater than ρ this quantity is large in the region $r<R$. The introduction of V_F is then not of much use and would even lead to erroneous results for scattering if one used Fermi's equation (6.2) exactly. In fact, the law in accordance with which V_F and R should be varied together in order to obtain equivalence for scattering is much more closely $V_FR^2=$constant than $V_FR^3=$constant, and it is the latter way of varying V_F with R that follows from Eq. (7). This way is therefore not right, and one should not apply Fermi's equation in this manner. It is thus seen also that Fermi's equation cannot give even approximately correct results for scattering if one replaces the function δ_R by Dirac's δ function and calculates with the resultant equation exactly. The latter replacement corresponds to approaching the limit of $R=0$ in Eq. (7) which corresponds to varying the internal phase as

$$\left(\frac{M}{h^2}|V_F|\right)^{\frac{1}{2}}R=\left[\frac{3|a|}{R}\right]^{\frac{1}{2}}$$

which gives for F of Eq. (2.3) a limiting behavior for $R \ll a$

$$\left(\frac{rdF}{Fdr}\right)_{r\cong R} \cong \left[\frac{3|a|}{R}\right]^{\frac{1}{2}} \cot\left[\frac{3|a|}{R}\right]^{\frac{1}{2}}$$

which is indeterminate for $R \to 0$ while the limiting value of this quantity should be

$$\left(\frac{rdF}{Fdr}\right)_{r\cong R} = \left[\frac{rd(r+a)}{(r+a)dr}\right]_{r=R} = \frac{R}{R+a} \cong \frac{R}{a}\left(1-\frac{R}{a}\right).$$

These two results are obviously inconsistent, indicating that one should only use Dirac's delta function in Fermi's equation for purposes of calculating the scattering to the first order of Born's method, but that an exact solution of this equation would lead to incorrect results. For this reason the explanation in the present section of the paper is concerned not with the equation which Fermi recommends for solution by the Born procedure but with the form (6.2) in which the δ_R function is employed. A simplified presentation of Fermi's equation is taken up next.

The radius R can be made several times a, and the potential energy V_F can thereby be made small compared with the nuclear interaction potential $g(r)$ and yet large in comparison with the molecular potential energy acting on the proton. By making R sufficiently large one can make the modification of the wave function due to the action of V_F quite gentle and keep the term of $a\psi/R$ small compared with ψ. Born's first approximation can be thus made to be a good approximation for Eq. (6.2). The margin of available orders of magnitude is not exceedingly great for this choice of R but is nevertheless sufficient to make this point of view have good sense. Thus, e.g., one can make

$$R = 20(\hbar/(Mm)^{\frac{1}{2}}c) = 1.8\times 10^{-11} \text{ cm},$$

which is reasonably large compared with the maximum value of a that comes under consideration, *viz.* $a = 2\times 10^{-12}$ cm. The averaging sphere is still small in comparison with the molecular vibration amplitude which is of the order 10^{-9} cm. This choice gives

$$V_F = -\frac{3a}{R}\frac{mc^2}{20^2} = -\frac{1}{3}\frac{510000}{400} \text{ ev} = -433 \text{ ev}.$$

The kinetic and potential energies of molecular motion are seen to be small compared with V_F and can be neglected in the region $r<R$. Under these conditions the dependence of ψ on r inside $r<R$ is expressible as the product of a nearly constant factor and the function χ. The dependence of the latter on r is for an attractive V_F, i.e., $a>0$

$$F = r\chi = \text{const.}\times\sin[(M|V_F|/\hbar^2)^{\frac{1}{2}}r]$$

so that

$$(rdF_-/F_-dr)_{r=R} \cong 1-\frac{1}{3}\left[\frac{3a}{R}\frac{\hbar^2}{MR^2}\right]\frac{M}{\hbar^2}R^2 = 1-\frac{a}{R}, \tag{7.1}$$

which is precisely the value needed to join on smoothly to the function $F=r+a$ for $r>R$. In fact for the latter

$$(rdF_+/F_+dr)_{r=R} = R/(R+a) = 1-a/R+\cdots. \tag{7.2}$$

If V_F is repulsive rather than attractive, the sign of the terms in $1/R$ in *both* of the above expressions is changed, and the internal function can be still joined smoothly to the external one. It is seen, thus, that the potential energy V_F is such that for $R \gg a$ the solution of Eq. (6.2) gives the correct value of $rd\chi/\chi dr$. Within the limitations already discussed this equation must give, therefore, the solution of the problem.

It has been noted above that the margin available for the choice of R is not very great. The question naturally arises as to the order of precision of calculations that assume the validity of Eq. (6.2) which has been seen to imply the possibility of choosing R so that it is both large in comparison with the range of nuclear forces and small as compared with molecular dimensions.

7. TRANSFORMATIONS OF THE BACKGROUND

In order to estimate the accuracy of the calculation, one has to know the coefficient of a in Eq. (5). For this purpose it will be transformed into a different form. By means of Eq. (1.1) one obtains

$$\int u_s^*(\mathbf{r}')f(\mathbf{r}')\frac{e^{ik_s|\mathbf{r}'-\mathbf{r}_\nu|}}{|\mathbf{r}'-\mathbf{r}_\nu|}d\mathbf{r}'=\frac{1}{E_s}\int f(\mathbf{r}')\,U(\mathbf{r}')u_s^*(\mathbf{r}')\frac{e^{ik_s|\mathbf{r}'-\mathbf{r}_\nu|}}{|\mathbf{r}'-\mathbf{r}_\nu|}d\mathbf{r}'-\frac{\hbar^2}{2ME_s}\int f(\mathbf{r}')\frac{e^{ik_s|\mathbf{r}'-\mathbf{r}_\nu|}}{|\mathbf{r}'-\mathbf{r}_\nu|}\Delta u_s^*(\mathbf{r}')d\mathbf{r}', \tag{8}$$

and one further has for any regular $\varphi(\mathbf{r})$

$$\int\frac{e^{i\kappa r}}{r}(\Delta+\kappa^2)\varphi(\mathbf{r})d\mathbf{r}=-4\pi\varphi(0). \tag{8.1}$$

Letting

$$\varphi(\mathbf{r})=f(\mathbf{r})u_s^*(\mathbf{r})$$

and combining Eqs. (8), (8.1) one obtains

$$\sum_s u_s(\mathbf{r}_\nu)\int u_s^*(\mathbf{r}_\nu')f(\mathbf{r}_\nu')\frac{2e^{ik_s|\mathbf{r}_\nu'-\mathbf{r}_\nu|}}{|\mathbf{r}_\nu'-\mathbf{r}_\nu|}d\mathbf{r}_\nu'=(2\pi\hbar^2/M)f(\mathbf{r}_\nu)\sum_s u_s^*(\mathbf{r}_\nu)u_s(\mathbf{r}_\nu)/E_s+\text{other terms}. \tag{8.2}$$

By means of a similar transformation one finds

$$\sum_s u_s(\mathbf{r}_\nu)\int u_s^*(\mathbf{r}_\nu')\frac{f(\mathbf{r}_\nu')}{|\mathbf{r}_\nu'-\mathbf{r}_\nu|}d\mathbf{r}_\nu'=(2\pi\hbar^2/M)f(\mathbf{r}_\nu)\sum_s u_s^*(\mathbf{r}_\nu)u_s(\mathbf{r}_\nu)/E_s+\text{other terms}. \tag{8.3}$$

In Eqs. (8.2), (8.3) the first term is the same. This term approaches $f(\mathbf{r}_\nu)/r$ for small r. If, therefore, one subtracts (8.3) from (8.2), the result is free of the term in $1/r$. It is thus found that

$$B(\mathbf{r}_\nu,\mathbf{r}_\nu)=E\sum_s\frac{u_s(\mathbf{r}_\nu)}{E_s}\int f(\mathbf{r})\frac{e^{ik_s|\mathbf{r}-\mathbf{r}_\nu|}}{|\mathbf{r}-\mathbf{r}_\nu|}u_s^*(\mathbf{r})d\mathbf{r}+\sum_s\frac{u_s(\mathbf{r}_\nu)}{E_s}\int\frac{e^{ik_s|\mathbf{r}-\mathbf{r}_\nu|}-1}{|\mathbf{r}-\mathbf{r}_\nu|}$$
$$\times\left\{f(\mathbf{r})u_s^*(\mathbf{r})\,U(\mathbf{r})+\frac{\hbar^2}{2M}[2\nabla f(\mathbf{r})\cdot\nabla u_s(\mathbf{r})+u_s^*\Delta f(\mathbf{r})]\right\}d\mathbf{r}. \tag{8.4}$$

The behavior of the first term in this formula will now be discussed. One finds by straightforward calculation that

$$[\Delta_\nu-(2M/\hbar^2)\,U(\mathbf{r}_\nu)]X=-4\pi\delta(\mathbf{r}_\nu-\mathbf{r}_\nu)$$

where

$$X=(2\pi\hbar^2/M)\sum_s u_s^*(\mathbf{r}_\nu)u_s(\mathbf{r}_\nu)/E_s.$$

It follows, therefore, that for small $r=|\mathbf{r}_\nu-\mathbf{r}_\nu|X$ behaves as $1/r$. For large r and fixed $\mathbf{r}_\nu$ the quantity X vanishes much more rapidly than $1/r$ on account of the rapid decrease of the $u_s(\mathbf{r}_\nu)$. In (8.4) the first term contains on performing the summation contributions of the order

$$(M/2\pi\hbar^2)Ef/|\mathbf{r}-\mathbf{r}_\nu|^2$$

for small value of $|\mathbf{r}-\mathbf{r}_\nu|$ modified by the presence of the exponentials. This term has, therefore,

the approximate magnitude

$$Ef(\mathbf{r}_\tau)\frac{2M\bar{R}}{\hbar^2}=\frac{E}{(\hbar^2/2M\bar{R}^2)}\frac{f(\mathbf{r}_\tau)}{\bar{R}}, \tag{8.5}$$

where $\bar{R}$ is a mean length at which the changes in f and in the exponentials containing κ_s decrease the integrand appreciably in comparison with the approximation just mentioned. This length is roughly of the order of $1/\bar{\kappa}$, where $\bar{\kappa}$ is a mean value of κ, and the length is, therefore, of molecular dimensions. The energy of the neutron enters, therefore, in comparison with the centrifugal barrier for molecular dimensions, and besides one, has the factor $f/\bar{R}$. Therefore, one expects the order of magnitude of the effect of the background on the cross section to be 10^{-12} cm/10^{-9} cm $=0.001$, which amounts to a tenth of a percent.

Another convenient form is found by introducing the quantity

$$F(\mathbf{r}_\tau, \mathbf{r}')=\sum_{s=0}^{\infty} u_s(\mathbf{r}_\tau)u_s^*(\mathbf{r}')e^{-2M(E_s-E_0)\tau/\hbar^2}, \tag{8.6}$$

where E_0 is the lowest E_s. One verifies readily that

$$\{\Delta_\tau+(2M/\hbar^2)[E_0-U(\mathbf{r}_\tau)]\}F=\partial F/\partial\tau, \tag{8.7}$$

and one obtains

$$\sum_{s=0}^{\infty} f_s=\sum_{s=0}^{\sigma} f_s+\int_{\tau=0}^{\infty}\frac{\exp\left\{-\dfrac{|\mathbf{r}_\nu-\mathbf{r}'|^2}{4\tau}+\dfrac{2M}{\hbar^2}(E-E_0)\tau\right\}}{2(\pi)^{\frac{1}{2}}\tau^{\frac{1}{2}}}$$

$$\cdot[F(\mathbf{r}_\tau, \mathbf{r}')-\sum_{s=0}^{\sigma} u_s(\mathbf{r}_\tau)u_s^*(\mathbf{r}')e^{-2M(E_s-E_0)\tau/\hbar^2}]d\tau, \tag{8.8}$$

where

$$f_s=u_s(\mathbf{r}_\tau)u_s^*(\mathbf{r}')e^{ik_s|\mathbf{r}'-\mathbf{r}_\nu|}/|\mathbf{r}'-\mathbf{r}_\nu|, \tag{8.9}$$

which is useful for the evaluation of B (Cf. Appendix II). This transformation is especially convenient for $E=E_0$. It can be employed also for other values of E. In applying Eq. (8.8), one represents the collection of terms due to the -1 in the numerator of Eq. (5′) as

$$-\frac{1}{r}=-\frac{1}{2\pi^{\frac{1}{2}}}\int_0^{\infty}\frac{\exp(-r^2/4\tau)}{\tau^{\frac{1}{2}}}d\tau. \tag{8.9′}$$

It is found then that in the limit of $r=0$, the two definite integrals over τ entering the representation of B combine to give a convergent integral. In evaluating B for $E>E_0$ the number σ in (8.8) must be chosen so as to make $E_\sigma<E<E_{\sigma+1}$. The terms $\sum_{s=0}^{\sigma}f_s$ represent the effect of the diverging waves.

8. FREE PROTONS

The equations will be illustrated first in the case of free protons. There might be reasonable doubt regarding their applicability because the free protons recoil and the proton waves have sources of diverging waves on a par with the neutron waves. These sources are not obviously present in Eq. (6), however.

The protons will be quantized in a fundamental volume with a periodic boundary condition. The wave function ψ_0 will be taken to be

$$\psi_0=e^{i\mathbf{k}_0\mathbf{r}_\nu}, \quad \mathbf{k}_0=i\mathbf{p}_0/\hbar \tag{9}$$

corresponding to the collision of neutron and proton waves of unit amplitude. The momentum

of the incident neutrons is $\mathbf{p}_0$. The proper functions for the protons are

$$u_s(\mathbf{r}_\nu) = V^{-\frac{1}{2}} e^{i\mathbf{k}_s \mathbf{r}_\nu}, \quad \mathbf{k}_s = \mathbf{p}_s/\hbar, \tag{9.1}$$

where V is the fundamental volume. In the usual manner the summation over s can be replaced by

$$V \int d\mathbf{k}_s / 2\pi^3. \tag{9.2}$$

One has thus for the sum that is multiplied by $2a$ on the right of Eq. (6)

$$\sum_s = \frac{1}{8\pi^3} \int\int |\mathbf{r}' - \mathbf{r}_\nu|^{-1} \exp\{i[\mathbf{k}(\mathbf{r}_\nu - \mathbf{r}') + \mathbf{k}_0 \mathbf{r}' + (k_0^2 - k^2)^{\frac{1}{2}} |\mathbf{r}' - \mathbf{r}_\nu|]\} d\mathbf{r}' d\mathbf{k}, \tag{9.21}$$

where in accordance with the convention that has been followed for κ one must set

$$(k_0^2 - k^2)^{\frac{1}{2}} = |(k_0^2 - k^2)^{\frac{1}{2}}| \quad (k_0 > k) \tag{9.22}$$

$$(k_0^2 - k^2)^{\frac{1}{2}} = i|(k^2 - k_0^2)^{\frac{1}{2}}| \quad (k > k_0). \tag{9.23}$$

The quantity needed for the integral equation is

$$\langle \sum_s \rangle = \frac{1}{8\pi^3} \int\int \frac{\sin kr}{kr|\mathbf{r}' - \mathbf{r}_\nu|} \cdot \exp\{i[\mathbf{k}(\mathbf{r}_\nu - \mathbf{r}') + \mathbf{k}_0 \mathbf{r}' + (k_0^2 - k^2)^{\frac{1}{2}} |\mathbf{r}' - \mathbf{r}_\nu|]\} d\mathbf{r}' d\mathbf{k}. \tag{9.24}$$

On introducing $\mathbf{r}'' = \mathbf{r}' - \mathbf{r}_\nu$ and integrating over directions of $\mathbf{r}''$ one finds

$$\langle \sum_s \rangle = \frac{e^{i\mathbf{k}_0 \mathbf{r}_\nu}}{2\pi^2} \int \left\{ \int_0^\infty \frac{\sin(kr) \sin(|\mathbf{k}_0 - \mathbf{k}| r'')}{kr|\mathbf{k}_0 - \mathbf{k}|} \exp[i(k_0^2 - k^2)^{\frac{1}{2}} r''] dr'' \right\} d\mathbf{k}, \tag{9.25}$$

and integration over directions of $\mathbf{k}$ gives

$$\langle \sum_s \rangle = \frac{2e^{i\mathbf{k}_0 \mathbf{r}_\nu}}{\pi k_0 r} \int_0^\infty \int_0^\infty (1/r'') \sin(kr) \sin(k_0 r'') \sin(kr'') \exp\{i(k_0^2 - k^2)^{\frac{1}{2}} r''\} dr'' dk. \tag{9.26}$$

It will be noted that the integrals over r'' converge and that the integrations can be performed first over r'' by straightforward calculation.

$$I.P. \int_0^\infty (1/r'') \sin k_0 r'' \sin kr'' \exp[i(k_0^2 - k^2)^{\frac{1}{2}}] dr''$$

$$= (i/4) \int_0^\infty (1/r) \{\sin A_1 r + \sin A_2 r - \sin A_3 r - \sin A_4 r\} dr \tag{9.27}$$

with

$$\begin{aligned} A_1 &= \sqrt{} + k_0 - k; \quad A_2 = \sqrt{} - k_0 + k; \\ A_3 &= \sqrt{} + k_0 + k; \quad A_4 = \sqrt{} - k_0 - k; \end{aligned} \tag{9.28}$$

and

$$\sqrt{} = (k_0^2 - k^2)^{\frac{1}{2}}.$$

Contributions to the imaginary part are present only if $k_0 > k$. For this reason A_1, A_2, A_3 are positive, while A_4 is negative in Eq. (9.27). The right side of (9.27) becomes $\pi i/4$ and

$$I.P.\langle \sum_s \rangle = ie^{i\mathbf{k}_0 \mathbf{r}_\nu} \frac{1 - \cos k_0 r}{2k_0 r^2} \cong ie^{i\mathbf{k}_0 \mathbf{r}_\nu} k_0/4. \tag{9.3}$$

Similarly one obtains

$$R.P.\langle\sum_s\rangle=\frac{e^{ik_0r_r}}{2\pi k_0 r}\int_0^\infty \sin kr\,\log\left[\frac{k+k_0}{|k-k_0|}\right]dk=\frac{e^{ik_0r_r}}{2k_0r^2}\sin(k_0r)\cong\frac{e^{ik_0r_r}}{2r}\left(1-\frac{k_0^2r^2}{6}\right), \tag{9.4}$$

and in the limit of $r=0$, and $\mathbf{r}_r=\mathbf{r}_s$ one has from Eqs. (9.3), (9.4)

$$a\langle B\rangle_{r=0}=iak_0e^{ik_0r_s}/2. \tag{9.5}$$

Here use was made of the fact that one may keep either $\mathbf{r}_s$ or $\mathbf{r}_r$ fixed in the averaging over directions of $\mathbf{r}$ as has been explained in connection with Eq. (5.34). One may replace, therefore, the $\mathbf{r}_r$ in Eqs. (9.3), (9.4) by $\mathbf{r}_s$.

In the above calculation one has introduced into the calculation of B the approximate value of $f\cong\psi_0$ which follows from (5) if one neglects $a\langle B\rangle$, i.e., if one solves (5) by iteration. On account of Eq. (9.5) the corrected value of f is

$$f(\mathbf{r}_s)\cong(1+ik_0a/2)e^{ik_0r_s}. \tag{9.6}$$

The asymptotic behavior of the angular average over directions of $\mathbf{r}$ is

$$\langle\psi\rangle_{r=0}\cong(1+ik_0a/2)(1+a/r)e^{ik_0r_s}, \tag{9.7}$$

which can be compared with the exact value following from

$$\psi=\psi_0(\mathbf{r}_s,\,\mathbf{r}_r)+e^{ik_0R}\frac{\sin(k_0a/2)}{k_0r/2}e^{ik_0(r+a)/2} \tag{9.8}$$

according to which

$$\langle\psi\rangle_{r=0}\sim1+\frac{\sin(k_0a/2)}{k_0/2}e^{ik_0a/2}(1/r+ik_0/2)=e^{ik_0a/2}\left[\frac{a}{r}\frac{\sin k_0a/2}{k_0a/2}+\cos k_0a/2\right]\cong(1+ik_0a/2)(1+a/r). \tag{9.8'}$$

It is seen from Eq. (9.8′) that the wave function is not quite of the form $1+a/r$. The deviations from this form are seen, however, to be of the order $k_0^2a^2$, which is a very insignificant factor for thermal neutrons.

It is satisfying that to the order k_0a there is agreement between (9.8′) and (9.7). While even the terms in $ik_0a/2$ affect the cross section only by the insignificant factor $1+k_0^2a^2/4$, it is satisfactory to have the *phase* of the scattered wave correct to the order $k_0a/2$.

The agreement between (9.7) and (9.8) is seen to be no worse than the assumption that the factor $1+a/r$ represents correctly the variation with r of the s part of ψ at small r. The exact dependence is of the type

$$\frac{1}{kr}(\sin ka\,\cos kr+\cos ka\,\sin kr)\sim\cos ka\left[1+\frac{\tan ka}{ka}\cdot\frac{a}{r}\right].$$

The deviations from the assumed form are themselves representable by correction factors $1+k^2a/3$, and there is no apparent reason for expecting the agreement to be closer than that found.

If one makes a calculation for the cross section along standard lines with ψ_0 in place of f in Eq. (6), then one finds without difficulty that the differential cross section per unit solid angle in any given direction when corrected for the factor $1+k_0^2a^2/4$ is

$$\sigma_\omega=(4a^2+k_0^2)p_r/p_0.$$

The last correction goes outside of the limits of accuracy of the method and does not represent an

improvement over the simpler result

$$\sigma_w \cong 4a^2 p_r/p_0,$$

since this correction is given by the factor

$$\sin^2 k_0 a/2.$$

If all the corrections obtainable from the equations were as small as that just discussed, there would be no purpose in presenting the equations. It is found, however, that the actual correction factor involves the ratio of a to molecular dimensions to the first rather than to the second power and is not negligible, therefore.

A general idea of what one may expect can be obtained by considering the background for free protons as made of two parts, one of which comes from the region $k_s > k_0$, and the other from $k_s < k_0$. The evaluation can be carried out by means of Eq. (9.4) by replacing the integral by

$$\int_{k_0}^{\infty} \sin kr \log\frac{k+k_0}{k-k_0} dk = \frac{\cos k_0 r}{r}[C - Ci(2k_0 r) + \log 2k_0 r)] + \frac{\pi}{r}\sin(k_0 r) - \frac{\sin k_0 r}{r} Si(2k_0 r) \tag{9.9}$$

with

$$C = 0.5772\cdots = \text{Euler-Mascheroni constant}$$

$$Si(x) = \int_0^x \frac{\sin u}{u} du; \quad Ci(x) = -\int_x^{\infty} \frac{\cos u}{u} du.$$

By means of the above Eq. (9.9), one finds on substitution into Eq. (9.4) and on passing to the limit of $r \to 0$

$$R.P.\langle \sum_{k>k_0} \rangle \to e^{ik_0 r\pi}\left(\frac{1}{2r} - \frac{k_0}{2\pi}\right), \tag{10}$$

and one has similarly

$$R.P.\langle \sum_{k<k_0} \rangle \to e^{ik_0 r\pi}\left(\frac{ik_0}{4} + \frac{k_0}{2\pi}\right). \tag{10.1}$$

It is seen that the singularity in $1/r$ is contributed by the region of high k as could be expected since the representation of the δ function in Eq. (6.1) is impossible without the extension of the sum over the eigenfunctions to those of infinitesimal wave-length. It is seen also that there are two real contributions to $a\langle B\rangle$, one of amount

$$-ak_0/\pi = \text{part of } \langle B\rangle_{r=0} \text{ for } k > k_0, \tag{10.2}$$

and another of equal and opposite amount which comes from $k < k_0$. The effect of each of these parts on f is of the order of a fractional change of amount $2a/\lambda_0$, where λ_0 is the wave-length of the incident neutron which is of the order 10^{-3} for 1 ev neutrons, and 10^{-2} for 100 ev neutrons. When the protons are chemically bound, the balance of the contributions from $k > k_0$ and $k < k_0$ is upset, and there is a residual effect which can be expected to give changes in the scattering cross section of the order of tenths of a percent, since the molecular energies are of the order of 0.5 ev or 0.2 ev.

The evaluation of the background for neutrons having very small energies incident on harmonically bound protons is made in the next paper in this issue.[5] The results agree with the estimates made here in Section 7 above.

---

[5] G. Breit and P. R. Zilsel, Phys. Rev. **71**, 232 (1947).

ACKNOWLEDGMENTS

The work has received support from the Wisconsin Alumni Research Foundation and from the Office of Naval Research of the Navy Department.

APPENDIX I

Derivation of Eq. (4.9)

Substitution of K into the left side of Eq. (4.9) by means of Eqs. (4.2), (4.5) gives

$$\int \mathbf{K}(\ ,\ ')g(r')\psi(\ ')d\tau_\nu' d\tau_\nu' = \frac{2\pi M}{\hbar^2}\sum_s \int u_s(\tau_\nu)u_s^*(\tau_\nu')f(\tau_\nu')\left\{\int \frac{e^{i\kappa_s|\tau_\nu-\tau_\nu'|}}{|\tau_\nu-\tau_\nu'|}g(r')\chi(r')dr'\right\}d\tau_\nu' \quad \text{(I, 1)}$$

where the replacement

$$\psi(\tau_\nu, \tau_\nu) = f(\tau_\nu)\chi(r) \quad \text{(I, 2)}$$

has also been made. The latter involves the harmless approximations which have been justified in connection with Eqs. (1.2), (2.1), and (3). This discussion showed that to a very good approximation

$$\left[-\frac{\hbar^2}{M}\Delta + g(r)\right]\chi(r) = 0. \quad \text{(I, 3)}$$

As the range of nuclear forces ρ contracts in the process discussed for Eq. (3), one can make it small enough, for any pre-assigned τ_ν', τ_ν, so as to have

$$|\tau_\nu' - \tau_\nu| \gg \rho. \quad \text{(I, 4)}$$

When this condition is satisfied, one can set

$$\int \frac{e^{i\kappa_s|\tau_\nu-\tau_\nu'|}}{|\tau_\nu-\tau_\nu'|}g(r')\chi(r')dr' \cong \frac{e^{i\kappa_s|\tau_\nu-\tau_\pi'|}}{|\tau_\nu-\tau_\pi'|}\cdot I \quad \text{(I, 4.1)}$$

where

$$I = \int g(r')\chi(r')dr', \quad \text{(I, 4.2)}$$

and the employment of Eq. (I, 3) in the above formula gives

$$I = -\frac{\hbar^2 a}{\pi M}. \quad \text{(I, 4.3)}$$

In the calculation just described a appears as the value of $-r^2 d\chi/dr$ at the outer boundary of the region where $g(r) \neq 0$. Substitution of (I, 4.3) into (I, 4.2), of the latter into (I, 4.1), and of the result into (I, 1) yields Eq. (4.9) of the text.

In the above discussion no account was taken of the region in which (I, 4) is not fulfilled. As ρ approaches zero, the volume of the part of the space τ_π' in which (I, 4) does not hold also approaches zero, and the contribution to the sum on the right side of Eq. (4.9) due to an individual term is of the order

$$2\pi\rho^2 u_s^*(\tau_\nu)f(\tau_\nu). \quad \text{(I, 4.4)}$$

This is true only for terms with sufficiently low s. For high s, the strongly negative numbers $i\kappa_s$ make the contributions smaller. The series consists of terms like (I, 4.4) up to the point where $|\kappa_s|$ is of the order $1/\rho$. The sum on the right side of Eq. (4.9) contains thus

$$\sum_{s=0}^{|\kappa_s|\sim 1/\rho} u_s(\tau_\nu)u_s^*(\tau_\nu) = D(|\tau_\nu - \tau_\nu|) \quad \text{(I, 4.5)}$$

which is an approximation to the δ function and differs from the δ function by being distributed through a volume of approximate linear dimensions ρ. The whole sum on the right of Eq. (4.9) is thus of the order $f(\mathbf{r}_\nu)/\rho$, if $r=|\mathbf{r}_\nu-\mathbf{r}_\mu|$ is of the order ρ on account of (I, 4.4), (I, 4.5), which has to be true in order to cancel the term in $1/r$ on the left side of Eq. (4.95). In the description of the behaviour of the sum which has just been considered, the quantity ρ has no direct significance as the range of nuclear force, but can be made equal to it if desired. It is thus seen that the contribution to the sum owing to the region $|\mathbf{r}_\nu'-\mathbf{r}_\mu|$ is quite large for $|\mathbf{r}_\nu-\mathbf{r}_\mu|<\rho$ and cannot be said to be negligible everywhere. It is also seen, however, that on account of (I, 4.5), this contribution is very much smaller if $|\mathbf{r}_\nu-\mathbf{r}_\mu|>\rho$, because the D function in (I, 4.5) is concentrated mainly in a region having linear dimensions ρ.

In spite of the fact that the contributions to the sum in (4.9), caused by the region inside a sphere of radius ρ, are responsible for the term $f(\mathbf{r}_\nu)/\rho$, when $|\mathbf{r}_\nu-\mathbf{r}_\mu|=\rho$, the contraction procedure makes it possible to make ρ small enough so that for a given $|\mathbf{r}_\nu-\mathbf{r}_\mu|$ one can satisfy (I, 4).

APPENDIX II

Derivation of Eq. (8.8)

For real values of $i\kappa_s$, one can represent the quantity f_s which is defined by Eq. (8.9) as

$$f_s=[u_s(\mathbf{r}_\nu)u_s^*(\mathbf{r}')/2\pi^{\frac{1}{2}}]\int_{\tau=0}^{\infty}\tau^{-\frac{1}{2}}\exp\{-|\mathbf{r}_\nu-\mathbf{r}'|^2/4\tau-|\kappa_s|^2\tau\}d\tau. \qquad \text{(II, 1)}$$

This formula can be verified as follows. The factor in (8.9) which multiplies the product of u_s and u_s^* will be temporarily denoted by g_s. One can define g_s by

$$(\Delta_\nu+\kappa_s^2)g_s=0, \qquad \text{(II, 1.1)}$$

and the requirements: (a) $g_s\to 0$ for $\mathbf{r}_\nu\to\infty$; (b) g_s approaches $|\mathbf{r}_\nu-\mathbf{r}'|^{-1}$ as a limit for $|\mathbf{r}_\nu-\mathbf{r}'|\to 0$. It is seen that

$$h_s=(1/2\pi^{\frac{1}{2}})\int_0^{\infty}\tau^{-\frac{1}{2}}\exp[-|\mathbf{r}_\nu-\mathbf{r}'|^2/4\tau-|\kappa_s|^2\tau]d\tau \qquad \text{(II, 1.2)}$$

has the property (II, 1.1) of g_s

$$(\Delta_\nu+\kappa_s^2)h_s=(1/2\pi^{\frac{1}{2}})\int_0^{\infty}\frac{d}{d\tau}\{\tau^{-\frac{1}{2}}\exp[-|\mathbf{r}_\nu-\mathbf{r}'|^2/4\tau-|\kappa_s|^2\tau\}d\tau \qquad \text{(II, 1.3)}$$

and is, therefore, zero unless $|\mathbf{r}_\nu-\mathbf{r}'|=0$. In the latter case the right side of (II, 1.3) is infinite. It is also clear from the form of (II, 1.2) that h_s has the same asymptotic forms at small and at large distances as g_s. It follows that

$$g_s=h_s \qquad \text{(II, 1.4)}$$

as can be verified by integration of (II, 1.2). Substituting (II, 1.2) for g_s in Eq. (8.9) of the text one obtains Eq. (II, 1) for f_s. This transformation applies only for $\kappa_s^2<0$ because if κ_s is real, then f_s is an outgoing wave. Equation (8.8) now follows by straightforward substitution of (II, 1) for $s=\sigma+1, \sigma+2, \cdots$.

The Scattering of Slow Neutrons by Bound Protons

II. Harmonic Binding—Neutrons of Zero Energy

G. BREIT* AND P. R. ZILSEL*
University of Wisconsin, Madison, Wisconsin

(Received November 29, 1946)

The cross section for scattering of very slow neutrons by elastically bound protons is calculated by means of the method described in the preceding paper. The results are expressed in terms of a correction factor to be applied to Fermi's factor 4. According to Eq. (5) of the present paper this correction factor is $1+16aJ/\pi^{\frac{1}{2}}$ with J defined by Eq. (6) which is suitable for numerical work. The results of numerical calculations for the effects of anisotropy in molecules with axial symmetry are presented in Fig. 1 which has to be used with Eqs. (6.2), (6.3) of the text. For scattering by the H_2O molecule the correction to be applied to Fermi's result is only $\sim$.3 percent of the final value. Fermi's method is very accurate in this case.

1. INTRODUCTION AND NOTATION

THE method of the preceding paper[1] is here applied to the calculation of the scattering cross section for neutrons having zero energy from protons bound in molecules by simple harmonic oscillator forces. The F transformation of the background term[1] is used to reduce the computation of the background to the evaluation of a definite integral by numerical quadrature. It is found, in agreement with order of magnitude considerations discussed in the preceding paper, that Fermi's factor 4, representing the increase in the scattering cross section caused by chemical binding, is accurate to within a few tenths of a percent, and the value of the correction factor is worked out in the last section of this paper. The notation is as in[1] with the addition of the following symbols:

a = constant having dimensions of length defined so that radial wave function is of the form const.$(1+a/r)$ for small proton-neutron distances r.
α_x, α_y, α_z = elastic binding constants of proton in molecule.
$\xi=x/\alpha_x$; $\eta=y/\alpha_y$; $\zeta=z/\alpha_z$.
$H_n(\xi)=(-)^n e^{\xi^2}(d/d\xi)^n e^{-\xi^2}$ = Hermite polynomial of degree n.
$q_x=\exp(-2\tau/\alpha_x^2)$; $q_y=\exp(-2\tau/\alpha_y^2)$; $q_z=\exp(-2\tau/\alpha_z^2)$.
$4T_x=4\tau+\alpha_x^2(1-q_x^2)$; etc.
$Q=\frac{1}{2}+(1-e^{-\xi})/2\xi$.

The potential energy binding the proton in the molecule is taken as

$$U(\mathbf{r}_\tau)=\frac{\hbar^2}{2M}\left(\frac{x_\tau^2}{\alpha_x^4}+\frac{y_\tau^2}{\alpha_y^4}+\frac{z_\tau^2}{\alpha_z^4}\right), \tag{1}$$

for which the characteristic frequencies are

$$2\pi\nu_x=\hbar/M\alpha_x^2, \quad \text{etc.}, \tag{1.1}$$

so that the energy levels are given by

$$E_s=[(2n_x+1)/\alpha_x^2+(2n_y+1)/\alpha_y^2+(2n_z+1)/\alpha_z^2]\hbar^2/2M \tag{1.2}$$

and the proton eigenfunctions by[2]

$$u_s(\mathbf{r})=\prod[\alpha_x 2^{n_x} n_x!\pi^{\frac{1}{2}}]^{-\frac{1}{2}} H_{n_x}(x/\alpha_x)\exp(-x^2/2\alpha_x^2) \tag{1.3}$$

* Now at Yale University.
[1] G. Breit, Phys Rev 71, 215 (1947). This will be referred to as I in the text. Formulas occurring in I will be referred to by prefixing the roman numeral I ahead of the number of the formula.
[2] In this paper the symbol Π always stands for the product over x, y, z.

with

$$H_n(\xi) = \text{Hermite polynomial.} \tag{1.4}$$

The following notation will be used

$$\xi = x/\alpha_x, \quad \eta = y/\alpha_y, \quad \zeta = z/\alpha_z. \tag{1.5}$$

The complete wave function of the system is given by Eq. (I, 6) with f given by (I, 5) and B by (I, 5′).

2. CALCULATION OF THE BACKGROUND

Equation (I, 5′) can be evaluated by means of the transformation (I, 8.8). The first approximation to f is ψ_0, and the solution of Eq. (I, 5) by iteration leads, therefore, to an integral in which f is replaced by ψ_0 in (I, 5′). In the present case, with $E = E_0$ and u_0 given by (1.3), one can replace ψ_0 by

$$f = C \exp[-(\xi^2+\eta^2+\zeta^2)/2]. \tag{2}$$

Putting $H_n(\xi) = (-)^n \exp(\xi^2)(d^n/d\xi^n)\exp(-\xi^2)$ in (1.3) and substituting into Eq. (I, 8.6) one has

$$F(\mathbf{r}, \mathbf{r}') = \sum_{n_x, n_y, n_z} \prod \left\{ \frac{\exp[(\xi^2+\xi'^2)/2]}{\alpha_x 2^{n_x} n_x! \pi^{\frac{1}{2}}} (\partial^{2n_x}/\partial\xi^{n_x}\partial\xi'^{n_x}) \cdot \exp[-\xi^2-\xi'^2-2n_x\tau/\alpha_x^2] \right\}. \tag{2.1}$$

The summations in (2.1) can be performed by expressing the exponentials containing $-\xi^2-\xi'^2$ by means of Fourier-integrals. One obtains

$$\exp(-\xi^2) = \frac{1}{2\pi^{\frac{1}{2}}} \int_{-\infty}^{\infty} \exp(i\omega\xi - \omega^2/4) d\omega,$$

and thus

$$\exp(-\xi^2-\xi'^2) = \frac{1}{4\pi} \int_{-\infty}^{\infty}\int_{-\infty}^{\infty} \exp[i(\omega\xi+\omega'\xi') - (\omega^2+\omega'^2)/4] d\omega d\omega'.$$

Putting

$$q_x = \exp(-2\tau/\alpha_x^2), \quad q_y = \exp(-2\tau/\alpha_y^2), \quad q_z = \exp(-2\tau/\alpha_z^2), \tag{2.2}$$

one obtains the auxiliary formula

$$\sum_{n=0}^{\infty} \exp(-2n\tau/\alpha^2)(\partial^2/\partial\xi\partial\xi')^n \exp(-\xi^2-\xi'^2)/2^n(n!) = F_x$$

$$= \frac{1}{4\pi} \int_{-\infty}^{\infty}\int_{-\infty}^{\infty} \sum_{n=0}^{\infty} \frac{(q/2)^n}{n!} (-\omega\omega')^n \exp[i(\omega\xi+\omega'\xi') - (\omega^2+\omega'^2)/4] d\omega d\omega' \tag{2.3}$$

$$= \frac{1}{4\pi} \int_{-\infty}^{\infty}\int_{-\infty}^{\infty} \exp\{i(\omega\xi+\omega'\xi') - \tfrac{1}{4}(\omega^2+\omega'^2+2q\omega\omega')\} d\omega d\omega'.$$

The subscript x has been dropped for α, n, and q so as to simplify the notation.

The integrations over ω, ω' can be carried out by transforming the homogeneous quadratic form in ω, ω' in the exponent of the last form of (2.3) to a diagonal form. It is thus found that

$$F_x = (1-q_x^2)^{-\frac{1}{2}} \exp\{-[\xi^2+\xi'^2-2q_x\xi\xi']/(1-q_x^2)\}. \tag{2.4}$$

Comparing (2.1) and (2.3) one sees that

$$F = \prod \exp[(\xi^2+\xi'^2)/2] F_x/(\pi^{\frac{1}{2}}\alpha_x),$$

so that

$$F(\mathbf{r}, \mathbf{r}') = \frac{1}{\pi^{\frac{1}{2}}} \prod \frac{\exp\{(\xi^2+\xi'^2)/2 - (\xi^2+\xi'^2-2q_x\xi\xi')/(1-q_x^2)\}}{\alpha_x(1-q_x^2)^{\frac{1}{2}}}. \tag{3}$$

It follows from Eq. (I, 8.8), on noting that $E=E_0$, and thus setting $\sigma=0$, that

$$\sum_0^\infty u_s(\mathbf{r}_\tau)u_s^*(\mathbf{r}')\frac{2\exp(i\kappa_s|\mathbf{r}_\nu-\mathbf{r}'|)-1}{|\mathbf{r}_\nu-\mathbf{r}'|}=\frac{1}{\pi^{\frac{1}{2}}}\int_0^\infty \exp(-|\mathbf{r}_\nu-\mathbf{r}'|^2/4\tau)F(\mathbf{r}_\tau,\mathbf{r}')d\tau-\delta(\mathbf{r}_\tau-\mathbf{r}')/|\mathbf{r}_\nu-\mathbf{r}'|$$

$$=(1/\pi^{\frac{1}{2}})\int_0^\infty\left[\prod\frac{\exp\{-(\xi_\tau^2+\xi'^2)(1+q_z^2)/2(1-q_z^2)+2q_z\xi_\tau\xi'/(1-q_z^2)\}}{\pi^{\frac{1}{2}}\alpha_x(1-q_z^2)^{\frac{1}{2}}}-\frac{\delta(\mathbf{r}_\tau-\mathbf{r}')}{2}\right]$$

$$\times\frac{\exp(-|\mathbf{r}_\nu-\mathbf{r}'|^2/4\tau)}{\tau^{\frac{1}{2}}}d\tau. \quad (3.1)$$

where $1/|\mathbf{r}_\nu-\mathbf{r}'|$ is represented as

$$(1/2\pi^{\frac{1}{2}})\int_0^\infty[\exp(-|\mathbf{r}_\nu-\mathbf{r}'|^2/4\tau)/\tau^{\frac{1}{2}}]d\tau.$$

Putting (3.1) and (2) into (I, 5′) and performing the integration over $\mathbf{r}'$ it is found that

$$B(\mathbf{r}_\tau,\mathbf{r}_\nu)=(8/\pi^{\frac{1}{2}})f(\mathbf{r}_\tau)\int_0^\infty\{\prod(4T_x)^{-\frac{1}{2}}\exp\{-(x_\nu-q_zx_\tau)^2/4T_x\}-\exp(-|\mathbf{r}_\nu-\mathbf{r}_\tau|^2/8\tau)/(8\tau)^{\frac{1}{2}}\}d\tau \quad (3.2)$$

with

$$4T_x=4\tau+\alpha_x^2(1-q_z^2). \quad (3.25)$$

The limit of (3.2) as $\mathbf{r}_\nu\to\mathbf{r}_\tau$ is independent of the angle $(\mathbf{r}_\nu,\mathbf{r}_\tau)$ so that the averaging process required for Eq. (I, 5) reduces to

$$B(\mathbf{r}_\tau,\mathbf{r}_\tau)=(8/\pi^{\frac{1}{2}})f(\mathbf{r}_\tau)\int_0^\infty\{\prod(4T_x)^{-\frac{1}{2}}\exp\{-(1-q_z^2)x_\tau^2/4T_x\}-(8\tau)^{-\frac{1}{2}}\}d\tau. \quad (4)$$

In the calculation leading to this equation it was assumed that f can be replaced by a constant multiple of u_0. This is justifiable only if the molecule is originally in its lowest state, if the neutrons have a very low energy and if a is sufficiently small to make aB small compared with f. The latter assumption is justified *a posteriori* by the smallenss of the effect of B.

3. THE SCATTERING CROSS SECTION

For zero energy neutrons the amplitude of the scattered wave is proportional to

$$\int u_0^*(\mathbf{r}')f(\mathbf{r}')d\mathbf{r}'.$$

f is given by (I, 5) with B from (4), in which f is taken as $f=\psi_0=u_0$.

Thus,

$$\int u_0^*(\mathbf{r}')f(\mathbf{r}')d\mathbf{r}'=\int|u_0(\mathbf{r}')|^2\left(1+8a/\pi^{\frac{1}{2}}\int_{\tau=0}^\infty\{\ \}d\tau\right)d\mathbf{r}'=1+(8a/\pi^{\frac{1}{2}})J(\alpha_x,\alpha_y,\alpha_z). \quad (5)$$

The square of this factor, *i.e.*, the quantity $1+16aJ/\pi^{\frac{1}{2}}$, is the correction factor for the cross section. The quantity J occurring in this formula is given by

$$J(\alpha_x,\alpha_y,\alpha_z)=\int_0^\infty\{\prod[4\tau+2\alpha_x^2(1-q_z)]^{-\frac{1}{2}}-8\tau^{-\frac{1}{2}}\}d\tau \quad (6)$$

as is found by performing the integration over $\mathbf{r}'$.

The integral occurring in Eq. (6) has been evaluated numerically in a few cases, and the results

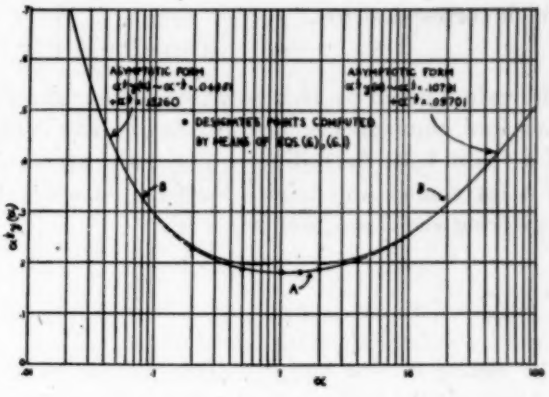

FIG. 1. Plot of $\alpha^{\frac{1}{2}}I(\alpha)$ vs. α. Curve A is drawn through points computed by means of Eqs. (6), (6.1). Curves B are the asymptotic forms given by Eqs. (6.3), (6.4). The ordinate of the graph can be used for the computation of the correction factor of Eq. (5) by means of Eqs. (6.1), (6.2) with α defined by Eq. (6.3).

are plotted in Fig. 1. In this figure the ordinate is the quantity

$$\alpha^{\frac{1}{2}}I(\alpha)=\alpha^{\frac{1}{2}}J(1,1,\alpha). \tag{6.1}$$

The asymptotic forms of this quantity for large and for small α are indicated on the graph, and their derivation is described in the Appendix. By means of the graph one can evaluate J for any harmonic oscillator with axial symmetry by means of the following formula

$$J(\alpha_x,\alpha_z,\alpha_s)=I(\alpha_s/\alpha_z)/\alpha_z. \tag{6.2}$$

The ordinate plotted is

$$\alpha^{\frac{1}{2}}I(\alpha)=\alpha_x^{\frac{1}{2}}\alpha_s^{\frac{1}{2}}J(\alpha_x,\alpha_z,\alpha_s);\quad \alpha=\alpha_s/\alpha_z. \tag{6.3}$$

The asymptotic forms of J are

$$\begin{aligned} &J(\alpha_x,\alpha_z,\alpha_s)\sim I_1/\alpha_s+2^{\frac{1}{2}}I_2/\alpha_x=0.0485/\alpha_s+0.1526/\alpha_x;\quad (\alpha\ll 1);\\ &J(\alpha_x,\alpha_z,\alpha_s)\sim I_2/\alpha_x+2I_1/\alpha_s=0.1079/\alpha_x+0.0970/\alpha_s;\quad (\alpha\gg 1), \end{aligned} \tag{6.4}$$

where

$$I_1=(1/16)\int_0^\infty (Q^{-\frac{1}{2}}-1)\xi^{-\frac{1}{2}}d\xi; \tag{6.5}$$

$$I_2=(1/16)\int_0^\infty (Q^{-1}-1)\xi^{-\frac{1}{2}}d\xi; \tag{6.6}$$

$$Q=\tfrac{1}{2}+(1-e^{-\xi})/2\xi. \tag{6.7}$$

The two asymptotic branches extrapolate to nearly the same value for an harmonic oscillator with spherical symmetry and agree rather well with values computed directly by means of Eqs. (6), (6.1).

4. APPLICATION TO THE WATER MOLECULE

In order to apply the present theory, the mass of the proton will be considered to be small in comparison with the mass of the molecule. One has then

$$\alpha=\frac{6.39\times 10^{-10}\text{ cm}}{[(h\nu)_{\text{ev}}]^{\frac{1}{2}}},$$

where the subscript ev indicates that the electron volt is the unit of energy. For H_2O Slater[3] lists the following frequencies:

$$h\nu \quad (\text{ev}) = \quad 0.443 \qquad 0.462 \qquad 0.248$$

[3] J. C. Slater, *Introduction to Chemical Physics* (McGraw-Hill Book Company, Inc., New York, 1939), p. 146.

which correspond to

$$\alpha \quad (\text{cm}) = 9.6\times10^{-10} \quad 9.4\times10^{-10} \quad 1.28\times10^{-9}.$$

The values given by Herzberg[4] are in essential agreement with the above. The lower frequency and, therefore, the higher α corresponds to a vibration roughly at right angles to the other two. The value of α_s/α_a is 1.35. According to Fig. 1 the anisotropy has no important effect in this case. The values of a for singlet and triplet scattering are $a_1 = 1.92\times10^{-12}$ cm; $a_3 = -0.584\times10^{-12}$ cm. For singlet scattering the correction factor is

$$1+0.82\frac{1.92\times10^{-12}}{1.06\times10^{-9}} = 1.0015.$$

The square of this factor matters for the scattered intensity. There is thus a correction of about 0.3 percent for the expected scattered intensity in the singlet state. Since slow neutrons are mostly scattered in the singlet state, this is the approximate magnitude of the correction for very slow neutrons.

ACKNOWLEDGMENTS

The authors would like to express their appreciation of the support given to this work by the Wisconsin Alumni Research Foundation and the Office of Naval Research of the Navy Department.

APPENDIX

Asymptotic Forms for $I(\alpha)$

The consideration will be carried out for $\alpha \ll 1$. It follows from Eqs. (6), (6.1) that

$$I(\alpha) = J(1, 1, \alpha) = \int_0^\infty \{[\tfrac{1}{2}+(1/4\tau)(1-e^{-2\tau})]^{-1}[\tfrac{1}{2}+(\alpha^2/4\tau)(1-\exp(-2\tau/\alpha^2))]^{-\frac{1}{2}}-1\}(8\tau)^{-\frac{1}{2}}d\tau. \quad \text{(A, 1)}$$

The integral will be represented as

$$I(\alpha) = A(\alpha)+B(\alpha), \quad \text{(A, 1.1)}$$

with

$$A(\alpha) = \int_0^{N\alpha^2} \cdots d\tau, \quad B(\alpha) = \int_{N\alpha^2}^\infty \cdots d\tau, \quad \text{(A, 1.2)}$$

where the integrand is the same as in (A, 1). The number N is chosen so as to satisfy the requirement

$$N \gg 1, \quad N\alpha^2 \ll 1. \quad \text{(A, 1.3)}$$

In the limit $\alpha = 0$ both of these requirements can be satisfied perfectly in the sense that N can be made to approach ∞ while $N\alpha^2$ approaches zero. Integral $A(\alpha)$ can be transformed through the introduction of the variable

$$\xi = 2\tau/\alpha. \quad \text{(A, 1.4)}$$

On account of the second condition (A, 1.3) the quantity $e^{-2\tau}$ can be expanded by Taylor's series, and the contributions to the integral form a rapidly converging series. Keeping the first two terms of the expansion one has

$$A(\alpha) = \int_0^{2N} (1/16\alpha)\{(1+\alpha^2\xi/4)[\tfrac{1}{2}+(1-e^{-\xi})/2\xi]^{-\frac{1}{2}}-1\}\xi^{-\frac{1}{2}}d\xi. \quad \text{(A, 2)}$$

The discussion of the contribution of the term in $\alpha^2\xi/4$ will be postponed. It will be shown later that its contribution to A approaches zero as α approaches zero. Only terms that do not approach

[4] G. Herzberg, *Infrared and Raman Spectra* (D. Van Nostrand Company, Inc., New York, 1945), p. 161.

zero with α will be kept. One has thus

$$A(\alpha)\sim\frac{1}{16\alpha}\left(\int_0^\infty-\int_{2N}^\infty\right)\left\{\left[\frac{1}{2}+\frac{1-e^{-\xi}}{2\xi}\right]^{-\frac{1}{2}}-1\right\}\xi^{-\frac{1}{2}}d\xi. \tag{A, 2.1}$$

The first integral will be kept in the above form. The second can be estimated as follows

$$-\frac{1}{16\alpha}\int_{2N}^\infty(2^{\frac{1}{2}}-1-2^{-\frac{1}{2}}\xi^{-1})\xi^{-\frac{1}{2}}d\xi\cong-\frac{2^{\frac{1}{2}}-1}{8\alpha(2N)^{\frac{1}{2}}}. \tag{A, 2.2}$$

The right side of (A, 2.2) becomes infinite for $\alpha=0$ on account of the second condition (A, 1.3). The omitted terms, however, are of order $N^{-\frac{1}{2}}\alpha^{-1}$. They can be made to approach zero by requiring

$$N^3\alpha^2\gg1. \tag{A, 2.3}$$

This means that N should be made to approach ∞ more strongly than $\alpha^{-\frac{1}{3}}$ which can be done consistently with the second condition (A, 1.3). Any dependence between α^{-2} and $\alpha^{-\frac{1}{3}}$ is satisfactory. With this additional restriction on N it suffices to consider only the right side of (A, 2.2).

In the evaluation of B one makes use of the smallness of $\alpha^2/\tau\ll1/N$. At the lower limit of integration

$$\left[\frac{1}{2}+\frac{\alpha^2}{4\tau}(1-\exp(-2\tau/\alpha^2))\right]_{\tau=N\alpha^2}^{-\frac{1}{2}}\cong2^{\frac{1}{2}}\left(1-\frac{1}{4N}+\cdots\right)\cong2^{\frac{1}{2}}. \tag{A, 3}$$

The omission of further terms here is justifiable because B turns out to be of the order $1/(N\alpha^2)^{\frac{1}{2}}$ so that (A, 2.3) will make negligible the term in $1/(4N)$ which has just been omitted. One obtains by means of (A, 3)

$$B(\alpha)\sim\frac{1}{16}\left(\int_0^\infty-\int_0^{N\alpha^2}\right)\left\{\left[\frac{1}{2}+\frac{1}{4\tau}(1-e^{-2\tau})-1\right]^{-1}-1\right\}\tau^{-\frac{1}{2}}d\tau+\frac{2-2^{\frac{1}{2}}}{16(N\alpha^2)^{\frac{1}{2}}}. \tag{A, 3.1}$$

The right side of the above relation contains $\int_0^{N\alpha^2}$. Its contribution is estimated by expanding the brace in a Taylor series. It is found to be $-(N\alpha^2)^{\frac{1}{2}}/16$ which vanishes on account of the second condition (A, 1.3).

Adding B to A the last term in (A, 3.1) is canceled by (A, 2.2). The integral I_1 of Eq. (6.5) of the text arises from (A, 2.1), the integral I_2 of Eq. (6.6) from (A, 3.1) and one obtains

$$I(\alpha)\sim\frac{I_1(\alpha)}{\alpha}+2^{\frac{1}{2}}I_2(\alpha),$$

which is equivalent to

$$J(\alpha_x,\alpha_x\alpha_z)\sim I_1/\alpha_x+2^{\frac{1}{2}}I_2/\alpha_x$$

on account of Eq. (6.2). This, together with numerical evaluations of I_1, I_2 gives the first line of Eq. (6.4).

It remains to explain the legitimacy of neglecting the term in $\alpha^2\xi/4$ in Eq. (A, 2). This term contributes to $I(\alpha)$ the amount

$$\frac{\alpha}{64}\int_0^{2N}\xi^{-\frac{1}{2}}\left[\frac{1}{2}+\frac{1-e^{-\xi}}{2\xi}\right]^{-\frac{1}{2}}d\xi.$$

The integral converges near $\xi=0$. The [ ] has the value 1 for $\xi=0$, and its value decreases to about $\frac{1}{2}$ for large ξ. The contribution is, therefore, less than

$$(2^{\frac{1}{2}}\alpha/64)\int_0^{2N}\xi^{-\frac{1}{2}}d\xi=(2^{\frac{1}{2}}\alpha/64)(2N)^{\frac{1}{2}}$$

which vanishes as $N\alpha^2$. The explanation of the first line of Eq. (6.4) has now been completed. The second line is obtained by very similar reasoning.

The Free Fall of Atoms and the Measurement of the Velocity Distribution in a Molecular Beam of Cesium Atoms

I. ESTERMANN, O. C. SIMPSON,* AND O. STERN**
Research Laboratory of Molecular Physics, Carnegie Institute of Technology, Pittsburgh, Pennsylvania
(Received November 29, 1946)

The free fall of atoms is observed in long molecular beams of potassium and cesium atoms. The measurement of the intensity distribution in a beam deflected by gravity represents the velocity distribution of the beam atoms and permits an accurate determination of this distribution. The results show that the measured values agree in general with those calculated for a modified Maxwellian velocity distribution in the beam. At larger deflections, i.e., for slow atoms, a deficiency of intensity was observed, which increased both with increasing deflection and with increasing pressure in the oven where the beam originates. This deficiency is explained by collisions in the immediate vicinity of the oven slit.

1. INTRODUCTION

A METHOD for the exact measurement of the Bohr magneton devised recently by one of us[1] is based on the compensation of the acceleration of gravity acting on a molecular beam of cesium atoms by the magnetic acceleration produced by an inhomogeneous magnetic field. The effect of gravity on atoms, that is their free fall, is easily observable in a long molecular beam. In a cesium beam 2 meters long, the fall distance of atoms having the most probable velocity corresponding to an oven temperature of about 450°K is approximately 0.2 mm. The magnetic inhomogenity required to compensate the acceleration of gravity is in this case only about 25 gauss/cm. It is, therefore, possible to produce the magnetic field by a current in a straight conductor of circular cross section; thus the magnetic inhomogeneity does not need to be measured, but can be calculated from the geometrical dimensions and the electric current. Hence, it is only necessary to measure the current I_0 through the conductor which produces a magnetic field of the inhomogeneity $(\partial H/\partial r)_0$ exactly compensating the acceleration of gravity for the Cs atoms with the largest magnetic moment μ_0 equal to one Bohr magneton. Since the compensation of the acceleration is independent of the velocity, this method is in principle independent of the velocity distribution in the beam. For the actual measurement of I_0, however, the exact knowledge of the velocity distribution in the beam is necessary.

FIG. 1. Principle of the method.

If the current I through the conductor is less than I_0, all the atoms in the beam are deflected downwards. If $I > I_0$, those with the largest magnetic moment are deflected upwards. The compensating current I_0 can be determined by placing a detector slightly above the plane of the beam (position D' in Fig. 1), and by increasing I gradually until atoms deflected upwards strike the detector. In practice, the beam intensity i striking the detector must be measured as a function of the current I, and I_0 is found by an extrapolation, which requires the knowledge of the actual velocity distribution in the beam.

From published measurements by Cohen and Ellett[2] of the velocity distribution in beams of alkali-metal atoms undergoing magnetic deflection, it appeared that in such beams the modified Maxwellian distribution was correct to within a few percent down to velocities of one-half of the most probable velocity. Experiments for the measurement of the Bohr magneton carried out by us from 1938 to 1942 showed, however, that considerable deficiencies of slow molecules (up to 50 percent of the number expected on the basis of Maxwell's law) are present even at oven pressures lower than those used in

* At present on leave to the Argonne National Laboratory, Chicago, Illinois.
** Now in Berkeley, California.
[1] O. Stern, Phys. Rev. 51, 852 (1937).
[2] V. W. Cohen and A. Ellett, Phys. Rev. 52, 502 (1937).

the magnetic deflection experiments of Cohen and Ellett.* It was, therefore, necessary to determine these deviations from the modified Maxwellian distribution as a preliminary work. Since the apparatus designed for the measurement of the Bohr magneton allowed such measurements by means of deflection by gravity ("free fall"), this method was used.

2. PRINCIPLE OF THE METHOD

To observe the free fall of molecules, the following arrangement was used (Fig. 1). A beam of Cs atoms produced by the oven slit O and the collimating slit S was detected by a hot tungsten wire D. Both slits as well as the detector wire were horizontal. The Cs atoms striking the detector wire became ionized and the ions were collected on a negatively charged cylinder surrounding the wire (Langmuir-Taylor method).[3] The ion current between the detector wire and the collecting cylinder gave directly the number per second of Cs atoms impinging upon the wire. The dotted lines show the path of Cs atoms with different velocities.

We assume $OS=SD=l$. Then for an atom with the velocity v, the fall distance is $S=gl^2/v^2$ (not $gl^2/2v^2$). For Cs atoms of the most probable velocity α the fall distance S_α is 0.174 mm† for an oven temperature $T=450°$K and for $l=100$ cm. Since the width of the slits defining the beam and the thickness of the detector wire in our experiments was only 0.02 mm, this fall distance is easily observable. For potassium atoms, S_α is approximately 0.04 mm, which is still well observable under our experimental conditions. The intensity distribution in the beam deflected by gravity measured in the vertical direction pictures the velocity distribution of the atoms in the beam.

With slits of the width b, the intensity distribution in the undeflected beam is given by a trapezoid (Fig. 2). Assuming Maxwellian distribution in the oven, the fraction of atoms in the beam in the velocity interval between v and

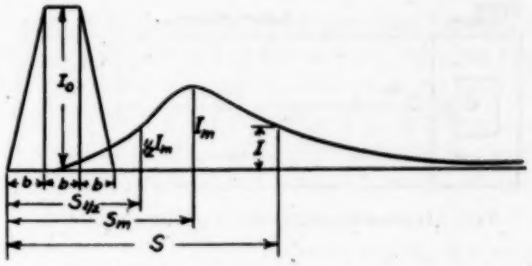

FIG. 2. Intensity distribution in a molecular beam deflected by gravity.

$v+dv$ is

$$\frac{dn}{n_0}=\frac{2v^2}{\alpha^3}\exp\left[-\frac{v^2}{\alpha^2}\right]d\left(\frac{v}{\alpha}\right)=x\cdot e^{-x}dx; \qquad x=\left(\frac{v}{\alpha}\right)^2. \tag{1}$$

The intensity at the displacement S is given by:

$$\frac{i}{i_0}=\frac{S_\alpha}{b}\left[\frac{S}{S_\alpha}\exp\left[-\frac{S_\alpha}{S}\right]-\frac{S-b}{S_\alpha}\exp\left[-\frac{S_\alpha}{S-b}\right]-\frac{S-2b}{S_\alpha}\exp\left[-\frac{S_\alpha}{S-2b}\right]+\frac{S-3b}{S_\alpha}\exp\left[-\frac{S_\alpha}{S-3b}\right]\right]. \tag{2}$$

This is the intensity distribution as function of the displacements which would be measured with an infinitely thin detector wire. The finite width of the detector can easily be taken into account by integration; in our Cs experiments, this correction amounted to less than 1½ percent near the maximum of the intensity distribution and was negligible elsewhere.

To compensate for the force of gravity by a magnetic force, one must produce a magnetic force on the Cs atoms of the same magnitude, but of direction opposite to the gravitational force. This can be accomplished by an electric current I underneath and parallel to the beam. At a distance d from the current, the magnetic field strength is $H=2I/d$, the inhomogeneity $\partial H/\partial r=2I/d^2$, and the force F on an atom whose component of magnetic moment in the direction of the field is μ_H is $F=\mu_H\cdot 2I/d^2$. Compensation takes place if

$$\mu_H\cdot 2I_0/d^2=mg, \tag{3}$$

* Because of a different slit form, their "effective" pressure at the oven slit might have been much lower than their measured pressure. A comparison of their results with our results is, therefore, not possible.

[3] J. B. Taylor, Zeits. f. Physik. **57**, 242 (1929).

† The value 0.177 mm given in reference 1 is incorrect.

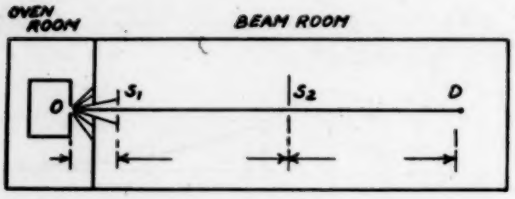

FIG. 3. General arrangement of the apparatus.

where m is the mass of the atom and g the acceleration of gravity. Because of the nuclear spin (7/2) of the Cs atom and the use of "weak" fields (not strong enough to uncouple the nuclear and electronic moments) the cesium beam is split by space quantization into 16 beams, each beam consisting of atoms with different values of μ_H. One-half of these values of μ_H result in a magnetic force in the same direction as gravity; for the other half, compensation is possible and will take place for those with the largest value of μ_H at the smallest value of I. (One-sixteenth of all the atoms will have the largest value of $\mu_H=\mu_B-\mu_N$, where μ_B is the Bohr magneton and μ_N the magnetic moment of the nucleus, which is of the order of magnitude of 1/1000 of the Bohr magneton.)

To measure I_0, the detector is placed a small distance above the position of the undeflected beam (position D'). As long as $I<I_0$, all atoms are deflected downwards and no atoms strike the detector. As soon as $I>I_0$, all the atoms with the largest magnetic moment ($\frac{1}{16}$ of the total number) will be deflected upwards and those in the proper velocity interval will strike the detector. As stated before, this method of measuring of I_0 is in principle independent of the velocity distribution in the beam. However, for practical reasons (small intensity of deflected atoms and background of scattered atoms) the intensity of the deflected atoms has to be measured at several detector positions as a function of I, and I_0 must be found by extrapolation. The extrapolation requires the knowledge of the actual velocity distribution in the beam. This is the reason for the experiments described in this paper.

To find the value of μ_B, the quantities m, g, and d in addition to I_0 have to be known. The mass*

* If Eq. (3) is multiplied by Avogadro's number N, it becomes $N\mu_B 2I_0/d^2=M_B\cdot 2I_0/d^2=Mg$, where M is the atomic weight. Therefore, we measure actually the Bohr magneton per mole, M_B, with the accuracy discussed here.

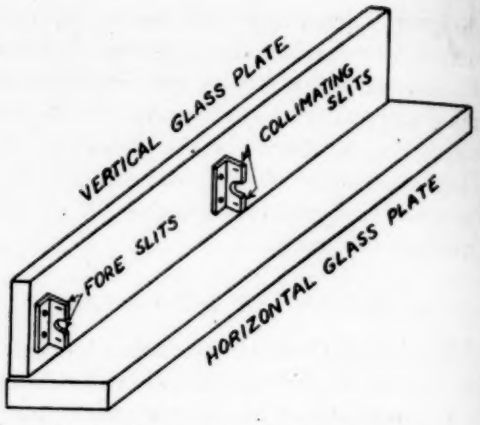

FIG. 4. Glass plates carrying slit system.

m is known to an accuracy of about one part in 10^4, and g, of course, at least to one part in 10^6. However, d is not only difficult to measure, but it is not simple to design an arrangement in which d is sufficiently defined and constant.

If we want the result to be exact to one part in 1000, the distance d between the center line of the current and the center of the beam has to be exact to one part in 2000. In our apparatus, this distance d was 2 cm. It is not possible to make this distance much larger, because then I_0 would be too large. Even with $d=2$ cm, I_0 is about 500 amp. Therefore, d has to be exact to 1/100 mm. Even with a solid rod as conductor it is not easy to have the radius exact to 1/100 mm over a length of more than 2 meters, nor is it easy to hold this rod in such a fashion that the center line is straight and parallel to the beam within this accuracy. Moreover, because of the heat developed by the current, it is necessary to provide cooling. This requires the use of a tube instead of a rod. Even in the best precision tubes obtainable, the wall thickness was not uniform to 1/100 mm.

To overcome this difficulty, we used the following arrangement: In addition to the beam above the conductor, a second beam was arranged at the same distance below. If we determine the I_0 for both beams and take the average, this value will be the I_0 for d equal to one-half of the distance between the two beams within the following accuracy: If δ is the deviation from the 2-cm distance between the beam and the center line of the conductor, then the error in the average I_0 for both beams is of the order of mag-

nitude $(\delta/d)^2$. The reason for this is that if the distance in one place is too small for one of the beams by the amount δ, it is too large by the same amount for the other beam. The distance between the two beams can be defined and measured very accurately by using a slit system in which both the source slits and the collimating slits are so designed that the edges of a single piece of metal form the lower jaw of the upper slit and the upper jaw of the lower slit. The distance between these edges was measured with a micrometer slide to a few thousandths of a mm. Even if the center line of the conductor should be misaligned by as much as 0.1 mm, the error produced hereby is only of the order of magnitude 10^{-4}. In our experiments, the error in alignment was less than 0.05 mm.

3. APPARATUS

(a) General Arrangement (Fig. 3)

The molecular beam was produced by Cs vapor streaming out from an oven slit and was defined by a foreslit S_1 and a collimating slit S_2. The introduction of a foreslit was necessary for two main reasons: First, in order to get a good vacuum in the "beam room," it was necessary to separate the latter from the "oven room." By this separation, it was possible to maintain a very good vacuum (10^{-7} mm Hg or better) in the beam room, where, because the beam was 2 m long, a long mean free path was required. In the oven room, the pressure was usually around 10^{-6} mm, but the beam length there was only 10 cm. Secondly, it was easier to maintain the correct mechanical alignment between foreslit, collimating slit, and detector than between the oven slit and the other slits, since the oven position is not exactly fixed and changes during the heating. The alignment was the most important and difficult part of the experiments. For the magnetic deflection experiments, the detector was placed only a few hundredths of a mm above the "undeflected" beam, since the intensity i of deflected atoms decreases rapidly with increasing distance. In order to obtain the compensating current I_0, this intensity i was measured as a function of the current I producing the magnetic field. During these measurements, the relative position of the slits and the detector had to remain constant to about one-thousandth of a mm. Since the distance between the two slits and between the collimating slit and the detector was one meter in each case, the demands on the rigidity of the apparatus were considerable. In the first apparatus, the detector and the slits were mounted on a self-contained metal framework which was supported inside the evacuated beam room, but this construction did not produce the necessary rigidity. We finally chose the following arrangement.

The slits and detectors were mounted on a slab of plate glass ("vertical glass plate") 204 cm long, 9.5 cm high, and 1.9 cm thick, as shown in Fig. 4. The slits were mounted horizontally. The high degree of rigidity is, therefore, required only in the vertical direction, where the glass plate was very rigid with respect to bending because of its height of 10 cm. A slight displacement of the slits in the horizontal direction (up to 1/10 mm) does not affect the accuracy. The vertical glass plate was resting on another glass plate 210 cm long, 3 cm high, and 11.5 cm wide, which was mounted horizontally. This glass plate carried a

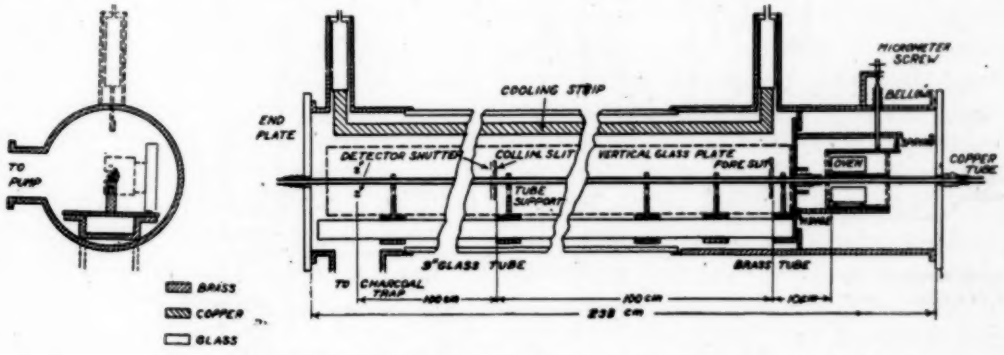

FIG. 5. (a) End view, (b) side view of apparatus.

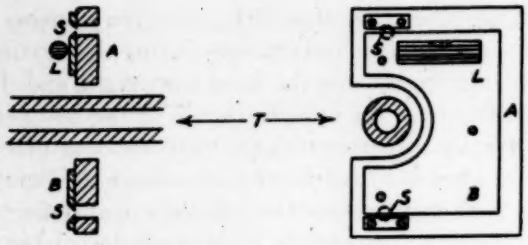

FIG. 6. (a) End view, (b) front view of slit system.

copper tube (0.947 cm O.D. and 0.47 cm I.D.) which served as conductor for the current producing the magnetic field. The horizontal glass plate was supported by two brass rings inside the vacuum envelope.

(b) Vacuum Envelope

The envelope consisted of a glass tube approximately 9″ in diameter with two brass end pieces as shown in Fig. 5. The glass tube had two side arms in the center for the shutter and for gas inlets, while the brass end pieces carried pump connections, traps, etc. It was divided by a brass plate into an oven room about 20 cm long, located inside one of the brass end pieces, and a beam room about 210 cm long. The oven room was evacuated by one large octoil diffusion pump,[4] and the beam room by two similar pumps. Large liquid-air cooled traps were arranged between pumps and apparatus. The dividing plate had a central hole for the copper tube conductor and two narrow channels for the two beams. The central hole was equipped with a bushing mounted on a sylphon bellows which permitted a slight motion of the tube but furnished a seal of high flow resistance. The channels for the beams were 20 mm long, 5 mm wide, and 1 mm high. The total flow between the two parts was about 1 liter/sec. as compared with a pumping speed of more than 50 liters/sec. for the beam room; that means that a pressure of 10^{-6} mm Hg in the oven room produced only 2×10^{-8} mm in the beam room. The ends were closed with plate glass disks of 26 cm and 1.9 cm ($\frac{3}{4}$″) thickness which were equipped with central holes of 2 cm and with bushings carried by sylphon bellows allowing a slight motion of the copper tube. All vacuum seals were made with Apiezon sealing compound *Q*.

In order to obtain the required vacuum of the order of magnitude of 10^{-8} mm, it was necessary to pump for several days. For the efficient condensation of vapors, a copper strip 4.5 cm high, 0.5 cm thick, and 185 cm long was suspended parallel to the beam from two metal Dewar vessels filled with liquid nitrogen. For the mag-

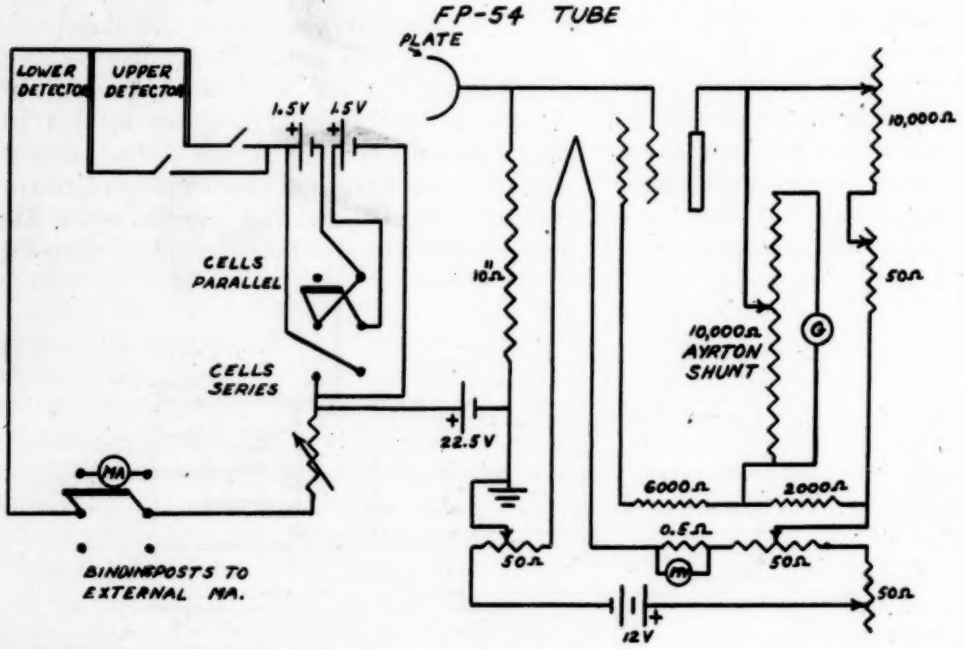

FIG. 7. Detector and amplifier circuit.

[4] L. Malter and N. Marcuvitz, Rev. Sci. Inst. 9, 92 (1938).

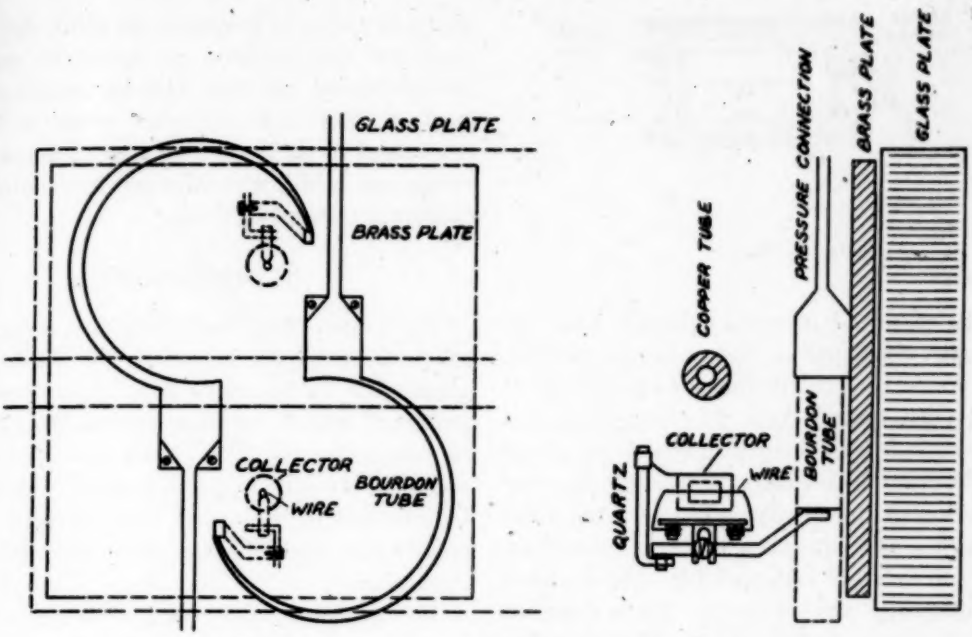

FIG. 8. (a) Side view, (b) end view of detector assembly and mounting.

netic deflection measurements, this copper strip could not be cooled, since it did not reach temperature equilibrium for several hours and changed the position of the beam during this period, apparently by changing the temperature of the slit system unevenly.

(c) Slit and Receiver System

The two foreslits and two collimating slits were each 3 mm long and the distance between the upper and lower slits was 4 cm. The upper slits were 0.022 mm and the lower slits 0.026 mm wide. They consisted of a base plate *A* and a slit plate *B* (Fig. 6). Plate *A* was made of brass and was screwed to a brass angle which in turn was fastened to the vertical glass plate by means of screws inserted through holes in the glass plate. The plates *A* and *B* had cut-outs for the copper tube *T* and plate *A* had two 3-mm holes underneath the slits, defining the "length" of the beams. The centers of the holes were 4 cm apart and in the same plane as the center of the copper tube. The upper jaw of the lower slit and the lower jaw of the upper slit were formed by the sharp edges of the center piece *B*. The distances between these edges were 3.994 cm for the foreslits and 3.991 cm for the collimating slits. They were measured with a microscope and a Gaertner micrometer slide to a few thousandths of a mm. The upper jaw of the upper slit and the lower jaw of the lower slit were formed by two small brass pieces screwed to the base plate *A*. The width of the slits was determined by two methods: First, by a direct measurement with microscope and eyepiece micrometer, and secondly, by measuring the distance of diffraction fringes with sodium light.

(d) Detector

The beam atoms were detected by the Langmuir-Taylor method, in which each Cs atom striking a hot tungsten wire is re-evaporated as an ion and collected on a negatively charged plate. The plate current gives directly the number per second of atoms striking the wire surface, or the intensity of the beam. This current was measured with a FP-54 DC amplifier circuit and a galvanometer (Fig. 7). The FP-54 tube and the grid leak resistor of $10^{11}\Omega$ were mounted inside the vacuum in a side tube (see Fig. 5) and the connecting wire between the collector plates and the grid cap of the FP-54 tube was self-supporting. Each detector consisted of a tungsten wire of 0.02-mm diameter and 15-mm length

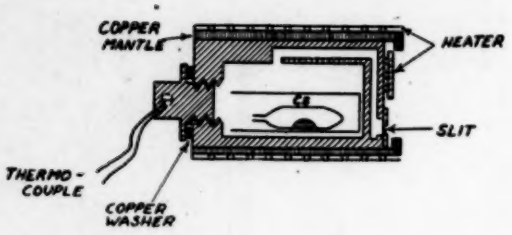

FIG. 9. Oven.

which was mounted between springs. The collector plates consisted of nickel cylinders with windows for letting the beam through and were insulated with quartz rods. The detectors had to be movable in the vertical direction by about 1.5 mm in order to measure the beam intensity as a function of the displacement. A movement which was insensitive against vibration, free from friction, and reliably reproducible was obtained in the following way (Fig. 8). Each detector assembly was attached to the tip of a Bourdon tube from a pressure gauge. This Bourdon tube was connected by a very flexible metal tube, wound in the form of a spiral, to a thin copper tube which was soldered through the vacuum mantle and led to a small glass bulb in which the pressure could be changed from vacuum to about two atmospheres. Calibration with a micrometer showed that a pressure change of 1 cm Hg produced a displacement of the detector wire by almost exactly 1/100 of a mm. The pressure was measured with a mercury manometer and adjusted with a mercury leveling bulb to about 1/10 mm. The position of the detector wire was therefore reproducible with an accuracy of 1/1000 mm, the actual displacements were measured to better than one percent.

(e) Alignment

The parallelism of foreslit, collimating slit, and detector wire was insured by making all of them horizontal. Each slit plate B was provided with a small level bulb L. Both edges of the slit plates were machined to be accurately parallel. Then a surface plate was made horizontal by means of a sensitive level. The slit plate was put on the surface plate so that the edges were horizontal, and finally the level bulbs were so adjusted that the bubble was in the center position. After mounting the slit plates on the vertical glass plate, it was only necessary to bring the bubbles back to this position in order to guarantee parallelism of the slits with an accuracy of one part in 1000. The detector wires were made horizontal with the aid of a microscope with a cross hair, which was adjusted horizontally with respect to the same level.

(f) Conductor Tube

The copper tube conducting the current for the magnetic field was mounted on the horizontal glass plate. It rested on ten "chairs" spaced 20 cm apart, which were fastened to the glass plate by brass clamps. The chairs were lined up by means of stretched tungsten wires. The tube was loosely tied to the chairs with thread so that it could move parallel to its axis to allow for thermal expansion.

The position of the slits with respect to the tube, that is of the two molecular beams, had to be invariable to a few thousands of a mm, but did not have to be known to better than one-tenth of a mm because of the two-beam arrangement. For the slit alignment, the vertical glass plate rested on two supports on the horizontal glass plate, and its position was secured with stops and springs. The slits were then adjusted so that the center lines of the beams were directly above and below and equally distant from the center line of the copper tube. This adjustment was made with the aid of a microscope and adjustable parallel blocks and had to be accurate only to one-tenth of a mm. The whole alignment was made outside the vacuum envelope. The two glass plates could be separated and reassembled without destroying the alignment.

TABLE I. Ratio of measured to calculated intensities of the cesium beam.

T °K	p mm Hg	I_{meas}/I_{calc} for $S\alpha$	$2S\alpha$	$3S\alpha$	Beam
439	1.9×10^{-2}	1.01	0.87		Lower
443	2.27	0.90	0.79	0.66	Lower
449	2.95	0.93	0.75	0.67	Upper
453	3.52	0.91	0.75		Lower
453	3.52	0.93	0.75	0.56	Lower
456	3.99	0.93	0.77	0.58	Lower
457	4.17	0.94	0.70		Lower
476	8.87	0.79	0.51	0.33	Upper
477	9.23	0.86	0.52	0.35	Lower
478	9.59	0.82	0.52	0.39	Upper

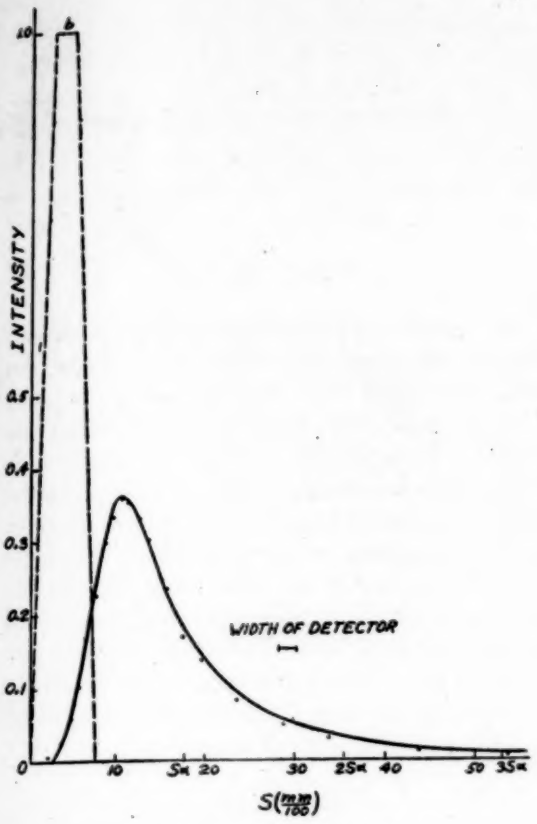

FIG. 10. Gravity deflection of a cesium beam.

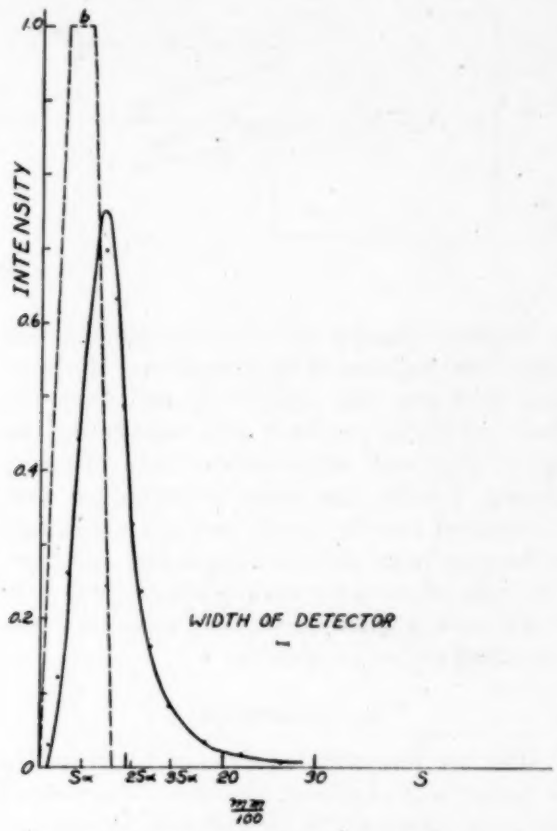

FIG. 11. Gravity deflection of a potassium beam.

(g) Ovens

The ovens were made of monel metal as shown in Fig. 9. The cesium was contained in sealed-off glass capsules holding about ½ g. They were broken inside the ovens in a nitrogen atmosphere, and the plugs were closed immediately thereafter. The ovens were mounted in a cylindrical copper tube heated by a Nichrome coil. Another small heater unit was screwed on to the front of the oven near the slit. A thermocouple was attached to the back of each oven. In a separate test, a second thermocouple was attached to the front of the oven near the slit and the temperature difference between the two thermocouples (about 5°C) was recorded for different temperatures. The ovens were mounted in a cradle which could be moved inside the vacuum in a vertical direction by means of a micrometer screw and a sylphon bellows. The cradle was also equipped with a level in order to make the oven slits horizontal. The size of the slits was 3 mm ×0.06 mm. Each oven rested on 3 pins which insured the reproducibility of its position.

(h) Assembly

After the alignment was completed, the horizontal glass plate carrying the copper tube was inserted in the vacuum apparatus. Then, the brass plate separating the beam room from the oven room was attached to the front end of this glass plate. The brass plate was equipped with a sylphon bellows and a bushing for the copper tube and with two channels for the beams. (See Fig. 5.) The cradles for the ovens were also attached to it. Next, the vertical glass plate carrying slits and detectors was slid into the vacuum envelope and moved into its correct position where it was held by two springs. Then the electrical connections between the detectors and the amplifier tube, etc. and the vacuum and pressure connections between the Bourdon tubes and the outside were made. A shutter operated

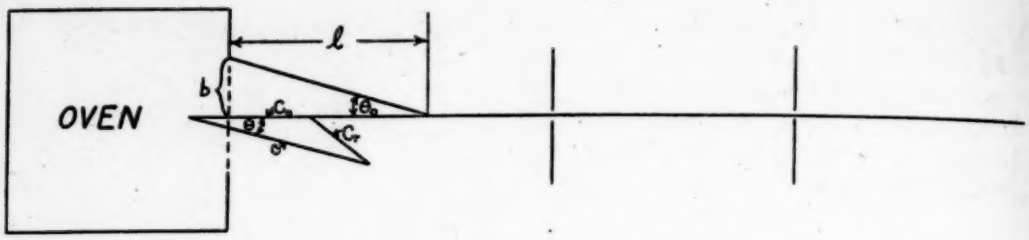

FIG. 12.

by pressure changes in a sylphon bellows was inserted through one of the side arms of the large glass tube near the collimating slit. Then the glass end plates provided with bellows for the copper tube were attached and tightened with Apiezon. Finally, the ovens were charged with Cs, inserted into the cradle through a side hole in the oven room and after the heater and thermocouple connections were made and the hole closed with a glass plate, the apparatus was evacuated as fast as possible.

4. PROCEDURE

After the necessary vacuum of 10^{-7} mm Hg or better was obtained, the oven was heated slowly to about 450°K and allowed to stabilize at a certain temperature in that region. The detector was moved to the position of maximum intensity and the oven was shifted up and down until the oven slit covered the collimating slit completely. The beam intensity was measured during this operation and the resulting "oven displacement curve" served as a check for the slit alignment. With the oven slit in the correct position, the detector was moved in the vertical direction through the beam in steps of one or several hundreds of a millimeter and the gravity deflection curve was obtained. For deflections of more than 0.1 mm from the maximum, it was necessary to move the oven slit slightly downwards with respect to the foreslit in order to keep all the slits, as well as the detector, on the parabolic trajectory of the atoms with the velocity corresponding to the detector position. The intensity of the beam was checked frequently by returning the detector to the maximum position, and a possible shifting of the position of the beam was controlled by checking a few points on the steep, upper side of the gravity deflection curve. The position of the "undeflected" beam was calculated from the measured points on the upper side of the gravity deflection curve, essentially from the position of the point at which the intensity is one-half of the maximum intensity. This distance S_i from the upper edge of the undeflected beam (Fig. 2) can be calculated for given values of b and S_α. Another method for the determination of the position of the undeflected beam, which was also used occasionally, is to send a compensating current I_0 through the copper conductor tube. The magnetic field produced by this current will bring $\frac{1}{16}$ of the atoms into the position of the undeflected beam, which can thus be measured out directly.

5. RESULTS

Experiments were carried out with potassium and cesium at different oven temperatures. The gravity displacement curves obtained agreed in general with the calculated curves. Figure 10 shows the results for a cesium beam, Fig. 11 for a potassium beam. The curves are calculated, the dots show the measured points. For larger deflections, *viz.*, $S\alpha$, $2S\alpha$, and $3S\alpha$, the measured intensity values were definitely lower than the calculated values. This deficiency increased with increasing deflection (slower atoms) and also with increasing oven temperature (pressure).

TABLE II. Values of $F(\gamma)$.

$\gamma = c/c_0$	$\gamma' = c_0/c$	$F(\gamma)$	$F(\gamma)^*$	$\frac{F(\gamma)-F(\gamma)^*}{F(\gamma)}$
0	∞	0.5000	0.5000	0
0.250	4	0.4080	0.4045	0.87%
0.333	3	0.3804	0.3754	1.31%
0.500	2	0.3322	0.3248	2.24%
0.667	1.5	0.2952	0.2883	2.34%
0.833	1.2	0.2737	0.2703	1.24%
0.909	1.1	0.2711	0.2697	0.51%
1	1	0.2761	0.2761	0
1.1	0.909	0.2982	0.2967	0.51%
1.2	0.833	0.3285	0.3244	1.24%
1.5	0.667	0.4428	0.4324	2.34%
2.0	0.500	0.6645	0.6495	2.24%
3.0	0.333	1.1412	1.1261	1.31%
4.0	0.250	1.6320	1.6179	0.87%

Table 1 shows the deficiency; expressed as the ratio of the measured and calculated intensities I_{meas}/I_{calc} for the positions $S\alpha$, $2S\alpha$, and $3S\alpha$ for different experiments with cesium. $S\alpha$, $2S\alpha$ and $3S\alpha$ are measured from the center of the undeflected beam (not from the upper edge as in Fig. 2).

6. DISCUSSION

The experiments serve as a demonstration that individual atoms follow the laws of free fall in the same way as other pieces of matter. Moreover, they permit a more accurate determination of the velocity distribution in molecular rays than those carried out earlier. The knowledge of this distribution is of great importance for many molecular beam experiments. It has usually been assumed that the Maxwellian distribution law is valid as long as the mean free path of the molecules in the oven is several times as large as the width of the oven slit. These experiments show, however, that there is a considerable deficiency of slow molecule seven at much lower pressures. This deficiency is probably caused by collisions in the immediate vicinity of the oven slit (see appendix).

7. APPENDIX

(a) Calculation of the Distortion of the Velocity Distribution

To estimate the order of magnitude of the distortion in the velocity distribution in the beam through collisions in the neighborhood of the oven slit ("cloud"), we calculate this effect under the following simplifying assumptions: The number of collisions is calculated for rigid spheres on the basis of the classical kinetic theory. The cross section of the spheres is taken from the experimental determination of the mean free path. It is assumed that every collision throws the beam molecule out of the beam. This assumption is certainly justified in our case where a deflection as small as 10^{-3} radian (1/100 mm to 1 m) removes the molecule from the beam. Furthermore, we assume that the density of the molecules inside the oven is uniform and that it and the velocity distribution of the molecules inside the oven are undisturbed up to the oven slit. We also neglect the number of molecules thrown into the beam by collisions outside the oven.* Finally, we consider the case of a circular oven opening and regard the beam, which is defined by the foreslit and the collimating slit, as emerging from the center of the oven opening perpendicular to it and with a cross section which is small compared to the area of the oven opening.

TABLE III. Values of $\bar{F}$ as a function of c_0/α.

$x_0=c_0/\alpha$	$S/S\alpha=x_0^{-2}$	$\bar{F}$
3	1/9	0.3664
2	¼	0.3261
$\sqrt{3}$	⅓	0.3172
$\sqrt{2.5}$	1/2.5	0.3148
$\sqrt{2}$	½	0.3167
1.3	1/1.69	0.3225
1.2	1/1.44	0.3320
1	1	0.3707
$1/\sqrt{2}$	2	0.5232
$1/\sqrt{3}$	3	0.6690
½	4	0.8018
1/2.5	6¼	1.0624
⅓	9	1.3319
¼	16	1.8827

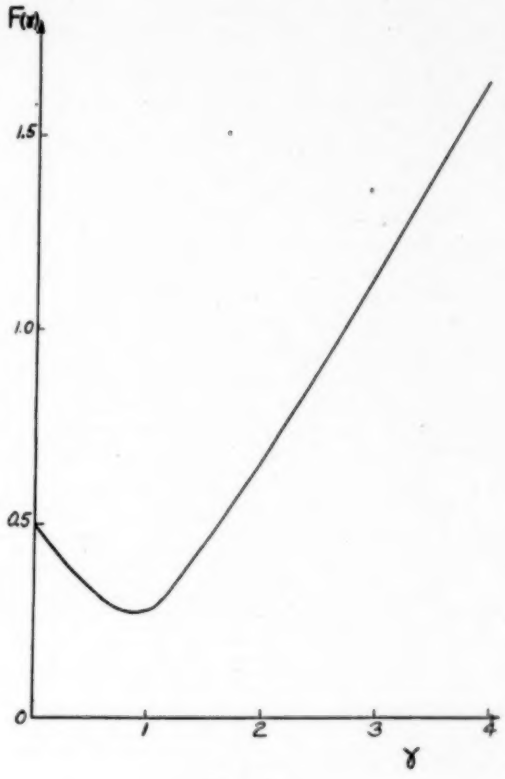

FIG. 13.

Let l be the distance from the oven hole (see Fig. 12), b the radius of the oven hole, n the number of molecules with the velocity c_0 passing the cross section of the beam at l per second, and N the number of molecules per cm³ in the oven with the velocity c. We consider first the case $c>c_0$. The angle between c and c_0 may be θ. Therefore the relative velocity is $c_r=(c^2+c_0^2-2cc_0\cos\theta)^{\frac{1}{2}}$. The number of collisions at l during the time dt is:

$$dn=ndl\cdot\pi\sigma^2N\int_0^{\theta_0}c_r\tfrac{1}{2}\sin\theta d\theta \qquad (4)$$

where $\pi\sigma^2$ is the collision cross section and $\tan\theta_0=b/l$. The decrease of n in traversing the distance $dl=c_0dt$ is therefore

* On the basis of some rough numerical estimates we believe that this assumption should not change the order of magnitude of our results.

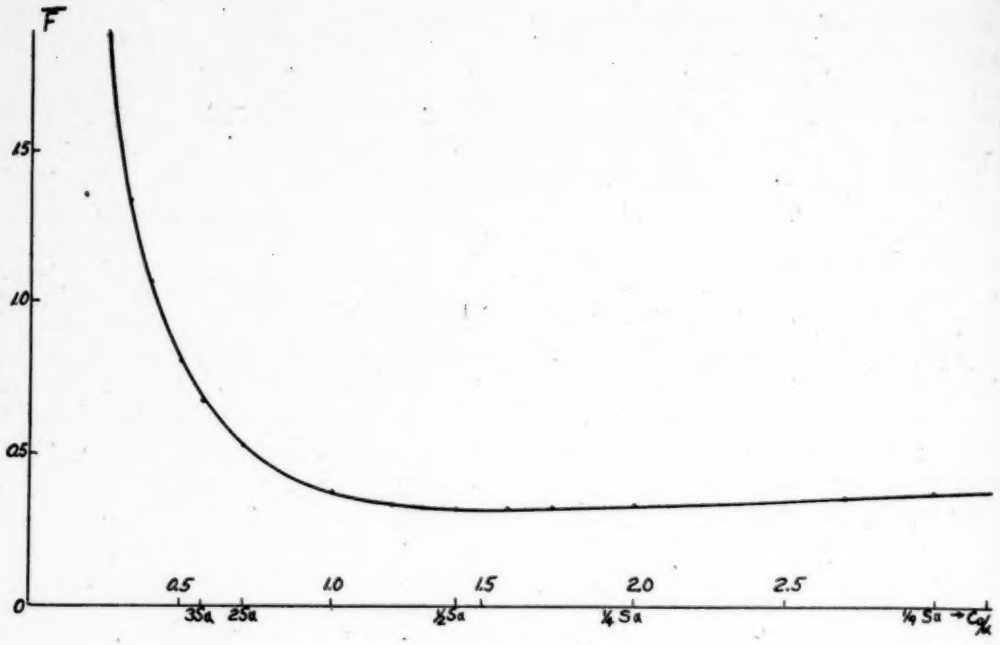

FIG. 14.

given by:

$$-d\ln n/dl=\pi\sigma^2(N/c_0)\int_0^{\theta_0}c_r\tfrac{1}{2}\sin\theta d\theta$$

$$=\pi\sigma^2(N/c_0)\int_{c_{r(0)}}^{c_{r(\theta_0)}}(c_r^2/2cc_0)dc_r$$

$$=[\pi\sigma^2N/(6cc_0)][c_{r(\theta_0)}{}^3-c_{r(0)}{}^3] \quad (5)$$

since $2c_rdc_r=2cc_0d\cos\theta$. Considering θ_0 as function of l ($\tan\theta_0=b/l$), and setting $(1/6cc_0)[c_{r(\theta_0)}{}^3-c_{r(0)}{}^3]=f(l)$ we get

$$n/n_0=\exp[-\pi\sigma^2N\int_0^{\infty}f(l)dl] \quad (6)$$

where n_0 is the number of beam molecules with the velocity c_0 leaving the oven slit per second. We are allowed to integrate to $l=\infty$ because at larger distances ($l\gg b$) the number of collisions is negligible. Substituting again θ_0 for l, setting $dl=(-b/\sin^2\theta_0)d\theta_0$, we obtain finally:

$$n/n_0=\exp[-\pi\sigma^2Nb\int_0^{\pi/2}f(\theta_0)d\theta_0] \quad (6a)$$

with

$$f(\theta_0)=[(c^2+c_0^2-2cc_0\cos\theta_0)^{\frac{1}{2}}-(c-c_0)^3]/6cc_0\sin^2\theta_0.$$

For the case $c_0>c$ we have to replace $(c-c_0)$ by (c_0-c).

The numerical value of the integral

$$\int_0^{\pi/2}f(\theta_0)d\theta_0=F(\gamma)$$

depends only on $\gamma=c/c_0$. For $\gamma>1$, we have:

$$f(\theta_0)=[(\gamma^2+1-2\gamma\cos\theta_0)^{\frac{1}{2}}-(\gamma-1)^3]/6\gamma\sin^2\theta_0 \quad (7)$$

for $\gamma<1$ with $\gamma'=1/\gamma=c_0/c>1$;

$$f(\theta_0)=[(\gamma'^2+1-2\gamma'\cos\theta_0)^{\frac{1}{2}}-(\gamma'-1)^3]/6\gamma'^2\sin^2\theta_0 \quad (7a)$$
$$F(\gamma)=F(\gamma')/\gamma'$$

and for $\gamma=1$,

$$f(\theta_0)=(2-2\cos\theta_0)^{\frac{1}{2}}/6\sin^2\theta_0. \quad (7b)$$

Limiting expressions are:

$\gamma\gg1$ (slow beam molecules) $F(\gamma)=\frac{1}{2}\gamma-\pi/8=\frac{1}{2}\gamma-0.3927$
$\gamma\ll1$ (fast beam molecules) $F(\gamma)=\frac{1}{2}-\pi\gamma/8=\frac{1}{2}-0.3927\gamma$.

Table II and Fig. 13 give some values of $F(\gamma)$.* The weakening of the beam molecules with the velocity c_0 by collisions with oven molecules of the velocity c is therefore given by:

$$n/n_0=\exp(-\pi\sigma^2bNF);\quad F=F(\gamma)=F(c/c_0), \quad (8)$$

where N is the number of oven molecules per cm³ with the velocity c. If we take c as the average velocity and N as the total number N_0 of molecules per cm³ we get already a fair approximation, especially for the case of slow beam molecules. It is, however, not difficult to take into account the velocity distribution of the oven molecules. We simply replace N according to Maxwell by

$$dN=N_0\frac{4}{\sqrt{\pi}}\exp[-c^2/\alpha^2](c^3/\alpha^3)d(c/\alpha).$$

---

* $F(\gamma)$ was calculated by numerical integration and by the formula

$$F(\gamma)=\tfrac{1}{3}(\gamma^2+1)^{\frac{1}{2}}+[(\gamma+1)/6\gamma](\gamma-1)^2\delta\mathbf{F}$$
$$-[(\gamma+1)/6\gamma](\gamma^2+1)\delta\mathbf{E},$$

where

$$\delta\mathbf{F}=\mathbf{F}(\kappa,\pi/2)-\mathbf{F}(\kappa,\pi/4)$$
$$\delta\mathbf{E}=\mathbf{E}(\kappa,\pi/2)-\mathbf{E}(\kappa,\pi/4);$$

and

$$\kappa^2=4\gamma/(\gamma+1)^2.$$

$\mathbf{F}$ and $\mathbf{E}$ are the elliptic integrals of the first and the second kind.

Since the e-factors of the molecules with different velocities multiply, we get:

$$n/n_0=\prod_{c=0}^{c=\infty}\exp[-\pi\sigma^2 bFdN]=\exp\left[-\pi\sigma^2 b\sum_{c=0}^{\infty}FdN\right]$$
$$=\exp[-\pi\sigma^2 bN_0\bar{F}] \quad (9)$$

where

$$\bar{F}=\int_0^\infty F\frac{4}{\sqrt{\pi}}\exp[-c^2/\alpha^2](c^2/\alpha^2)d(c/\alpha).$$

To evaluate $\bar{F}$, the following approximation formula F^* was used for F:

$$\text{For } \gamma>1;\quad F^*=\frac{1}{2}\gamma-\frac{\pi}{8}+\frac{0.16884}{\gamma^2};$$

$$\text{For } \gamma<1;\quad F^*=\frac{1}{2}-\frac{\pi}{8}\gamma+0.16884\gamma^3;$$

$$\gamma=c/c_0.$$

This formula gives the right limiting expressions for small and large values of γ. The factor 0.16884 of the third term is so chosen that the value of F for $\gamma=1$ is correct. In the intervals $0<\gamma<1$ and $1<\gamma<\infty$, the largest deviation from the correct value is less than $2\frac{1}{2}\%$ (compare Table II).

The resulting values of $\bar{F}$ as function of c_0/α are given in Table III and Fig. 14.

(b) Comparison with the Experiments

Our theoretical formula gives the "weakening factor" Φ

$$\Phi=n/n_0\exp[-\pi\sigma^2 Nb\bar{F}].$$

The cross section for collisions of Cs atoms with Cs atoms was measured by Foner:*

$$\pi\sigma^2=2.35\times10^{-13}\text{ cm}^2.$$

The number N of Cs atoms per cm³ in the oven is:

$$N=p/kT=2.1\times10^{14}\times p',$$

where p' is the pressure of the Cs vapor in the oven in units of 10^{-2} mm Hg. For the temperature we took an average value $T=460°$K.

The width of the oven slit in our experiments was 5×10^{-3} cm. In our theoretical equation, b is the radius of a circular oven opening. If we set $b=5\times10^{-3}$ cm we should get the right order of magnitude.

With these numerical values we have:

$$\Phi=(n/n_0)\exp[-0.25p'\bar{F}].$$

To compare our experimental results with this formula we have to consider that our I_{meas}/I_{calc} (see Table I) refers to an I_{calc} which sets arbitrarily $\Phi=1$ in the neighborhood of the maximum of the deflection curve. In reality we know only that Φ is approximately constant in this region. This follows directly from our experimental result that in the neighborhood of the maximum the shape of the measured intensity curve agrees with the shape calculated from the modified Maxwellian distribution. It also agrees with our theoretical result for $\bar{F}$ (see Fig. 14). We assume therefore that our I_{calc} corresponds to the minimum value of $\bar{F}=0.32$. If we call the weakening factor in this region Φ_0, we have:

$$\Phi_0=\exp[-0.25p'\times0.32]=\exp[-0.080p'].$$

For the deflection $S\alpha$, the velocity of the beam molecules is α, and from our curve for $\bar{F}$ we take $\bar{F}=0.37$, and finally obtain

$$\Phi_{S\alpha}=\exp[-0.25\times p'\times0.37]=\exp[-0.0925p'].$$

Hence, for the deflection $S\alpha$, our I_{meas}/I_{calc} is

$$I_{meas}/I_{calc}=\Phi_{S\alpha}/\Phi_0=\exp[-0.0125p'].$$

Correspondingly we have for the deflections $2S\alpha$ and $3S\alpha$:

$2S\alpha$: $c_0=\alpha/\sqrt{2}$; $\bar{F}(1/\sqrt{2})=0.52$;
$I_{meas}/I_{calc}=\Phi_{2S\alpha}/\Phi_0=\exp[-0.050p']$

$3S\alpha$: $c_0=\alpha/\sqrt{3}$; $F(1/\sqrt{3})=0.67$;
$I_{meas}/I_{calc}=\Phi_{3S\alpha}/\Phi_0=\exp[-0.0875p']$.

The following Table IV gives some calculated values of I_{meas}/I_{calc}:

TABLE IV. Calculated values of I_{meas}/I_{calc}.

p'	$S\alpha$	$2S\alpha$	$3S\alpha$
2	0.98	0.90	0.84
4	0.95	0.82	0.70
8	0.90	0.67	0.50

A comparison with the measured values in Table I shows agreement in the dependence on pressure and velocity as well as in the order of magnitude of the numerical values. Generally, the measured deviations are somewhat larger than the calculated ones. That may be due to additional collisions, either with foreign gas molecules in the oven room, or directly at the oven slit with foreign gas molecules originating in the oven. The fluctuations in the measurements corroborate this explanation. The discrepancy could also be due, at least in part, to the choice of b. A slightly larger value of b ($7\frac{1}{2}\times10^{-3}$) would give agreement within the limits of error of the measurements. Considering the number of serious simplifications made in the calculations we cannot expect a better agreement than in the order of magnitude.

* S. N. Foner, Thesis, Carnegie Institute of Technology, Pittsburgh, 1945 (see also the following paper).

The Mean Free Paths of Cesium Atoms in Helium, Nitrogen, and Cesium Vapor

I. ESTERMANN, S. N. FONER,* AND O. STERN**
Research Laboratory of Molecular Physics, Carnegie Institute of Technology, Pittsburgh, Pennsylvania
(Received November 29, 1946)

The mean free paths of cesium atoms in helium, nitrogen, and cesium vapor were measured with a molecular beam apparatus permitting the measurement of scattering deflections of about 5 seconds of arc. Utilizing the free fall of the beam atoms, the variation of the mean free path with the velocity of the beam atoms could be determined directly. This variation was found to be in agreement with the equations calculated on the basis of classical theory treating the atoms as elastic spheres. The measured values of the sums of the effective atomic radii are 12.0×10^{-8} cm for Cs-He, 17.2×10^{-8} for Cs-N_2, and 27.3×10^{-8} cm for Cs-Cs collisions. These values correspond to mean free paths of 2.1 meters in He, 2.2 meters in N_2, and 1.36 meters in Cs-vapor of 10^{-6}-mm Hg pressure for cesium atoms with a velocity corresponding to the maximum intensity of the gravity deflection curve.

AS pointed out in a previous paper,[1] the deficiency of slow atoms in a molecular beam of Cs-atoms can be explained as arising from the scattering of the beam atoms in the immediate vicinity of the oven slit. For a quantitative estimate of the effect of this scattering, it is necessary to know the effective cross section for the Cs-Cs collision. The present investigation was undertaken to measure the mean free path of cesium atoms in cesium vapor, helium, and nitrogen, and to determine the velocity dependence of the mean free path.

1. THEORY

In the quantum-mechanical treatment of scattering, Massey and Mohr[2] consider a beam of atoms with the DeBroglie wave-length $\lambda=h/Mv$ incident upon an atom which is at rest in the coordinate system. The scattering cross section Q is defined as

$$Q=2\pi\int_0^\pi I(\theta)\sin\theta d\theta, \qquad (1)$$

where $I(\theta)$ is the scattering intensity per unit solid angle of the beam atoms scattered through an angle θ from the direction of the incident beam. For a hard sphere model, Massey and Mohr[2] have given as a rough approximation the angular dependence of $I(\theta)$ shown in Fig. 1 as curve A. Here r_0 is the sum of the "classical" atomic radii and $k=2\pi/\lambda$, where $\lambda=h/Mv_R$ is

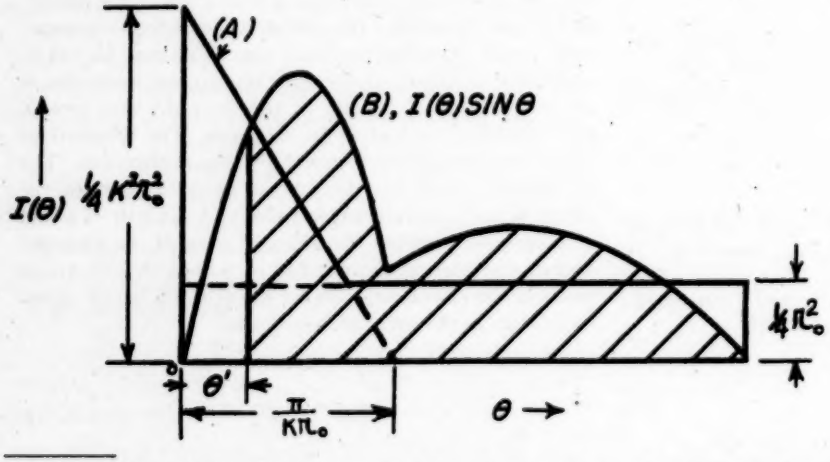

FIG. 1. Scattering intensity as function of angle.

* Now at Applied Physics Laboratory, Johns Hopkins University, Silver Spring, Maryland.
** Now in Berkeley, California.
[1] I. Estermann, O. C. Simpson, and O. Stern, Phys. Rev. 71, 238 (1947); referred to as I.
[2] H. S. W. Massey and C. B O. Mohr, Proc. Roy. Soc. 141, 454 (1933).

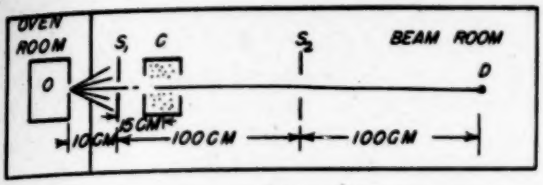

FIG. 2. Schematic diagram of apparatus.

the DeBroglie wave-length associated with the system; $M=m_1m_2/(m_1+m_2)$ being the reduced mass and v_R the relative velocity of the atoms. The large increase in scattering intensity for small angles makes the cross section Q about twice the classical value πr_0^2. Curve B in Fig. 1 represents $I(\theta)\sin\theta$. The experimentally measured cross section depends on the resolving power of the apparatus. If a scattering corresponding to an angle θ' can be detected, the error made in measuring the total scattering cross section is found by comparing the unshaded area under curve B in Fig. 1 with the total area. The resolving power necessary to get meaningful results is reached if an increase in the resolving power will not materially increase the measured cross section. In our experiments, this condition was fulfilled.

If an attractive potential of the form $V=-C/r^S$ exists, the total cross section is given by[3]

$$Q=[\pi(2S-3)/(S-2)]f^{2/(S-1)}(C/k)^{2/(S-1)}, \quad (2)$$

where k is again $2\pi/\lambda=2\pi Mv_R/h$ and f is a known function of s. Assuming dipole-dipole Van der Waals forces with a potential $V=-C/r^6$, Q takes the form

$$Q=Bv_R^{-2/5}, \quad (3)$$

where B is a constant, so that the cross section varies as the inverse $\frac{2}{5}$ power of the relative velocity. The expected dependence of Q on the relative velocity is therefore a slowly varying function, with the result that the variation of Q with the beam atom velocity is still smaller, so that for the range of velocities encountered in the experiments we can consider Q a constant, especially in view of the accuracy of the measurements and the degree of monochromization of the beam.

[3] H. S. W. Massey and C. B. O. Mohr, Proc. Roy. Soc. 144, 188 (1934).

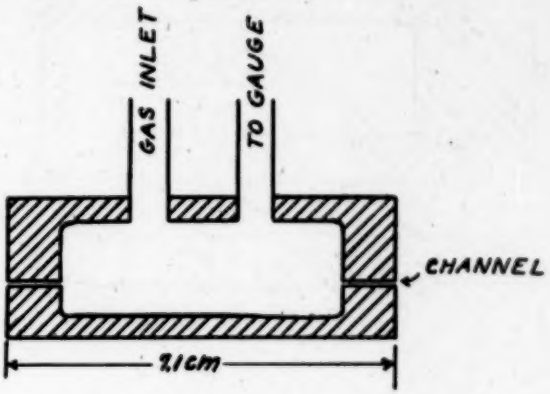

FIG. 3. Scattering chamber for nitrogen and helium.

2. EXPERIMENTAL ARRANGEMENT

The mean free path was determined by measuring the weakening of a molecular beam of cesium atoms passing through a scattering chamber filled with helium, nitrogen, or cesium vapor. The apparatus used for these experiments was the one described in paper I, with a scattering chamber C mounted between the foreslit and the collimating slit of the upper beam, as shown in Fig. 2. For helium and nitrogen as scattering gases, the scattering chamber was made of two brass pieces (Fig. 3). The lower piece had a milled groove 0.4 mm deep and 5 mm wide, which together with the upper piece formed two channels 0.4 mm high, 5 mm wide, and 1 cm long through which the beam passed. The large flow resistance of these channels and the high pumping speed in the rest of the apparatus permitted the maintenance of a pressure ratio of about 1000 to 1 between the chamber and the apparatus. The gas was fed into the chamber through a flexible pipe line from a 5-liter flask outside the apparatus. The pressure in the chamber was controlled by a sensitive needle valve and measured with an ionization gauge connected to the chamber through another tube. A by-pass permitted the outgassing of the ionization gauge.

For the cesium-cesium experiments, the scattering chamber had to be made of a metal not affected by cesium. Monel metal was found to be satisfactory. As shown in Fig. 4, this scattering chamber was machined from a solid metal block. The scattering took place in a tube T 3.5 cm long and 0.476 cm in diameter through which

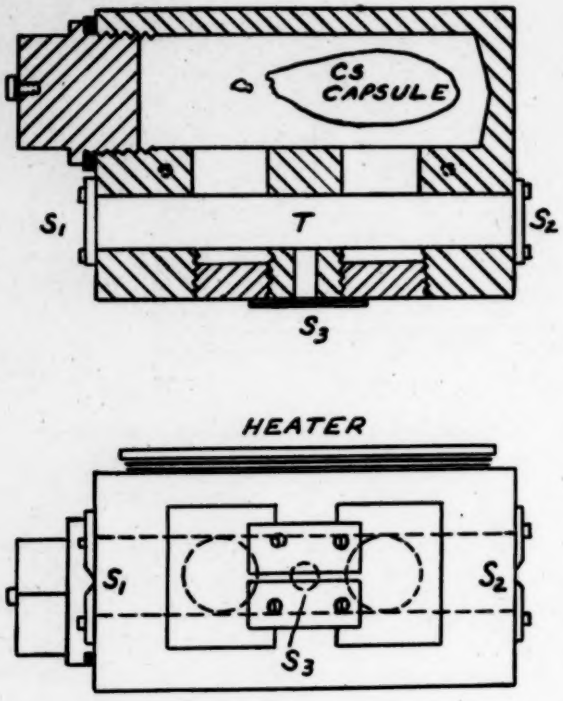

FIG. 4. Scattering chamber for cesium vapor.

the beam passed. The cesium vapor was supplied from a cesium capsule in the second part of the scattering chamber, which was connected to the first by two $\frac{1}{4}$-inch holes. Since the cesium vapor escaping from the scattering chamber was quickly condensed at the cooled copper strip (see Fig. 5 of paper I), it was possible to use slits S_1 and S_2 instead of channels at the ends of the scattering tube without materially increasing the pressure in the apparatus. A Nichrome ribbon heater was fastened to the top of the chamber and a thermocouple to the plug. For better thermal insulation, the chamber was mounted on a glass plate and supported by brass angles attached to the vertical glass plate (see Fig. 4 of paper I), which also carried the slit and detector system.

It was found that the Cs pressure in the scattering chamber could not be calculated reliably from the temperature measured by the thermocouple. In order to measure the pressure of the scattering Cs vapor, a third slit S_3 was attached to the side of the scattering tube and an auxiliary hot tungsten wire detector was mounted 2.3 cm away from the side slit. A collimating slit and a magnetically operated shutter were mounted between this detector and the side slit. From the intensity of the cesium beam striking the side detector and the geometry of the arrangement, the pressure of Cs atoms in the scattering tube could be calculated. It was also calculated from the intensity of the Cs beam which originated from the scattering chamber. This intensity was measured with the beam detector after displacing the oven sufficiently as to cut out all the atoms originating in the oven. Because of the efflux of cesium vapor through the slits at the ends of the scattering tube, the pressure inside the chamber was not quite uniform. An appropriate correction for this effect was applied in the calculations.

3. RESOLVING POWER

The resolving power of the apparatus follows from the geometry of the molecular beam. The source slit (fore slit) and collimating slit were both 0.02 mm wide and 100 cm apart. The detecting wire had a diameter of 0.02 mm and was located 100 cm beyond the collimating slit. The distance between the middle of the scattering chamber and the collimating slit was 85 cm. Hence, if the direction of the velocity vector of a beam atom passing through the scattering chamber is changed by an angle of 2.4×10^{-5} radian or 5 seconds of arc (0.02 mm in 85 cm), the atom cannot pass through the collimating slit and is, therefore, measured as "scattered." The actual resolution will be slightly lower since atoms can be scattered into the beam from the 0.1-mm broad beam wedge inside the scattering chamber, which is formed by the oven slit and the fore slit.

In the theory of scattering, the angle of scattering is the angle through which the relative velocity vector v_R is turned. What is measured experimentally is the deviation of the beam atom. In the case of small angular deviations, this is roughly half the angle through which the relative velocity vector is turned.[4]

By using the hard sphere model and the Massey and Mohr approximation (Fig. 1) for Cs-Cs scattering, the angle $\theta_0=\pi/kr_0$ at which quantum scattering begins to make itself noticed, turns out to be 0.3°, if the effective radius for the Cs atom is taken from our experi-

[4] W. H. Mais, Phys. Rev. 45, 773 (1934).

ments as equal to approximately 10×10^{-8} cm. This means that beam atom deflections of less than 0.15° will show "quantum scattering" (see Fig. 1). Since the apparatus has a resolving power 100 times larger than this, the interpretation of the measurements seems justified, even allowing for the fact that there is no *a priori* reason for assuming that large atoms like Cs will behave in collisions like hard spheres, and that, therefore, the actual form of the angular function $I(\theta)$ is not known.

4. PROCEDURE

(a) Helium and Nitrogen Experiments

With the scattering chamber evacuated, the beam was stabilized in the manner described in paper I, and the gravity deflection curve of the unscattered beam was measured out. Then, a certain gas pressure was introduced into the scattering chamber. The measurement of the gravity curve was repeated for different scattering pressures between 8 and 33×10^{-6} mm Hg.

(b) Cesium Experiments

For the cesium experiments, the scattering chamber was charged with a Cs capsule which was broken in a N_2 atmosphere before assembling the apparatus. After a vacuum of better than 10^{-6} mm was obtained, both the oven and the scattering chamber were heated slowly to a temperature somewhat higher than the operating temperatures and outgassed for several hours. Then the scattering chamber was allowed to cool off to room temperature and the unscattered beam was measured out. The scattering chamber was then heated again until the beam intensity was cut to $\frac{1}{2}$ or $\frac{1}{3}$ of its original value; and after stabilization, the gravity curve was measured again. Since part of the intensity measured by the beam detector came from cesium atoms originating in the scattering chamber, the oven was later displaced sufficiently as to cut out all the atoms originating from the oven, and the residual intensity was measured out. These measurements served as a second determination of the pressure in the scattering chamber. In some experiments, a check of the original beam intensity was made by letting the scattering chamber cool off again to room temperature.

5. RESULTS

(a) Helium and Nitrogen Scattering

Gravity deflection curves obtained in the helium and nitrogen experiments are shown in

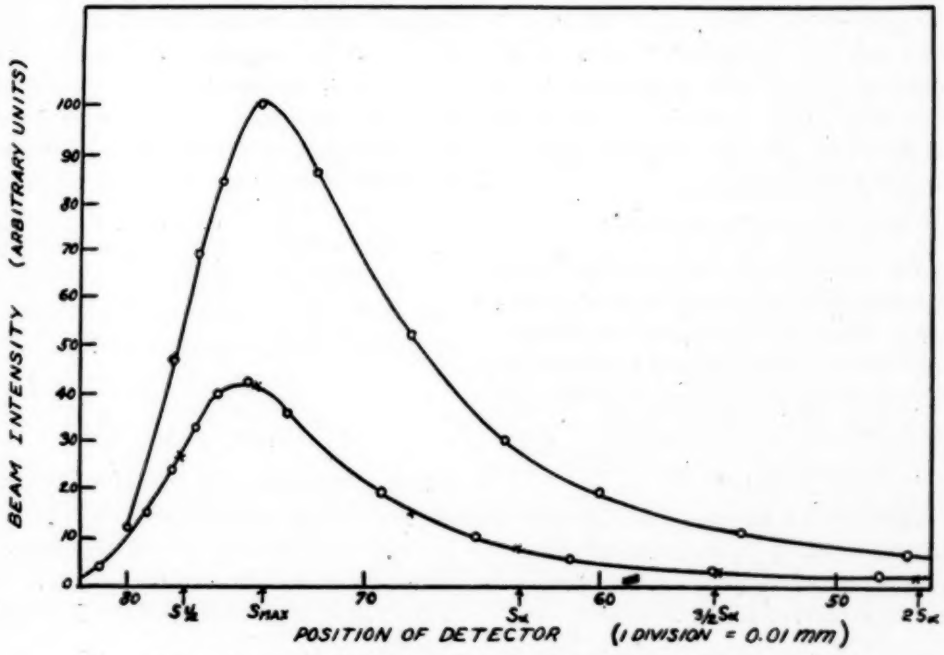

FIG. 5. Intensity distribution in cesium beam scattered by helium (o measured points, x calculated points).

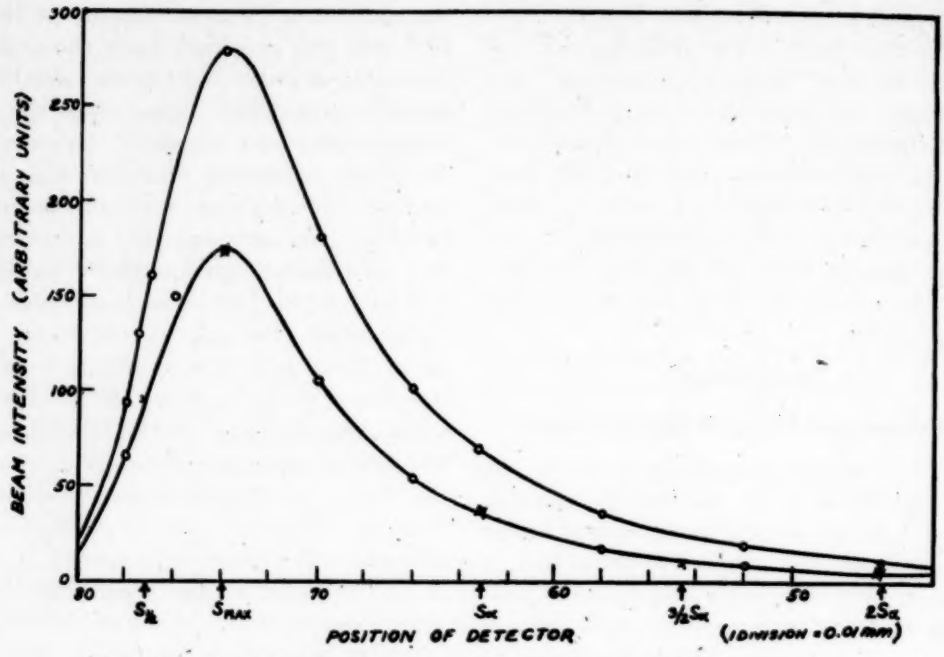

FIG. 6. Intensity distribution in cesium beam scattered by nitrogen (o measured points, x calculated points).

Figs. 5 and 6, respectively. In both figures the higher intensity curve represents the "unscattered" beam. Similar curves were obtained with helium pressures of 8.5×10^{-6} mm and 17.9×10^{-6} mm Hg, and a nitrogen pressure of 18.0×10^{-6} mm Hg.

The points marked "calculated" were found in the following way: The weakening of a homogeneous beam (i.e., a beam in which all atoms have the same velocity) from an intensity I_0 to an intensity I is given by

$$I=I_0\exp(-l/\lambda)=I_0\exp(-lp/\lambda_0), \qquad (4)$$

where p is the scattering pressure, l the length of the scattering chamber, λ the mean free path, and $\lambda_0=\lambda/p$ a constant independent of pressure. If we consider the actual beam as a superposition of a number of homogeneous beams of different velocities c, we can write

$$I^c=I_0^c\exp(-lp/\lambda_0^c), \qquad (4a)$$

where the superscript c denotes that the symbol pertains to the velocity c. If the weakening of the beam by a certain scattering pressure p is known for two velocities c and c', then

$$\frac{\lambda^{c'}}{\lambda^c}=\frac{\ln(I_0^c/I^c)}{\ln(I_0^{c'}/I^{c'})}. \qquad (5)$$

Because of the finite width of the slits, all the atoms striking the detector at a given deflection position S do not have the same velocity. Calculations given elsewhere[5] show, however, that the average of the free paths of all these atoms does not deviate appreciably from the free path of the atoms reaching the position S and originating from the center of the undeflected beam. We may, therefore, define an effective velocity c corresponding to every detector position S, and, since the deflections are inversely proportional to c^2; $c^2/\alpha^2=S_\alpha/S$, where α refers to the most probable velocity of the beam atoms, and S_α to the corresponding deflection. Comparing all the free paths with the free path of the atoms in the maximum of the gravity curve, we get

$$\frac{\lambda_0^m}{\lambda_0^c}=\frac{\ln(I_0^c/I^c)}{\ln(I_0^m/I^m)}, \qquad (5a)$$

where the superscript m, refers to the atoms in the maximum of the gravity curve. If the relationship between λ_0^c and λ_0^m is known, the scattered curve can be calculated from the unscattered curve if one point of the scattered curve is known.

[5] S. N. Foner, Thesis, Carnegie Institute of Technology, 1945.

TABLE I. Mean free paths for cesium atoms in helium and nitrogen.

S (10^{-2} mm)	S_a/S	c/α	Scattering gas: Helium I^e/I_0^m	Helium λ_0^e/λ_0^m	Nitrogen I^e/I_0^m	Nitrogen λ_0^e/λ_0^m
3.0	5.70	2.38	0.268	1.460	0.346	1.212
6.4	2.67	1.63	0.415	1.000	0.620	1.000
12.8	1.34	1.16	0.148	0.711		
14.1	1.00	1.00	0.069	0.613	0.125	0.700
22.7	0.67	0.82	0.019	0.503	0.040	0.586
28.2	0.50	0.71	0.007	0.435	0.017	0.519

For helium scattering, the cesium atoms traversing the scattering chamber are essentially stationary targets for the much faster He atoms, hence the probability of a cesium atom being scattered out of the beam is simply proportional to the time spent in the chamber $t=l/c$. Therefore, $\lambda_0^m/\lambda_0^c=c^m/c$, and the intensity distribution in the scattered beam is given by

$$\ln(I_0^c/I^c)=(c^m/c)\ln(I_0^m/I^m)$$
$$=(S_a/S^m)^{\frac{1}{2}}/(c/\alpha)\ln(I_0^m/I^m). \quad (6)$$

For the collisions between cesium atoms and nitrogen molecules, the relationship between free path and velocity is more complicated. Calculations for this case are given elsewhere.[5-7]

The absolute value of the mean free path of the cesium atoms is given for those atoms which make up the maximum of the gravity curve, since there the measurements are most accurate. For these atoms, and a scattering pressure of 10^{-6} mm Hg, the mean free path is

$\lambda_0^m=209$ cm/10^{-6} mm Hg for cesium in helium,

and

$\lambda_0^m=216$ cm/10^{-6} mm Hg for cesium in nitrogen.

The calculated values for the intensity I^e in the scattered beam as function of the deflection S are indicated on Figs. 5 and 6. They are also given in Table I together with the relative values for the mean free path for cesium atoms of different velocities in helium and nitrogen.

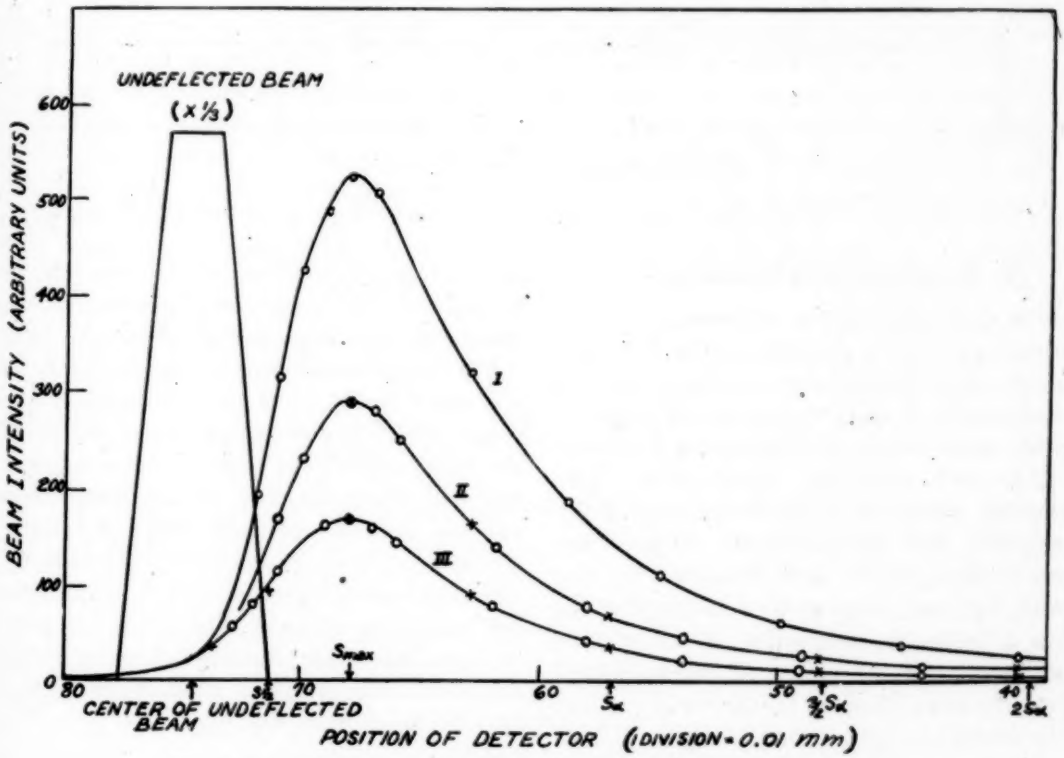

FIG. 7. Intensity distribution in cesium beam scattered by cesium vapor (0 measured points, x calculated points).

[6] O. E. Meyer, *Kinetic Theory of Gases* (London, 1899).
[7] J. H. Jeans, *Dynamic Theory of Gases* (Cambridge, 1916) second edition.

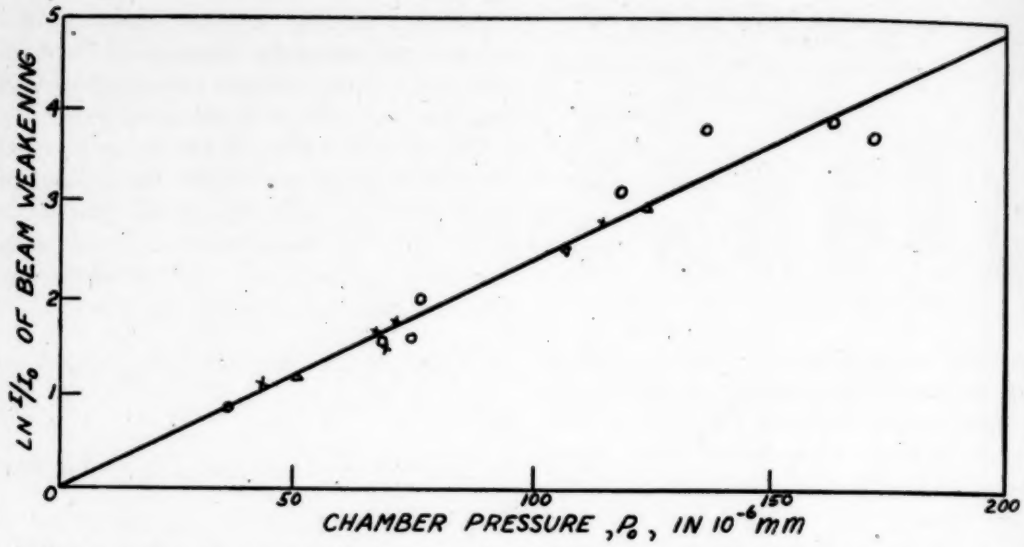

FIG. 8. Weakening of cesium beam scattered by cesium vapor as function of scattering pressure.

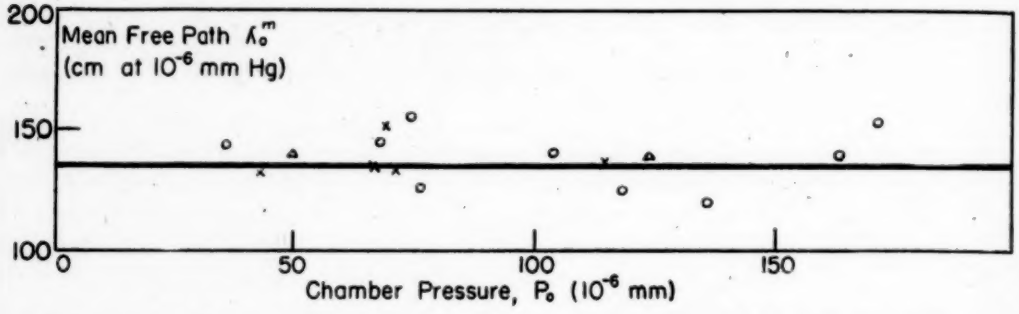

FIG. 9. Values of λ_0^m of cesium atoms in cesium vapor as a function of the scattering pressure.

(b) Cesium-Cesium Scattering

Gravity deflection curves obtained in Cs-Cs scattering experiments are given in Fig. 7. Curve I shows the unweakened beam, curves II and III the beam passing through the scattering chamber filled with cesium vapor of a pressure of 4.9×10^{-6} and 12.4×10^{-6} mm Hg, respectively. The "undeflected" beam curve, as calculated from the slit geometry and the maximum of the "unweakened" beam curve and indicated by the trapezoid, has been reduced by a factor of three to allow a better representation of the gravity curves. The calculated points of the weakened beam curves were obtained by the same method as in the nitrogen scattering experiments. The intensity of the unweakened curve as calculated on the basis of a Maxwellian velocity distribution in the undeflected beam indicates a deficiency of slow molecules (9 percent at $S=S_a$, 30 percent at $S=2S_a$). This effect is discussed in detail in paper I. Otherwise, the agreement between measured and calculated values is very good.

For the determination of the absolute value of the mean free path of cesium atoms in cesium vapor, a series of measurements of $\ln(I_0^m/I^m)$ in the maximum of the gravity curve was carried out, with the pressure in the scattering chamber varying between 35 and 200×10^{-6} mm Hg. These results are given in Fig. 8, while Fig. 9 shows the resulting values of λ_0^m as a function of the scattering pressure. The mean free path λ_0^m at a pressure of 10^{-6} mm Hg is 136 cm. Values for other velocities are given in reference (5) and can be calculated from Eq. (7).

(c) Collision Cross Sections for Cesium Atoms

From the mean free path at a given pressure, the classical collision cross section $\pi\sigma_{AG}^2$ can be

calculated[7] by means of Eq. (7),

$$\lambda_x = x^2/(\pi^{\frac{1}{2}}\nu_G\sigma_{AG}^2\psi(x)), \qquad (7)$$

where

$$x = c_A(m_G/2kT_G)^{\frac{1}{2}},$$

and ν_G is the number of scattering atoms per cm³, c_A the velocity of the beam atoms, T_G the absolute temperature of the scattering gas, k Boltzmann's constant, m_A and m_G the mass of beam and scattering gas atoms, respectively, and

$$\psi(x) = xe^{-x^2} + (2x^2+1)\int_0^x e^{-y}dy.$$

Since

$$\tfrac{1}{2}m_G\alpha_G^2 = kT_G \quad \text{and} \quad \tfrac{1}{2}m_A\alpha_A^2 = kT_A,$$

where the subscripts G and A refer to the scattering gas and the beam atoms, respectively, we have $x=(c_A/\alpha_A)(T_Am_G/T_Gm_A)^{\frac{1}{2}}$. For c_A, we choose the velocity of the atoms in the maximum of the intensity curve. From this curve, we take $c_A=1.64\alpha_A$. Using the data for $\lambda_x=\lambda_0^m$ corresponding to this velocity, we obtain the values for the cross sections given in Table II, where σ_{AG} is the sum of the effective radii, $\pi\sigma_{AG}^2$ the quantum-mechanical collision cross section and r_0 the classical sum of the atomic radii calculated under the assumption[2] that the classical cross section is one-half of the quantum-mechanical cross section.

The values of the mean free path are estimated to be accurate within 10 percent, hence the accuracy of the effective radii should be 5 percent. It is interesting to compare the classical radii for the Cs-Cs and Cs-He collisions. The radius of the Cs atom in the latter is 9.6×10^{-8} cm, which is larger than the sum of the radii of the Cs-He collision, which is 8.5×10^{-8} cm. This means, of course, that attractive forces are present in the Cs-Cs encounters.

TABLE II. Effective collision radii and cross sections.

Encounter	$\sigma_{AG}^2\times10^{16}$ cm	$\sigma_{AG}\times10^{8}$ cm	$\pi\sigma_{AG}^2\times10^{16}$ cm	$r_0\times10^{8}$ cm
Cs-He	142	12.0	446	8.5
Cs-N_2	298	17.2	936	12.1
Cs-Cs	743	27.3	2350	19.3

The effective collision radius for Cs-He encounters was measured by Rosin and Rabi,[8] who found $\sigma_{AG}=7.18\times10^{-8}$ cm, which is about 40 percent lower than our value. Their apparatus was much smaller (beam length about 10 cm), and the resolving power of the order of 1 minute of arc as compared with 5 seconds of arc in our apparatus. A possible explanation for this discrepancy is that the scattering intensity for small angles may be much higher than is expected on the basis of the simplified quantum theoretical treatment of the atoms as hard spheres.

[8] S. Rosin and I. I. Rabi, Phys. Rev. **48**, 373 (1935).

Electron Waves in the Magnetic Dipole Field of a Neutron

CHARLES L. CRITCHFIELD
University of Minnesota, Minneapolis, Minnesota
(Received October 21, 1946)

The relativistic wave functions for an electron moving in the field of a central magnetic dipole that has spin $\frac{1}{2}\hbar$ are studied. Spin inertia and retardation of the central field are neglected. In general, there are then four, first-order, coupled differential equations for the radial dependence of the electron waves; and these are equivalent to two coupled Schroedinger equations having a positive definite potential energy operator. In the particular case that the total angular momentum of the system is zero, however, the equations are equivalent to a single Schroedinger equation in which the potential energy is positive at all radii only for the electron-neutron interaction. The positron-neutron potential becomes strongly negative in a small region near a separation of the order of e^2/Mc^2, where M is the mass of the neutron. The attraction is just sufficient to form a bound $P_{\frac{1}{2}}$-state of the positron with zero binding energy. The reality of such neutron-positron state is open to question because of the simplifications that have been made and also because the magnetic dipole moment of the neutron is most probably of extended origin. The single equation obtained when the total angular momentum vanishes is the Mathieu differential equation which may be solved in terms of an integral function by a method developed by Lindemann. Asymptotic forms of these solutions, as well as of the fourth-order equation for total angular momentum unity are presented. The results indicate agreement with those obtained in various applications of perturbation methods. In particular, the ambiguity of the wave functions discussed previously by Bloch is apparent in the solutions for unit angular momentum.

1. INTRODUCTION. THE WAVE EQUATIONS

A THEORY of elementary particles must contain, to some degree, an interpretation of electromagnetic fields near singularities. An interesting portion of the singular behavior lies in the magnetic field arising from the dipole carried by the particles. For electrons and positrons, and presumably for charged mesons, the magnetic field is concomitant with the singular electric field. For protons and neutrons, most of the magnetic field is thought of as arising from an extended source characteristic of the interaction between nucleons and mesons. In either case, further knowledge of the properties of the magnetic fields is desirable. It is the purpose of this paper to present a theoretical investigation of a simple manifestation of magnetic dipole forces, *viz.*, the relativistic motion of an electron in the field of a point dipole. The line of approach taken here is chosen to be as parallel as possible to the familiar treatment of two-body problems where electric forces are dominant, i.e., the hydrogen atom and scattering by the Coulomb field. It is not the purpose of this work to replace, or refine, previous considerations made by many authors on hyperfine structure of spectral terms, magnetic scattering of electrons by nuclei and the scattering of neutrons by ferromagnetic substances for which perturbation methods are adequate.

If the magnetic field in which the electron moves were due to a magnetic dipole, $\boldsymbol{\mu}$, fixed at the origin of coordinates, the potential acting on the electron would be the vector potential, $\mathbf{A}$, which does not vary with time,

$$\mathbf{A}=(\boldsymbol{\mu}\times\mathbf{r})/r^3. \tag{1}$$

The wave equation for the electron would then be found by putting $\mathbf{A}$ in its proper place in the relativistic Hamiltonian function, as given by Dirac's theory. Then, if the self-energy of the dipole field is neglected, the situation is quite analogous to the result of the usual procedure when the central force is electrostatic (overlooking the fact that angular momentum will not be conserved under the postulates made so far).

If the magnetic dipole is associated with an elementary particle that is heavy compared with the electron, it is appropriate to fix its position at the origin of coordinates but not to fix its direction in space. The direction of the dipole is rather to be correlated with the spin axis of the central particle. In the present work we consider only the case for which the spin of the central particle is $\frac{1}{2}\hbar$. Using the Pauli spin vector operator $\boldsymbol{\sigma}$, the $\boldsymbol{\mu}$ in Eq. (1) must be considered as an

operator on the spin states of the heavy particle

$$\mu = \nu' \sigma, \tag{2}$$

where ν' is a dimensional constant. Since we also assume that the central particle does not carry an electric charge, the closest physical system to the one postulated here is the electron-neutron system. Comparison of the theory, which is for point dipoles, with neutron-electron systems suffers the obvious defect that the neutron's magnetic moment is probably not of point origin but rather arises in a region of radius comparable to the range of nuclear forces.

Correlating the central magnetic moment with the spin of the central particle means that the wave function depends not only on the position and spin coordinates of the electron but also on the spin of the neutron. It also means that the orientation of the magnetic field may change with time and this has two effects. First, the magnetic field must have some rotational inertia that should be added to the kinetic energy of the system and, secondly, the vector potential now varies with time after the fashion of retarded potentials. Generally speaking, the magnetic interaction is so weak that angular velocities induced in the central field should be relatively low and the effects of motion negligible. In the present paper, consequently, the rotational inertia and retardation effects will be disregarded, along with the self-energy of the field. The main criticism of this procedure is that for the most interesting consequence of the work, the possibility of bound states, the effects neglected are probably not small. On the other hand, bound neutron-positron systems are probably ruled out by the finite extension of the neutron's moment so that the whole question of the reality of bound states is better postponed until a study is made of the magnetic interaction of more elementary, and therefore charged, particles.

Under the conditions just set forth, the Hamiltonian function that is relativistic for the electron[1] but neglects the motion of the center of gravity of the neutron may be given the form:

$$H = c(\boldsymbol{\alpha}, \mathbf{p}) + e(\boldsymbol{\alpha}, \mathbf{A}) + \beta mc^2, \tag{3}$$

$$\mathbf{A} = \frac{\nu'}{r^3} \boldsymbol{\sigma} \times \mathbf{r}.$$

[1] P. A. M. Dirac, *Principles of Quantum Mechanics* (Clarendon Press, Oxford, 1935), second edition, Chap. XII.

Neither the angular momentum of the neutron, $\frac{1}{2}\boldsymbol{\sigma}\hbar$, nor the total angular momentum of the electron $\mathbf{M} = \mathbf{m} + \frac{1}{2}\boldsymbol{\sigma}\hbar$ commutes with H so that neither, alone, is a constant of the motion. However, it can be shown that H does commute with the total angular momentum

$$\mathbf{F}\hbar = \mathbf{M} + \tfrac{1}{2}\boldsymbol{\sigma}\hbar.$$

This means that the operator H couples the various states that can be formed with a given total angular momentum. In the terminology of hyperfine spectroscopy, the total angular momentum of nucleus plus electron is designated $F\hbar$. With a nuclear spin of $\frac{1}{2}\hbar$ and a single electron, the angular momentum in the electron state, $M\hbar$, may have either of two values given by $M = F + \frac{1}{2}$ and $M = F - \frac{1}{2}$, if $F > 0$; or just $M = \frac{1}{2}$ when $F = 0$. The complete wave function for a particular value of F will be a sum of product wave functions, each product containing one polarization of the electron wave and one polarization of the neutron wave. Each product is itself composed of the four components of the electron wave. Let the neutronic spin function be χ_s, where $s = \pm\frac{1}{2}$ designates the z-component of the spin state. Each product may thus be symbolized by

$$\{\psi_1, \psi_2, \psi_3, \psi_4\}\chi_s.$$

The only term in H that operates simultaneously on the ψ's and χ_s is that containing $\mathbf{A}$ and this may be written

$$e(\boldsymbol{\alpha}, \mathbf{A}) = \frac{\nu e^2 \hbar}{Mcr^2} Q, \quad \nu' = \nu \frac{e\hbar}{Mc},$$

$$Q \equiv \tfrac{1}{2} \begin{vmatrix} \alpha_x & \sigma_x & \sin\theta\cos\phi \\ \alpha_y & \sigma_y & \sin\theta\sin\phi \\ \alpha_z & \sigma_z & \cos\theta \end{vmatrix}.$$

More explicitly, the operation of Q on $\{\psi_1, \psi_2, \psi_3, \psi_4\}\chi_s$ may be written:

$$\begin{aligned} &Q\{\psi_1, \psi_2, \psi_3, \psi_4\}\chi_s \\ &= is\chi_s\{-e^{-i\phi}\psi_4, e^{i\phi}\psi_3, -e^{-i\phi}\psi_2, e^{i\phi}\psi_1\}\sin\theta \\ &\quad \tfrac{1}{2}\chi_{-s}\{(2s+1)\psi_4, (2s-1)\psi_3, \\ &\quad (2s+1)\psi_2, (2s-1)\psi_1\}\cos\theta \\ &\quad + \frac{i}{2}\chi_{-s}\{-\psi_3, \psi_4, -\psi_1, \psi_2\} \\ &\qquad \times (2s\cos\phi + i\sin\phi)\sin\theta. \end{aligned} \tag{4}$$

With this formula, it is a matter for direct computation to determine the wave equations for the electron. For that purpose, we adopt the method presented by Darwin[2] who expresses the angular dependence of the electron wave functions by writing the whole harmonic as

$$P_k^u=(-)^u(k-u)!\times\sin^{-u}\theta\left(\frac{d}{d\cos\theta}\right)^{k+u}\frac{(\cos^2\theta-1)^k}{2^k k!}e^{iu\phi}.$$

The notation differs from that in the reference only by the factor $(-)^u$ which arises from a different choice of representation of the rotation group.

Let a and b be functions of r alone, then one electron wave for which $M=k+\frac{1}{2}=M_z$ has the general form

$$\{(2k+1)P_k^k a,\ 0,\ iP_{k+1}^k b,\ -iP_{k+1}^{k+1}b\}.$$

Another form may be derived from this by interchanging function 1 with 3, and 2 with 4, and changing the sign of a relative to b. The latter is equivalent to transformation by the matrix $-i\alpha_x\alpha_y\alpha_z$ which commutes with every member of H except βmc^2 with which it anticommutes. Wave equations that one set of electron waves obeys can then be obtained from those that the other obeys by substituting $-mc^2$ for mc^2 in H and identifying b with a and a with $-b$.

A state of total angular momentum Fh and z-component $F_z h$, with $F=F_z=k+1$ is then the simple product

$$T_k(a,b)=\{(2k+1)P_k^k a,\ 0,\ iP_{k+1}^k b,\ -iP_{k+1}^{k+1}b\}\chi_1. \quad (5)$$

The state with which T_k is coupled by the operator Q is of the form

$$S_k(f.g)=\tfrac{1}{2}[\{P_{k+2}^{k+1}f,\ -P_{k+2}^{k+2}f,\ i(2k+3)P_{k+1}^{k+1}g,\ 0\}\chi_{-1}-\{P_{k+2}^{k}f,\ -P_{k+2}^{k+1}f,\ i(2k+2)P_{k-1}^{k}g,\ iP_{k+1}^{k+1}g\}\chi_1](k+1)^{-\frac{1}{2}}(k+2)^{-\frac{1}{2}}, \quad (6)$$

where f and g are functions of r alone. It can be verified, that under infinitesimal rotations, both T_k and S_k belong to the $(2k+3)$-dimensional representation of the group of rotations and that they belong to the same representation of the reflection group.[3] Interchanging ψ_1 with ψ_3 and ψ_2 with ψ_4 leads to two other total wave functions that belong to the same representation of the rotation group but to the alternate representation of the reflection group. Since Q is invariant under inversions these two types of total wave functions are not coupled by Q.

Operation by Q on T_k and S_k can then be calculated by using Eq. (4) and, with $F=k+1$, leads to

$$\begin{aligned}-(2F+1)QT_k(a,b)&=FT_k(b,a)+F^{\frac{1}{2}}(F+1)^{\frac{1}{2}}S_k(b,a),\\ -(2F+1)QS_k(f,g)&=F^{\frac{1}{2}}(F+1)^{\frac{1}{2}}T_k(g,f)+(F+1)S_k(g,f).\end{aligned} \quad (7)$$

Note that the order of the arguments (a,b), etc., is interchanged by Q. We introduce the characteristic length, w,

$$w=\nu(e^2/Mc^2)$$

(ν is just the number of nuclear magnetons in the spin direction) and combine Eq. (7) with the general considerations of reference 2 as they relate to Eq. (3) to obtain the differential equations in r that a, b, f and g must obey:

$$\begin{aligned}&\frac{da}{dr}-\frac{F-1}{r}a-\frac{F}{2F+1}\frac{w}{r^2}a-\frac{(F(F+1))^{\frac{1}{2}}}{2F+1}\frac{w}{r^2}f+\frac{mc^2+E}{\hbar c}b=0,\\ &\frac{db}{dr}+\frac{F+1}{r}b+\frac{F}{2F+1}\frac{w}{r^2}b+\frac{(F(F+1))^{\frac{1}{2}}}{2F+1}\frac{w}{r^2}g+\frac{mc^2-E}{\hbar c}a=0,\\ &\frac{dg}{dr}-\frac{F}{r}g+\frac{F+1}{2F+1}\frac{w}{r^2}g+\frac{(F(F+1))^{\frac{1}{2}}}{2F+1}\frac{w}{r^2}b+\frac{mc^2-E}{\hbar c}f=0,\\ &\frac{df}{dr}+\frac{F+2}{r}f-\frac{F+1}{2F+1}\frac{w}{r^2}f-\frac{(F(F+1))^{\frac{1}{2}}}{2F+1}\frac{w}{r^2}a+\frac{mc^2+E}{\hbar c}g=0,\end{aligned} \quad (8)$$

[2] C. G. Darwin, Proc. Roy. Soc. A118, 654 (1928).

[3] E. Wigner, *Gruppentheorie* (Vieweg, Braunschweig, 1931).

where E is the eigenvalue of H. Another set of equations for the same eigenvalue is obtained by changing the sign of m and exchanging the components of the electron wave function as described above.

Equation (8) can also be derived by a method parallel to that used by Dirac, reference 1, in obtaining the equations in spherical coordinates for the hydrogen atom. This may be done by defining an operator

$$K\hbar=(\sigma, \mathbf{M})+\hbar,$$

where σ still refers to the neutron spin, and making use of Dirac's operator

$$\epsilon=\rho_1(\sigma_r, \mathbf{r})/r.$$

It is readily verified that

$$Q=(K\epsilon-\epsilon K)/2i,$$
$$Q^2=Q^4=Q^6=\cdots,$$
$$Q^2K+KQ^2=K-\tfrac{1}{2},$$

and from these relations, and the fact that Q is a two-rowed matrix in S_k, T_k-space, Eq. (8) may be derived. This method was not used, here, as it is less clear how it may be extended to magnetic interaction with particles of higher spin.

The differential Eq. (8) may be reduced to a more compact form by the substitutions:

$$\begin{aligned}\gamma&=F^{\frac{1}{2}}(F+1)^{\frac{1}{2}},\\ \phi_1&=r[F^{\frac{1}{2}}b+(F+1)^{\frac{1}{2}}g],\\ \phi_2&=r[F^{\frac{1}{2}}g-(F+1)^{\frac{1}{2}}b],\\ \phi_3&=r[F^{\frac{1}{2}}f-(F+1)^{\frac{1}{2}}a],\\ \phi_4&=r[F^{\frac{1}{2}}a+(F+1)^{\frac{1}{2}}f],\end{aligned}\tag{9}$$

from which one obtains the first-order, coupled equations for the ϕ's

$$\begin{aligned}\frac{d\phi_1}{dr}+\left(\frac{w}{r^2}-\frac{1}{r}\right)\phi_1-\frac{\gamma}{r}\phi_2+\frac{mc^2-E}{\hbar c}\phi_4=0,\\ \frac{d\phi_2}{dr}-\frac{\gamma}{r}\phi_1+\frac{mc^2-E}{\hbar c}\phi_3=0,\\ \frac{d\phi_3}{dr}+\frac{\gamma}{r}\phi_4+\frac{mc^2+E}{\hbar c}\phi_2=0,\\ \frac{d\phi_4}{dr}+\left(\frac{1}{r}-\frac{w}{r^2}\right)\phi_4+\frac{\gamma}{r}\phi_3+\frac{mc^2+E}{\hbar c}\phi_1=0.\end{aligned}\tag{10}$$

The equations may also be expressed as two sets of coupled, second-order equations which are readily derived by differentiation and elimination in Eq. (10); let

$$c^2p^2=E^2-m^2c^4$$

then the second-order equations are:

$$\begin{aligned}\frac{d^2\phi_1}{dr^2}+\left(\frac{p^2}{\hbar^2}-\frac{\gamma^2}{r^2}-\frac{w^2}{r^4}\right)\phi_1+\frac{\gamma w}{r^3}\phi_2=0,\\ \frac{d^2\phi_2}{dr^2}+\left(\frac{p^2}{\hbar^2}-\frac{\gamma^2}{r^2}\right)\phi_2+\frac{\gamma w}{r^3}\phi_1=0,\end{aligned}\tag{11}$$

$$\begin{aligned}\frac{d^2\phi_3}{dr^2}+\left(\frac{p^2}{\hbar^2}-\frac{\gamma^2}{r^2}\right)\phi_3-\gamma\left(\frac{2}{r^2}-\frac{w}{r^3}\right)\phi_4=0,\\ \frac{d^2\phi_4}{dr^2}+\left(\frac{p^2}{\hbar^2}-\frac{2+\gamma^2}{r^2}+4\frac{w}{r^3}-\frac{w^2}{r^4}\right)\phi_4\\ -\gamma\left(\frac{2}{r^2}-\frac{w}{r^3}\right)\phi_3=0.\end{aligned}\tag{12}$$

Each of these sets of two equations can be regarded as a pair of coupled Schroedinger equations. The operator of the potential energy in Eq. (11) would then be

$$V_{10}=\frac{\hbar^2}{2m}\begin{Vmatrix}\frac{\gamma^2}{r^2}+\frac{w^2}{r^4} & -\frac{\gamma w}{r^3}\\ -\frac{\gamma w}{r^3} & \frac{\gamma^2}{r^2}\end{Vmatrix}$$

which is positive definite if $\gamma>0$, since both sum and product of its eigenvalues at any r are positive. If $\gamma=0$, V_{10} is diagonal and not negative. The dipole potential thus leads to no net attraction in the states ϕ_1 and ϕ_2 and no bound states of this type may be formed.

The potential operator in Eq. (12) is

$$V_{11}=\frac{\hbar^2}{2m}\begin{Vmatrix}\frac{2+\gamma^2}{r^2}-4\frac{w}{r^3}+\frac{w^2}{r^4} & \gamma\left(\frac{2}{r^3}-\frac{w}{r^4}\right)\\ \gamma\left(\frac{2}{r^3}-\frac{w}{r^4}\right) & \frac{\gamma^2}{r^2}\end{Vmatrix}$$

which is positive definite if $\gamma>\sqrt{2}$. At $\gamma=\sqrt{2}$, one eigenvalue of V_{11} is zero. The value $\gamma=\sqrt{2}$ is obtained when $F=1$. However, F may also be zero, in which case $\gamma=0$. Then V_{11} is diagonal

and has the single non-vanishing element

$$V_{11}=\frac{\hbar^2}{2m}\left(\frac{2}{r^2}-4\frac{w}{r^3}+\frac{w^2}{r^4}\right)$$

which is everywhere positive only if $w<0$. If $w>0$, as in the case of neutron-positron interaction, there is a region of strong attraction between the roots of V_{11}, *viz.*, $r'=\frac{1}{2}(2\pm\sqrt{2})w$. At $r=w$, the potential is $-\hbar^2/2mw^2$ and the range of negative potential is approximately $\sqrt{2}w$. Thus, the product of the potential and the square of the range is of the order of $\hbar^2/m$, as is required to form a bound system. It will be noted, also, that as r$\rightarrow$0, V_{11} becomes positive and infinite so that there is no difficulty with the solutions at that point.

The foregoing analysis shows that solutions of the wave equations may be expected to exist without altering the dipole potential near $r=0$. Of the possible solutions, the case of $\gamma=0$ is most interesting because, in this case alone, there is a net attractive potential in the system. Under this condition, however, the equations for ϕ_2 and ϕ_3 degenerate to those for plane waves, and the equation for ϕ_1 contains a repulsive potential for all radii. Thus, a bound state must be characterized by $\phi_1=\phi_2=\phi_3=0$. This condition is consistent with $\phi_4\neq 0$, according to Eq. (10), only if $E=mc^2$ and

$$\frac{d\phi_4}{dr}+\left(\frac{1}{r}-\frac{w}{r^2}\right)\phi_4=0. \tag{13}$$

Equation (13) can be integrated at once, up to a factor,

$$\phi_4=\frac{1}{r}e^{-w/r}. \tag{14}$$

That the solution, Eq. (14), represents a bound state is apparent from the fact that the wave function, $f=\phi_4/r$, falls off as r^{-2} with large r, so that most of the charge of the positron is concentrated within a radius of the order $|w|=|\nu|e^2/Mc^2$. The existence of such a state thus depends upon the dipole field persisting to radii small compared with the classical radius of the proton. This condition is not expected to be fulfilled in the case of the neutron because of the mesonic origin of its magnetic moment. But even if the range of the meson field were small compared with w there is serious doubt that effects connected with the time rate of change of the neutronic dipole moment would be neglible in a state of such small radius. In particular, the inertial effects in the magnetic field might be expected to be large and, since these contribute a positive energy, the bound state would disappear into the continuum.

2. SOLUTIONS FOR $F=0$

General solutions, for which $p^2\neq 0$, are obtainable for the waves in which $F=0$. As stated above, only two wave functions are involved, ϕ_1 and ϕ_4, and the solutions are determined by the equation of second order, Eq. (11)

$$\phi_1''+\left(\frac{p^2}{\hbar^2}-\frac{w^2}{r^4}\right)\phi_1=0, \tag{15}$$

plus one of the relations, Eq. (10), say

$$\phi_4=\frac{\hbar c}{E-mc^2}\left[\phi_1'+\left(\frac{w}{r^2}-\frac{1}{r}\right)\phi_1\right]. \tag{16}$$

First, we transform Eq. (15) to a resemblance of Bessel's equation by choosing a new dependent variable, y,

$$y=r^{-\frac{1}{2}}\phi_1,$$

$$y''+\frac{1}{r}y'+\left(\frac{p^2}{\hbar^2}-\frac{1}{4r^2}-\frac{w^2}{r^4}\right)y=0. \tag{17}$$

At large r this approaches the equation for $J_{\pm\frac{1}{2}}(pr/\hbar)$, the $\pm\frac{1}{2}$-order Bessel functions. If we write Eq. (17) with $1/r$ as the independent variable the form of the equation remains the same except that $p^2/\hbar^2$ is interchanged with $-w^2$. The asymptotic solutions at small r are, therefore, $J_{\pm\frac{1}{2}}(iw/r)$. We shall be particularly concerned with two forms of asymptotic solution, y_1 and y_2, and their product $Y=y_1y_2$:

$$\begin{aligned} y_1&\rightarrow(r/w)^{\frac{1}{2}}\sinh(w/r),\\ y_2&\rightarrow(r/w)^{\frac{1}{2}}\cosh(w/r),\\ Y&\rightarrow(r/2w)\sinh(2w/r). \end{aligned} \tag{18}$$

The differential Eq. (17) can be put in more familiar form by transformation of independent variable from r to x, such that

$$\begin{aligned} r&=(\hbar w/p)^{\frac{1}{2}}e^{i(x-\frac{1}{4}\pi)},\\ y(x)''&+\left(\frac{1}{4}+2i\frac{pw}{\hbar}\cos 2x\right)y(x)=0. \end{aligned} \tag{19}$$

Equation (19) is the Mathieu equation in its conventional form, but with complex parameters. The general solution of the Mathieu equation has been found by F. Lindemann.[4] The method is based on the proof that there are two independent solutions the product of which is an integral function of the variable z, which is related to x by

$$z=\cos^2 x.$$

If $Y(z)$ is the required integral function, the two solutions are given by

$$y(z)=Y^{\frac{1}{2}}\exp\left[\pm C\int_0^z \frac{dz}{Y[z(1-z)]^{\frac{1}{2}}}\right], \quad (20)$$

where C is a constant such that

$$y_1'y_2-y_2'y_1=2C\frac{dx}{dz}.$$

An asymptotic expression for Y appears in Eq. (18) and this may be written as a function of z:

$$\text{for } r^2\ll\hbar w/p,$$

$$z\to-\tfrac{1}{4}i(\hbar w/pr^2) \quad \text{and} \quad Y\to\frac{\sinh 4(ipwz/\hbar)^{\frac{1}{2}}}{4(ipwz/\hbar)^{\frac{1}{2}}}. \quad (21)$$

It is readily verified that if the product, Y, contained y_1^2 or y_2^2, as given in Eq. (18), its asymptotic form would not be an integral function of z. If we substitute Eq. (21) into Eq. (20) and integrate, we actually find

$$\begin{matrix} y_1\to[(r/w)\coth(-ipw/\hbar)^{\frac{1}{2}}]^{\frac{1}{2}}\sinh w/r \\ y_2\to[(r/w)\tanh(-ipw/\hbar)^{\frac{1}{2}}]^{\frac{1}{2}}\cosh w/r \end{matrix} \quad r\to 0,$$

so that the solution that is bounded and square integrable at $r=0$ must be of the form

$$y=y_2-y_1\tanh(-ipw/\hbar)^{\frac{1}{2}}. \quad (22)$$

Since $Y(z)$ is an integral function, the same asymptotic form of solution holds for all large z. If we apply the limiting process to Y, but such that

$$r^2\gg\hbar w/p, \quad z\to\tfrac{1}{4}i(pr^2/\hbar w),$$

we get

$$\begin{aligned} y_1&\to(\hbar/pr)^{\frac{1}{2}}[\tan(ipw/\hbar)^{\frac{1}{2}}]^{\frac{1}{2}}\cos(pr/\hbar), \\ y_2&\to(\hbar/pr)^{\frac{1}{2}}[\cot(ipw/\hbar)^{\frac{1}{2}}]^{\frac{1}{2}}\sin(pr/\hbar), \\ &\text{as } r\to\infty. \end{aligned}$$

Substituting these forms into Eq. (22) we get the asymptotic form at large r for the solution that is acceptable at $r=0$, *viz.*

$$\begin{aligned} y\to(\hbar/pr)^{\frac{1}{2}}&[\cot(ipw/\hbar)^{\frac{1}{2}}]^{\frac{1}{2}}[\sin pr/\hbar \\ &-\tan(ipw/\hbar)^{\frac{1}{2}}\tanh(-ipw/\hbar)^{\frac{1}{2}}\cos pr/\hbar]. \end{aligned} \quad (23)$$

Since w corresponds to a length of the order e^2/Mc^2, the product $pw/\hbar$ is of the order unity only in the neighborhood of billions of electron volts. Such energies, however, are beyond those allowable in this treatment because the relativistic properties of the neutron have been neglected. In application, therefore, $pw/\hbar$ must be much smaller than unity and, disregarding the constant factor, the solution for y is essentially*

$$y\to r^{-\frac{1}{2}}\sin p(r-|w|)/\hbar. \quad (24)$$

In brief, the electron waves manifest a phase-shift of $-p|w|/\hbar$ radians at large radii, if they form a state of total angular momentum zero, $F=0$, with the neutron. The same phase shift applies to both ϕ_1 and ϕ_4 components, as is evident from Eq. (16). The ${}_0S_{\frac{1}{2}}$ and ${}_0P_{\frac{1}{2}}$ waves at large r will be of the usual type, modified by this phase shift. This analysis holds for all finite p. When p is exactly zero the solution to the wave equations is the bound state presented in the preceding section.

3. NATURE OF SOLUTIONS NEAR THE ORIGIN

The behavior of the solutions of Eq. (10), or the equivalent Eqs. (11) and (12), near $r=0$ may be investigated by disregarding the zero power of r, i.e., setting $p^2=0$. The functions thus obtained will then be asymptotic forms of the complete solutions. Certain linear combinations of the asymptotic forms will be required, in general, in order to satisfy the boundary conditions at $r=0$. This study has been made for the states of lowest angular momentum, $F=0$ and $F=1$, which appear to be particularly tractable.

[4] F. Lindemann, Math. Ann. **22**, 117 (1883). The method is described in Forsyth, *Theory of Differential Equations*, Part III (Cambridge, 1902) p. 431 and also by P. Humbert, *Fonctions de Lamé et Fonctions de Mathieu, Memorial des Sciences Mathématique* (Gauthier-Villars, 1926).

* If $w<0$, the analysis holds with $p<0$ and the negative square root in Eq. (22).

In fact it was shown in the preceding section that the case of $F=0$ is readily soluble.

When $F=0$ we shall designate the asymptotic forms of ϕ_1 and ϕ_4 by u_1 and u_4, respectively. The functions ϕ_2 and ϕ_3 are irrelevant. The equation for u_1, as derived from Eq. (11) by setting $\phi_1=u_1$ and $p^2=0$, $\gamma=0$, is then

$$u_1''-\frac{w^2}{r^4}u_1=0. \tag{25}$$

This equation has the solutions, up to a factor,

$$u_1=r\exp -w/r \quad \text{and} \quad u_1=r\exp w/r. \tag{26}$$

One of these solutions is bounded, the other unbounded, at $r=0$ depending upon the sign of w. From Eq. (12) we get the equation for u_4

$$u_4''-\frac{1}{r^2}(2-4w/r+w^2/r^2)u_4=0, \tag{27}$$

which has the solutions

$$\begin{aligned} &u_4=\frac{1}{r}\exp -w/r, \\ &u_4=(r^2+wr+2w^2)e^{w/r}+4\frac{w^3}{r}e^{-w/r}\int_0^r e^{2w/r'}\frac{dr'}{r'}. \end{aligned} \tag{28}$$

The first form is bounded and square integrable at $r=0$ if $w>0$, the second if $w\leq 0$. The numerical factors with which u_1 and u_4 occur in the complete solutions are determinable from Eqs. (10). For $P_{\frac{1}{2}}$ waves we get directly from Eq. (10)

$$\begin{aligned} u_1'+(w/r^2-1/r)u_1&=0, \\ u_4'+(1/r-w/r^2)u_4+2(mc/\hbar)u_1&=0, \end{aligned}$$

with acceptable solutions

$$\begin{aligned} &u_1=re^{w/r}, \\ &u_4=-\frac{2}{3}\frac{mc}{\hbar}\Big[(r^2+wr+2w^2)e^{w/r} \\ &\qquad +4\frac{w^3}{r}e^{-w/r}\int_0^r e^{2w/r'}\frac{dr'}{r'}\Big], \\ &u_1=0, \quad u_4=\frac{1}{r}e^{-w/r}, \quad w>0. \end{aligned} \tag{${}_0P_{\frac{1}{2}}$}$$

The first set holds if $w\leq 0$. The second set is obviously the bound state described in Section 1.

For $S_{\frac{1}{2}}$ waves, we replace mc^2 in Eq. (10) by $-mc^2$ and set $E=mc^2$, $\phi_1=u_1$, $\phi_4=-u_4$, leading to

$$\begin{aligned} u_1'+(w/r^2-1/r)u_1+2(mc/\hbar)u_4&=0, \\ u_4'+(1/r-w/r^2)u_4&=0, \end{aligned}$$

with the solutions

$$\begin{aligned} &u_1=re^{w/r}, \quad u_4=0, \quad w\leqslant 0, \\ &u_1=re^{-w/r}, \quad u_4=-(\hbar w/mc)\frac{1}{r}e^{-w/r}. \end{aligned} \tag{${}_0S_{\frac{1}{2}}$}$$

The asymptotic forms of solution for $F=1$, i.e., $\gamma=\sqrt{2}$ in Eq. (10) may be found by a series of transformations and quadratures with $p^2=0$. The steps in this process will be omitted here and the results converted to those for a, b, f and g of Eq. (8). It is to be understood that these letters stand for solutions with $p^2=0$ as used in this section. In particular, E is set equal to mc^2 in Eq. (8). There are four solutions in this case:

$$a=1-\frac{w}{3r}, \quad f=\frac{w\sqrt{2}}{6r}, \quad b=0, \quad g=0, \tag{29}$$

$$\left.\begin{aligned} a&=\left(6+4\frac{w}{r}+\frac{w^2}{r^2}\right)e^{-w/r}, \\ f&=\sqrt{2}\left(\frac{w^2}{r^2}+\frac{w}{r}\right)e^{-w/r}, \quad b=0, \quad g=0, \end{aligned}\right\} \tag{30}$$

$$\left.\begin{aligned} f&=\left(r^2-\frac{w^2}{9}-\frac{2w^3}{9r}\right)e^{w/r}+\frac{2}{9}\frac{w^3}{r}\int_0^r e^{w/r'}\frac{dr'}{r'} \\ &\qquad -\frac{4w^2}{9r^2}(w^2+wr)e^{-w/r}\int_0^r e^{2w/r'}\frac{dr'}{r'}, \\ a&=\frac{w}{\sqrt{2}}\Big\{-\left(r+\frac{13}{9}w+\frac{2}{9}\frac{w^2}{r}\right)e^{w/r} \\ &\qquad +\frac{4}{3}w\left(1-\frac{w}{3r}\right)\int_0^r e^{w/r'}\frac{dr'}{r'} \\ &\qquad -\frac{4}{9}w\left(\frac{w^2}{r^2}+4\frac{w}{r}+6\right)e^{-w/r}\int_0^r e^{2w/r'}\frac{dr'}{r'}\Big\}, \\ b&=\frac{5w}{6\sqrt{2}}\frac{\hbar}{mc}e^{w/r}, \quad g=\frac{5}{6}(w-3r)\frac{\hbar}{mc}e^{w/r}, \end{aligned}\right\} \tag{31}$$

$$\left.\begin{aligned} f&=r^2+wr+\frac{7}{18}w^2+\frac{w^3}{9r}-\frac{2w^2}{9r^2}(w^2+wr)\\ &\qquad\times e^{-w/r}\int_{r_0}^{r}e^{w/r'}\frac{dr'}{r'},\\ a&=-\tfrac{1}{2}\sqrt{2}\Big[wr+\frac{7}{9}w^2+\frac{8w^3}{9r}\\ &\quad+\frac{2w^2}{9r^2}(w^2+4wr+6r^2)e^{-w/r}\int_{r_0}^{r}e^{w/r'}\frac{dr'}{r'}\Big],\\ b&=\frac{5\sqrt{2}}{12}\Big(\frac{w^2}{r}+w\Big)\frac{h}{mc},\\ g&=-\frac{5}{12}\Big(6r+4w+\frac{w^2}{r}\Big)\frac{h}{mc}. \end{aligned}\right\}\quad(32)$$

If $w>0$ the solution of Eq. (31) is unacceptable. Equation (32) defines a D-wave that is unique except for an undetermined lower limit, r_0, in the integrals. This lower limit must be finite, however, and admixes the solution (30) in terms of the order w^2. Both solutions (29) and (30) are acceptable S-waves. It is evident, consequently, that the solutions are not completely defined and that additional boundary conditions should be imposed at $r=0$. Such boundary conditions might be stated by defining the central dipole more closely as the limiting case of approaching magnetic charges or as a shrinking amperian current. This was first pointed out by Bloch[5] as having a major influence on the total scattering cross section. Its effect thus evidently appears in first order (in w) in states of higher angular momenta, but does not appear at all for $F=0$. In the above solutions for $F=1$ the uncertainty appears only in second, and higher, power of w. To first order, Eq. (29) and Eq. (30) are identical and the two independent solutions may be written

$$_1S_{\frac{1}{2}}:\quad a\to 1-\frac{w}{3r},\quad f\to\frac{\sqrt{2}w}{6r},\quad b\to 0,\quad g\to 0,\qquad(33)$$

$$_1D:\quad a\to\frac{w}{\sqrt{2}r},\quad f\to r^2+wr,\quad b\to\frac{5w}{6\sqrt{2}}\frac{h}{mc},$$
$$g=-5\frac{h}{mc}\Big(\frac{r}{2}+\frac{w}{3}\Big).\qquad(34)$$

If $w<0$, Eq. (30) is unacceptable, but Eq. (29) becomes a unique S-wave. Both (31) and (32) provide D-wave solutions, if $r_0=0$, and they are identical to first order in w. The approximate solutions in this case are then those in (33) and (34), as before.

In addition to the $_1S_{\frac{1}{2}}$ and $_1D_{3/2}$ waves there are the $_1P_{\frac{1}{2}}$ and $_1P_{3/2}$. The equations for the latter may be obtained essentially from Eq. (8), or their transformations Eq. (10), by replacing mc^2 by $-mc^2$. The second-order equations (11), which determine b and g, are unchanged in the transformation. The solutions for b and g presented in (31) and (32) can thus be combined to give solutions for ϕ_1 and ϕ_2. These solutions are

$$\begin{aligned} &\phi_1=(wr-2r^2)e^{w/r},\quad &&\phi_2=-\sqrt{2}r^2e^{w/r},\\ &\phi_1=-(2r^2+wr)\sqrt{2},\quad &&\phi_2=-(2r^2+2rw+w^2). \end{aligned}\qquad(35)$$

However, Eq. (11) must have four sets of solutions. The remaining two sets can be derived from (35) by noting that Eq. (11) is invariant to the simultaneous substitutions $w\to -w$, $\phi_1\to-\phi_1$. Hence two new solutions are obtained from (35)

$$\begin{aligned} &\phi_1=(wr+2r^2)e^{-w/r},\quad &&\phi_2=-\sqrt{2}r^2e^{-w/r},\\ &\phi_1=\sqrt{2}(2r^2-wr),\quad &&\phi_2=-(2r^2-2rw+w^2). \end{aligned}\qquad(36)$$

Again, the wave functions are unambiguous only to first order. The result may be written:

$$_1P_{\frac{1}{2}}:\quad b\to r-\tfrac{2}{3}w,\quad g\to-\frac{\sqrt{2}}{6}w,$$
$$a\to\frac{1}{2}\Big(3-\frac{w}{r}\Big)\frac{h}{mc},\quad f\to\frac{w\sqrt{2}}{4r}\frac{h}{mc},\qquad(37)$$

$$_1P_{3/2}:\quad b\to-\frac{\sqrt{2}}{6}w,\quad g\to r+\tfrac{2}{3}w,\quad a\to 0,\quad f\to 0.\qquad(38)$$

4. SOLUTIONS TO FIRST ORDER IN w FOR $F=1$

Equation (8) may be expressed as two sets of coupled, second-order differential equations.

[5] F. Bloch, Phys. Rev. 51, 994 (1937).

When $F=1$ these equations are

$$\begin{aligned}
&a''+2\frac{a'}{r}+\frac{p^2}{\hbar^2}a+\sqrt{2}\frac{w}{r^3}f-\frac{w^2}{3r^4}(a+\sqrt{2}f)=0,\\
&f''+2\frac{f'}{r}+\left(\frac{p^2}{\hbar^2}-\frac{6}{r^2}\right)f+\sqrt{2}\frac{w}{r^3}a\\
&\qquad+\frac{4w}{r^3}f-\frac{\sqrt{2}w^2}{3r^4}(a+\sqrt{2}f)=0,\\
&b''+2\frac{b'}{r}+\left(\frac{p^2}{\hbar^2}-\frac{2}{r^2}\right)b-\frac{4w}{3r^3}b\\
&\qquad-\frac{\sqrt{2}w}{3r^3}g-\frac{w^2}{3r^4}(b+\sqrt{2}g)=0,\\
&g''+2\frac{g'}{r}+\left(\frac{p^2}{\hbar^2}-\frac{2}{r^2}\right)g+\frac{4w}{3r^3}g\\
&\qquad-\frac{\sqrt{2}w}{3r^3}b-\frac{\sqrt{2}w^2}{3r^4}(b+\sqrt{2}g)=0.
\end{aligned}\tag{39}$$

If $w=0$, these equations become four independent differential equations closely related to Bessel's equations of order, $\frac{1}{2}$, 3/2, and 5/2. The solutions of Eq. (39) that are bounded at $r=0$ are then, to zero order in w

$$\begin{aligned}
a_0&=(\pi\hbar/2pr)^{\frac{1}{2}}\alpha_0 J_{\frac{1}{2}}(pr/\hbar),\\
b_0&=(\pi\hbar/2pr)^{\frac{1}{2}}\beta_0 J_{3/2}(pr/\hbar),\\
g_0&=(\pi\hbar/2pr)^{\frac{1}{2}}\gamma_0 J_{3/2}(pr/\hbar),\\
f_0&=(\pi\hbar/2pr)^{\frac{1}{2}}\delta_0 J_{5/2}(pr/\hbar),
\end{aligned}\tag{40}$$

where α_0, β_0, γ_0, and δ_0 are constant factors.

Expanding the solutions of Eq. (39) in an ascending power series in w, the functions Eq. (40) appear as the leading terms. The functions that are multiplied by the first power of w may be found by substituting the functions of Eq. (40) in those terms of Eq. (39) that appear to the first power, neglecting the terms in w^2 and solving the resulting, inhomogeneous differential equations. The integrals will consist of two parts, a particular integral and a complementary function; the latter is chosen to be orthogonal to the solutions Eq. (40) at large r. Let α_1, β_1, γ_1, and δ_1 be the factors with which the complementary functions in a, b, g, and f are added, respectively. The solutions to first order are then computed to be

$$\begin{aligned}
a&=\left(\frac{\pi}{2\xi}\right)^{\frac{1}{2}}\Big[\alpha_0 J_{\frac{1}{2}}(\xi)+\alpha_1 J_{-\frac{1}{2}}(\xi)\\
&\qquad-\delta_0\frac{\sqrt{2}w}{r\xi}J_{3/2}(\xi)\Big],\quad \xi\equiv\frac{pr}{\hbar},\\
b&=\left(\frac{\pi}{2\xi}\right)^{\frac{1}{2}}\Big[\beta_0 J_{3/2}(\xi)+\beta_1 J_{-3/2}(\xi)\\
&\qquad+\frac{4\beta_0+\sqrt{2}\gamma_0}{12}\frac{w}{r\xi}J_{\frac{1}{2}}(\xi)\Big],\\
g&=\left(\frac{\pi}{2\xi}\right)^{\frac{1}{2}}\Big[\gamma_0 J_{3/2}(\xi)+\gamma_1 J_{-3/2}(\xi)\\
&\qquad+\frac{\sqrt{2}\beta_0-4\gamma_0}{12}\frac{w}{r\xi}J_{\frac{1}{2}}(\xi)\Big],\\
f&=\left(\frac{\pi}{2\xi}\right)^{\frac{1}{2}}\Big\{\delta_0 J_{5/2}(\xi)+\delta_1 J_{-5/2}(\xi)\\
&\qquad-2\delta_0\frac{w}{r\xi^2}J_{3/2}(\xi)-\Big[4\delta_0+\sqrt{2}\alpha_0\\
&\qquad+\frac{E+mc^2}{cp}(\gamma_0-\tfrac{1}{4}\sqrt{2}\beta_0)\Big]\frac{w}{3r\xi}J_{-\frac{1}{2}}(\xi)\Big\}.
\end{aligned}\tag{41}$$

Reversal of the sign of mc^2, as is done for half of the solutions changes only the form of f as evidenced in the explicit appearance of mc^2. For the rest, the numerical coefficients in Eq. (41) may be determined to fit onto the asymptotic forms near $r=0$, as presented in Section 3. Making use of the asymptotic forms of the Bessel functions[6] for large $pr/\hbar$, the induced phase shifts are brought into evidence.

The asymptotic forms, at large r for the solutions Eq. (41) that fit onto the accepted

[6] Jahnke Emde (B. G. Teubner, Leipzig, 1933), second edition, p. 203, for example.

behavior near $r=0$ are as follows:

$$
\begin{aligned}
&a\rightarrow\frac{1}{r}\sin p\left(r-\frac{w}{3}\right)\Big/\hbar,\\
&b\rightarrow\frac{1}{r}\left(\frac{E-mc^2}{E+mc^2}\right)^{\frac{1}{2}}\cos p\left(r-\frac{w}{3}\right)\Big/\hbar,\qquad :{}_1S_{\frac{1}{2}}\\
&f\rightarrow-\frac{\sqrt{2}}{12}\frac{pw}{\hbar r}\cos pr/\hbar,\\
&g\rightarrow-\frac{\sqrt{2}}{12}\frac{pw}{\hbar r}\left(\frac{E-mc^2}{E+mc^2}\right)^{\frac{1}{2}}\sin pr/\hbar,
\end{aligned}
\tag{42}
$$

$$
\begin{aligned}
&f\rightarrow-\frac{1}{r}\sin p\left(r+\frac{w}{3}\right)\Big/\hbar,\\
&g\rightarrow\left(\frac{E-mc^2}{E+mc^2}\right)^{\frac{1}{2}}\frac{1}{r}\cos p\left(r+\frac{w}{3}\right)\Big/\hbar,\qquad :{}_1D_{3/2}\\
&a\rightarrow\frac{\sqrt{2}}{12}\frac{pw}{\hbar r}\cos pr/\hbar,\\
&b\rightarrow\frac{\sqrt{2}}{12}\left(\frac{E-mc^2}{E+mc^2}\right)^{\frac{1}{2}}\frac{pw}{\hbar r}\sin pr/\hbar,
\end{aligned}
$$

and the related expressions for ${}_1P_{\frac{1}{2}}$ and ${}_1P_{3/2}$ which are obtained by exchanging a with $-b$, f with g, and sin for cos in the expressions for ${}_1Ss$ and ${}_1D_{3/2}$, respectively. The results of the above tabulations may be summarized as follows: electron states forming a state of total angular momentum $\hbar$, with the neutron, show a phase shift of $\frac{1}{3}pw/\hbar$ radians if $j=3/2$ and $-\frac{1}{3}pw/\hbar$ radians if $j=\frac{1}{2}$. In addition, each wave is attended by the factor $\pm(\sqrt{2}pw/12\hbar)$ times the unbounded wave belonging to the alternate state of the same j. This is to be compared with the phase shift $-p|w|/\hbar$ radians for ${}_0P_{\frac{1}{2}}$ and ${}_0S_{\frac{1}{2}}$ states.

5. CONCLUSION

The foregoing results for the phase shifts indicate that the scattering of an electron by a magnetic dipole is characterized by a cross section of the order of πw^2. This has been pointed out already by Massey.[7] For the electron-neutron interaction, therefore, the cross section is of the order of 10^{-30} cm^2. The theory predicts, however, that under certain circumstances the amplitudes of waves scattered from many neutrons in a nucleus should reinforce even though the spins of the neutrons are distributed statistically. This appears to be the case for S-waves, for example (the same argument applies to $P_{\frac{1}{2}}$-waves), since the phase shift in ${}_0S_{\frac{1}{2}}$-states is $-p|w|/\hbar$ and that in ${}_1S_{\frac{1}{2}}$ states is $-pw/3\hbar$. The weighted average phase shift is then $-\frac{1}{2}pw/\hbar$ if $w>0$ and zero if $w<0$. Thus, if the magnetic moment of a neutron is localized sufficiently that each neutron in a nucleus of N-neutrons acts as an individual scattering center, and if the wave-length of the incident particle is long compared with nuclear diameters, the cross section for positron scattering ($w>0$) in S-waves should be of the order of N^2w^2, whereas that for electron scattering in S-waves would be of the order w^2 and would depend upon the resultant magnetic moment of the nucleus.

Similar conclusions to those found for the neutron-positron interaction probably can be drawn for the electron-proton system. In particular, the strong attractive potential in the ${}_0P_{\frac{1}{2}}$-state may have some effect upon the term values of the hydrogen atom that would illuminate the consequences of some of the assumptions that have been made. In general, the motion of an electron in a combined electric monopole and magnetic dipole field should be of more fundamental interest than that in the magnetic field alone. Such solutions, especially if generalized to include unit spin for one of the particles, would apply to the interaction of the "elementary" particles for which electric charge and magnetic moment are necessarily associated. On the other hand, the chief interest in such solutions probably would center on the possibility of bound states and the theory of such states is rather clouded by the uncertainties due to spin inertia and effects of retardation.

The work reported in this paper was done during the author's association with The George Washington University and The Department of Terrestrial Magnetism, Carnegie Institution of Washington, and it is a pleasure to acknowledge the support of these institutions.

[7] H. S. W. Massey, Proc. Roy. Soc. **A127**, 666 (1930).

Letters to the Editor

PUBLICATION of brief reports of important discoveries in physics may be secured by addressing them to this department. The closing date for this department is, for the issue of the 1st of the month, the 8th of the preceding month and for the issue of the 15th, the 23rd of the preceding month. No proof will be sent to the authors. The Board of Editors does not hold itself responsible for the opinions expressed by the correspondents. Communications should not exceed 600 words in length.

Note on the Scattering of Radiation in an Inhomogeneous Medium†

C. L. PEKERIS
Columbia University, New York, New York*
January 23, 1947

WE consider the scattering of a plane sound wave when passing through a medium in which the sound velocity c fluctuates slightly and irregularly around the mean value $\bar{c}$. The corresponding problem of the scattering of electromagnetic radiation in an optically inhomogeneous medium can be treated along similar lines. We write

$$c(x, y, z)=\bar{c}+\Delta c(x, y, z), \tag{1}$$

and compute the intensity of sound scattered by a volume V of the medium, which is large enough to contain several oscillations in sign of Δc. We choose a coordinate system centered at V and assume an incident plane wave traveling in the negative z direction. If φ denotes the sound potential then we have

$$\varphi=e^{ik(ct+z)}+\varphi_1,$$
$$\varphi_1=-\frac{k^2}{2\pi}\int\left(\frac{\Delta c}{c}\right)'\frac{\exp[ik(ct+z'-R)]}{R}dv', \tag{2}$$

where

$$dv=dx'dy'dz', \quad R=[(x-x')^2+(y-y')^2+(z-z')^2]^{\frac{1}{2}}, \tag{3}$$

and c has been written for $\bar{c}$. From an analysis of the scattering by a sphere of radius a of slightly different sound velocity it is found that expression (2) is valid if $(ak)(\Delta c/c)\ll 1$. We should, therefore, expect the perturbation method used in deriving (2) to be valid if $(a'k)(\Delta c/c)\ll 1$, where a' denotes the dominant "wave-length" of Δc.

If the distance r of the point of observation is large in comparison with the wave-length, we have

$$R\cong r-\frac{xx'}{r}-\frac{yy'}{r}-\frac{zz'}{r}, \quad f'\equiv z'+\frac{xx'}{r}+\frac{yy'}{r}+\frac{zz'}{r},$$
$$\varphi_1=-\frac{k^2}{2\pi r}\int\left(\frac{\Delta c}{c}\right)'\cos k(ct+f'-r)dv', \tag{4}$$

where we have taken the real part of (2). The energy E scattered in an elementary solid angle $d\Omega$ is given by

$$E=-\rho\frac{\partial\varphi}{\partial t}\cdot\frac{\partial\varphi}{\partial r}r^2d\Omega=c\rho k^2\left(\frac{k^2}{2\pi}\right)^2d\Omega\int\left(\frac{\Delta c}{c}\right)'$$
$$\times\cos k(ct+f'-r)dv'\int\left(\frac{\Delta c}{c}\right)''\cos k(ct+f''-r)dv''. \tag{5}$$

We now average over time, and writing $E_0=\frac{1}{2}\rho ck^2$, obtain

$$E=E_0\left(\frac{k^2}{2\pi}\right)^2d\Omega\int\left(\frac{\Delta c}{c}\right)'dv'$$
$$\times\int\left(\frac{\Delta c}{c}\right)''\cos k\left[\left(1+\frac{z}{r}\right)\gamma+\frac{\alpha x}{r}+\frac{\beta y}{r}\right]$$
$$=E_0\left(\frac{k^2}{2\pi}\right)^2d\Omega\int\left(\frac{\Delta c}{c}\right)'dv'$$
$$\times\int\frac{\Delta c}{c}(x'+\alpha, y'+\beta, z'+\gamma)$$
$$\times\cos k\left[\left(1+\frac{z}{r}\right)\alpha+\frac{x\beta}{r}+\frac{y\gamma}{r}\right]d\alpha d\beta d\gamma, \tag{6}$$

with

$$\alpha=x''-x', \quad \beta=y''-y', \quad \gamma=z''-z'.$$

The axes of α, β, γ are parallel to the axes of the original system, and the limits of α, say, are $-(x_1+x_2)$ and $+(x_1+x_2)$ if the limits of x are $-x_1$ and $+x_2$. In particular we have

$$\left(1+\frac{z}{r}\right)\alpha+\frac{x\beta}{r}+\frac{y\gamma}{r}=\cos\theta_0(1+\cos\theta)$$
$$+\sin\theta_0\sin\theta\sin(\varphi-\varphi_0), \tag{7}$$

where θ_0, φ_0 refer to the direction of r, and θ, φ are the spherical coordinates in the (α, β, γ) system. *We now define the autocorrelation* $R(\alpha, \beta, \gamma)$[1] *of the values of* $(\Delta c/c)$ *at two points inside* V *whose* x', y', z' *coordinates differ, respectively, by* α, β, γ *by:*

$$\iiint\frac{\Delta c}{c}(x', y', z')\frac{\Delta c}{c}(x'+\alpha, y'+\beta, z'+\gamma)dx'dy'dz'$$
$$=V\left\langle\left(\frac{\Delta c}{c}\right)^2\right\rangle_{Av}R(\alpha, \beta, \gamma). \tag{8}$$

Substituting in (6) we get

$$E=E_0\left(\frac{k^2}{2\pi}\right)^2d\Omega V\left\langle\left(\frac{\Delta c}{c}\right)^2\right\rangle_{Av}\iiint R(\alpha, \beta, \gamma)$$
$$\times\cos k\left[\left(1+\frac{z}{r}\right)\gamma+\frac{x\alpha}{r}+\frac{y\beta}{r}\right]d\alpha d\beta d\gamma. \tag{9}$$

In the case of spherical isotropy we have

$$R(\alpha, \beta, \gamma)=R(\rho), \quad \rho=[\alpha^2+\beta^2+\gamma^2]^{\frac{1}{2}}, \tag{10}$$

and using the relation

$$\int_0^\infty\rho^2R(\rho)d\rho\int_0^\pi\sin\theta d\theta\int_0^{2\pi}\cos k[\cos\theta_0(1+\cos\theta)$$
$$+\sin\theta_0\sin\theta\cos(\varphi-\varphi_0)]d\varphi$$
$$=4\pi\int_0^\infty\rho^2R(\rho)\left(\frac{\sin bk\rho}{bk\rho}\right)d\rho, \quad b=2\cos(\theta_0/2), \tag{11}$$

we obtain

$$E=E_0\frac{k^4}{\pi}d\Omega V\left\langle\left(\frac{\Delta c}{c}\right)^2\right\rangle_{Av}\int_0^\infty\rho^2R(\rho)\left(\frac{\sin bk\rho}{bk\rho}\right)d\rho. \tag{12}$$

For a Markoffian autocorrelation function[2]

$$R(\rho)=e^{-\rho/a}, \tag{13}$$

where a represents a measure of the "size" of the scattering elements, and Eq. (12) yields

$$E=E_0\frac{2a^3k^4}{\pi}d\Omega V\left\langle\left(\frac{\Delta c}{c}\right)^2\right\rangle_{Av}\left[1+4a^2k^2\cos^2\left(\frac{\theta_0}{2}\right)\right]^{-2}. \tag{14}$$

It should be noted that θ_0 is measured from the negative z

axis. If the angle is measured from the forward direction of the incident wave, $\cos(\theta_0/2)$ in (11) and (14) should be changed to $\sin(\theta_0/2)$.

In the interpretation of light scattering in solutions, it is customary to assume a model for the scattering elements, say a sphere of radius a, and apply the theory of scattering by a cloud of randomly distributed spheres.[3] Experiments indicate, however, that a has a considerable statistical scatter. The model of randomly distributed spheres of variable radii is perhaps not simpler to visualize than the autocorrelation function R itself, which is the only statistical property of the scatterers' population determining the angular distribution of scattered light, as shown in Eqs. (9) and (12).

This note is taken from a study of scattering problems made by the writer in May, 1942 for O.S.R.D., of which only the results were published. The manuscript was made available to members of Division 6 and was loaned to several members of Division 17 of O.S.R.D. Among the problems treated in this study, either exactly or approximately, are the scattering of sound by (1) a vortex sheet, (2) a cylindrical vortex, (3) a spherical vortex, (4) a convective cloud in which turbulence is isotropic, and (5) a corrugated surface.

† Publication assisted by the Ernest Kempton Adams Fund for Physical Research of Columbia University, New York, New York.
* On leave of absence from Massachusetts Institute of Technology.
[1] See G. I. Taylor, Proc. Lond. Math. Soc. 20, 196 (1920); Proc. Roy. Soc. A164, 478 (1938). N. Wiener, Acta Mathematica 55, 118 (1930); A. L. Patterson, Phys. Rev. 46, 372 (1934).
[2] C. L. Pekeris, Phil. Mag. [7] 33, 541 (1942).
[3] P. Debye, J. App. Phys. 15, 338 (1944).

The Half-Life of Be^{10}

D. J. Hughes, C. Eggler, and C. M. Huddleston
Argonne National Laboratory, P. O. Box 5207, Chicago 80, Illinois
January 9, 1947*

THE long-lived nucleus Be^{10} has been reported as formed only in the $Be^9(d, p)$ reaction.[1,2] The half-life could only be estimated to be in the range 10^3 to 10^7 years[1-3] because the yield of the reaction producing the Be^{10} is not known. Bretscher[4] tried to produce Be^{10} from the $Be^9(n, \gamma)$ reaction but found no activity. Levinger and Meiners[2] also found no Be^{10} activity in Be irradiated in the Clinton pile.

Because the extremely long half-life of Be^{10} is of interest theoretically, it was decided to attempt its measurement by isolation of the activity produced by the (n, γ) reaction in two BeO samples which had been irradiated for different periods of time in the Hanford pile (kindly supplied by O. C. Simpson of the Argonne Laboratory). Although the BeO was of high purity, it had a gross counting rate of about 5000 counts per min. per mg of Be. As the expected Be^{10} activity would be only a few counts per min. per mg, it was necessary to purify the samples carefully. The purification was carried out by group separation and the addition of suspected impurities of the third and fourth groups as carriers, the final specific separation for Be being the basic acetate process.[5] The main impurities were found to be carried with titanium in excess NaOH and with zinc in the H_2S-NH_4CH_3COO process.

The final samples, which did not decrease in activity with further purification, had activities of 3.3 counts per min. per mg of Be for one sample and 6.7 for another sample that had been irradiated twice as long. Absorption curves of the activities gave an energy of 0.58 ± 0.03 Mev which is in close agreement with the findings of Levinger and Meiners[2] and McMillan and Ruben[1] and the mass difference of Be^{10} and B^{10} (0.58 Mev[1]).

In order to obtain the half-life from the nvt and observed activity it is necessary to know the cross section of the (n, γ) reaction. The cross section for $Be^9(n, \gamma)$ was measured by comparing the effect on the reactivity of the Argonne graphite pile of several kilograms of BeO with that of graphite. The value obtained was 0.01 barn (barn $= 10^{-24}$ cm^2) in agreement with the measurements of S. K. Allison,[6] of A. Langsdorf,[6] and of R. Nobles.[6] The half-life of Be^{10} calculated from the activity, nvt, and the cross section is almost the same for the two samples, the average value being

$$T_{\frac{1}{2}} = 2.9 \times 10^6 \text{ years.}$$

The amount of activity to be expected in the Hanford graphite from the $C^{13}(n, \alpha)Be^{10}$ (fast neutron) reaction was then calculated, using the measured half-life and an (n, α) cross section estimated by comparison with measured pile cross sections for other endothermic reactions.[7] A small amount of graphite which had been in the Hanford pile for about a year was ignited, several mg of Be carrier added, and the Be purification carried out. An activity was obtained of magnitude within a factor of two of that predicted, which did not decay, and had the correct beta-energy for Be^{10}. It seems certain then that the activity was Be^{10} produced by the $C^{13}(n, \alpha)$ reaction and the finding constitutes additional support for the correctness of the half-life determination.

Because of the importance of obtaining Be^{10} in large amounts and of higher specific activity than can be done by the (n, γ) reaction, arrangements are now being made to irradiate boron in the Hanford pile for the production by the (n, p) reaction and subsequent chemical separation of the Be^{10}.

* Declassified January 6, 1947.
[1] E. M. McMillan and S. Ruben, Phys. Rev. 70, 123 (1946).
[2] J. Levinger and E. Meiners, Phys. Rev., to be published.
[3] G. T. Seaborg, Rev. Mod. Phys. 16, 1 (1944).
[4] E. Bretscher, Nature 146, 94 (1940).
[5] Noyes and Bray, *A System of Qualitative Analysis for the Rare Elements* (The Macmillan Company, New York, 1943).
[6] Unpublished Manhattan Project work (1943-46).
[7] D. J. Hughes, N. Goldstein, and W. D. B. Spatz (unpublished).

Photoelectric Emission from a Rough Surface*

Hugh Bradner
Radiation Laboratory, University of California, Berkeley, California
January 10, 1947

EXPERIMENTS on the normal energy distribution of photoelectrons from alkali metals ordinarily make use of evaporated metals which have a matte surface rather than the smooth surface considered in the Fowler-DuBridge[1] theory. The following is a modification of the theory for the case of a rough surface at zero degrees Kelvin.

At 0°K, the electron velocity distribution is uniform within a sphere of radius $(2\mu_0/m)^{\frac{1}{2}}$ in velocity space, where μ_0 = maximum energy of unexcited electrons, and m = electron mass. Assume that the energy of the photon adds to the electron energy in such a way that it increases only the component of electron velocity normal to the surface element. And assume further an excitation probability α proportional to the normal component of the electron velocity. Considering the transformations of the sphere by the excitation energy $h\nu$, the surface potential barrier W_a, and the retarding potential V_s applied at an angle δ to a surface element, one obtains an equation that is readily soluble when $V_s \geq (\mu_0+h\nu-W_a)\sin^2\delta$. The current from an element is

$$i=(2\pi em\alpha/h^3)\cos\delta\cdot[\mu_0+h\nu-W_a-V_s]^2,$$

which is just DuBridge's expression multiplied by $\cos\delta$.

The photoelectric current from a rough surface at 0°K thus shows the same dependence on retarding potential and on energy as that from a smooth surface, providing the surface is not too rough, and the retarding potentials are not too low. Assuming a maximum angle of 45° between surface element normals and the normal to the cathode, the formula is valid for $i \leq (2^{\frac{1}{2}}\pi em\alpha/h^3)(V_s)^2$.

The equation for $V_s < (\mu_0+h\nu-W_a)\sin^2\delta$ does not reduce to a simple form. From the equations it does follow, though, that the current will be less than DuBridge's expression, indicating that photoelectric saturation current curves for rough surfaces will be rounded even at 0°K.

The writer has examined the data of Overhage[2] on normal energy distribution to see whether the above arguments could explain any of the discrepancy between theory and his curves. They do not.

The writer wishes to express his indebtedness to Dr. W. V. Houston who suggested looking into this problem, and also suggested the mathematical treatment used.

* This work was done at the California Institute of Technology n 1941.

[1] L. A. DuBridge, Phys. Rev. 43, 727 (1933).
[2] C. F. J. Overhage, Phys. Rev. 52, 1039 (1937).

Neutron Induced Activities in Lutecium, Ytterbium, and Dysprosium

MARK G. INGHRAM, RICHARD J. HAYDEN, AND DAVID C. HESS, JR.
Argonne National Laboratory, University of Chicago, Chicago, Illinois
January 17, 1947

NITRIC acid solutions of Lu_2O_3, Yb_2O_3, and Dy_2O_3 were irradiated with neutrons in the Argonne heavy water pile. Decay curves of the irradiated lutecium sample showed 3.4-hour and 6.6-day activities as reported by Flammersfeld and Mattauch.[1] Decay curves of the ytterbium sample showed a 2.7-hour activity (probably the same activity reported by Marsh and Sugden[2] as 3.5 hours) and also a 102-hour activity not previously reported. No evidence of the 41-hour activity reported by Pool and Quill[3] was found. Decay curves of the dysprosium sample showed the 2.5-hour activity reported by Marsh and Sugden.[2]

Assignment of mass to three of these active isotopes was made as follows. A portion of the sample containing the activity in question was placed on the filament source of a mass spectrograph. Operation of the spectrograph separated the isotopes and deposited them on a photographic plate. The position of the active isotope on this plate was determined by placing a second photographic plate face to face with the original. The disintegration of the active isotopes on the first plate produced developable images on both plates. Comparison of the position of this active deposit with the normal mass spectrum on the original plate determined the mass of the active isotope. This method of mass assignment gives results without the necessity of assuming the nuclear reaction by which the isotope is formed and is therefore frequently valuable in establishing the nuclear reaction. Using these techniques the following masses were assigned: 6.6-day lutecium, 177; 102-hour ytterbium, 175; and 2.5-hour dysprosium, 165.

[1] Flammersfeld and Mattauch, Naturwiss. 31, 66 (1943).
[2] Marsh and Sugden, Nature 136, 102 (1935).
[3] M. L. Pool and L. L. Quill, Phys. Rev. 53, 437 (1938).

Interpretation of Anomalous Larmor Frequencies in Ferromagnetic Resonance Experiment

CHARLES KITTEL*
Research Laboratory of Electronics, Massachusetts Institute of Technology, Cambridge, Massachusetts
January 10, 1947

RECENTLY J. H. E. Griffiths[1] reported an important new ferromagnetic resonance experiment at microwave frequency. The experiment is essentially the ferromagnetic analog of the Purcell-Torrey-Pound nuclear resonance experiment. Griffiths found however the unusual result that the resonance frequencies he observed were greater than the calculated Larmor frequencies for electron spin by factors of about two to six. He attempted unsuccessfully to explain the anomaly by the introduction of the Lorentz cavity force, a step which is definitely not justified.

A theory of the resonance effect is given below which leads to values of the resonance frequency in close agreement with the experimental determination. It is shown that it is important to consider the dynamic coupling caused by the demagnetization field normal to the surface of the specimen. The result is that the appropriate Larmor frequency should be calculated as for a field strength $(BH)^{\frac{1}{2}}$ rather than for H.

A ferromagnetic specimen whose surface is the plane $y=0$ is subjected to a strong d.c. field H_z and a weak microwave field H_x. The magnetization $\mathbf{M}$ and the angular momentum density $\mathbf{J}$ are related by $\mathbf{M}=\gamma\mathbf{J}$, where γ is the gyromagnetic ratio. The equation of motion $\partial\mathbf{J}/\partial t=[\mathbf{M}\times\mathbf{H}]$ may be written

$$\partial\mathbf{M}/\partial t=\gamma[\mathbf{M}\times\mathbf{H}], \quad (1)$$

where the components of $\mathbf{H}$ are $(H_x, -4\pi M_y, H_z)$. Here $-4\pi M_y$ is written for H_y on the basis of the divergence relation $B_y=H_y+4\pi M_y=0$. The Lorentz and Weiss fields are omitted as they are always parallel to $\mathbf{M}$, and hence their vector product with $\mathbf{M}$ is identically zero. It is assumed that saturation obtains, and in fact that the d.c. field is sufficiently strong to outweigh the magnetic

TABLE I. Comparison of observed and calculated resonance frequencies.

	d.c. field H_z(Oe)	Angular frequencies for resonance: (rad/sec.) $\times 10^{-10}$ Calculated Larmor frequencies for H_z	for $(B_zH_z)^{\frac{1}{2}}$	Experimental frequencies
Fe	2800	5.0	14.5	15.4
	500	0.9	5.8	5.9
Co	510	0.9	5.3	5.9
Ni	5000	8.8	13.5	15.4
	3800	6.7	10.9	13.2
	1030	1.8	4.9	5.9

anisotropy forces so that in the static case the spin system always points in the direction of the resultant magnetic field. In this limit the whole specimen is supposed to behave as a single domain, so that there are no complications from the domain boundaries.

We have, neglecting products of small quantities,

$$\partial M_x/\partial t=\gamma(M_yH_z+4\pi M_yM_z)=\gamma B_zM_y; \quad (2)$$

$$\partial M_y/\partial t=\gamma(M_zH_x-M_xH_z); \quad (3)$$

$$\partial M_z/\partial t\leqq 0; \quad (4)$$

which gives $-\omega^2M_x=\gamma^2B_z(M_zH_x-M_xH_z)$. The susceptibility $\chi_x=M_x/H_x$ is given by

$$\chi_x=\chi_0/[1-(\omega/\omega_0)^2], \quad (5)$$

where the frequency for resonance is found to be $\omega_0=\gamma(B_zH_z)^{\frac{1}{2}}$ and is the Larmor angular frequency in the fictitious field $(B_zH_z)^{\frac{1}{2}}$. The static susceptibility χ_0 is equal to M_z/H_z and varies with the biasing field; here M_z may be taken as the saturation magnetization.

In Table I Griffiths' experimental values of ω_0 are compared with the calculated Larmor frequencies for fields H_z and $(B_zH_z)^{\frac{1}{2}}$. The gyromagnetic ratio is taken as the electron spin value. The induction B_z is calculated using 1700, 1400, and 500 as the saturation magnetization for Fe, Co, and Ni, respectively. The theory given here is seen to account quite well for the experimental results, considering that damping and anisotropy forces have been neglected.

The effect of relaxation is introduced by adding a term $-\lambda(\mathbf{M}-\chi_0\mathbf{H})$ to the right side of Eq. (1). We find

$$\frac{\chi_x}{\chi_0}=\frac{\omega_0^2+\lambda^2\mu_0+j\omega\lambda}{\omega_0^2+\lambda^2\mu_0-\omega^2+j\omega\lambda(1+\mu_0)}, \quad (6)$$

where $\mu_0=B_z/H_z$. From this it is seen that the demagnetizing field acts to increase the apparent damping.

The interpretation of a complex susceptibility in terms of the result of an electrical measurement is somewhat involved, but may be accomplished by the reasoning previously given.[2] The apparent permeability for a resistive measurement (such as a "Q" measurement) is $\mu_R=|\mu_x|(1-\sin\phi)$, where μ_x is the permeability derived from χ_x, and ϕ is the phase angle of μ_x; ϕ is always between 0 and $-\pi$.

* John Simon Guggenheim Memorial Foundation Fellow.
[1] J. H. E. Griffiths, Nature 158, 670 (1946).
[2] C. Kittel, Phys. Rev. 70, 281 (1946).

Biased Betatron in Operation

W. F. WESTENDORP
Research Laboratory, General Electric Company, Schenectady, New York
January 22, 1947

A BIASED betatron[1-2] with closed central core has been successfully operated. The guiding magnetic field consists of a direct-current field component with a sinusoidal component superimposed, while the closed central core carries only a sinusoidal component of flux maintained at the proper magnitude by the current in a bucking coil located in grooves in the polefaces. Figure 1 shows a schematic cross section of the machine and Fig. 2 is a diagram of the principal electrical components of the energizing circuit.[1] The turn ratio of main coils to bucking coil is chosen so that the proper flux ratio and thereby the betatron 2:1 rule is fulfilled. Although radically different from previous betatrons in which the 2:1 rule was established by means of air gaps, this principle of locating the electron orbit offered no difficulties. It has the advantage of a reduction of the size of the capacitor bank since less magnetic energy storage takes place in a machine with a closed central core. The application of a direct-current bias to the main coils to produce an increased guiding field and to the bucking coil to keep the constant component out of the central flux, proved to be not critical and was tried out successfully for all ratios between main coil direct-current and crest alternating-current between 0 and 0.866. The corresponding ratio of current components in the bucking coil was always smaller for maximum x-ray output, but not critical.

No compensating or phase correcting circuits of any kind were used. Even though the a.c. components in main and bucking coils are not exactly 180 degrees out of phase,[2] theory[3] predicts that the shift of the orbit produced is very small during most of the accelerating interval and this was checked experimentally by the use of an orbit tilt circuit by means of which the electrons are made to hit a target located above the orbit.

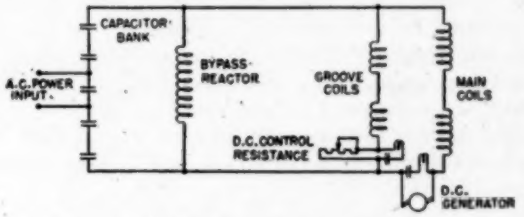

FIG. 1. Biased betatron with closed central core.

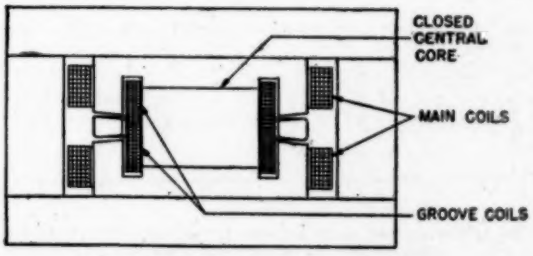

FIG. 2. Circuit diagram of biased betatron.

By means of a "megavolt meter,"[4] a direct reading of the electron energy and of the corresponding x-rays produced could be obtained in all cases. Thereby an instantaneous change from 11 Mev without d.c. bias to 20.5 Mev with d.c. bias could be produced and read by merely turning on the direct current and rephasing the electron injection pulse. In both cases, electron injection voltages as low as 8000 volts could be used indicating a high degree of uniformity of the magnetic guiding field with azimuth. With oil-cooled coils, the machine will produce 50-million volt x-rays.

[1] W. F. Westendorp, J. App. Phys. 16, 657 (1945).
[2] Donald W. Kerst, Phys. Rev. 68, 233 (1945).
[3] E. Amaldi and B. Ferretti, Rev. Sci. Inst. 17, 389 (1946).
[4] W. F. Westendorp, Rev. Sci. Inst. 17, 215 (1946).

The Capture Cross Section of Boron for Neutrons of Energies from 0.01 ev to 1000 ev*

R. B. Sutton,[1] B. D. McDaniel,[2] E. E. Anderson,[3] and L. S. Lavatelli[4]
University of California, Los Alamos Scientific Laboratory, Santa Fe, New Mexico
January 23, 1947

THE slow neutron capture cross section of boron has been measured for neutron energies from 0.01 ev to 1000 ev. The cross section was obtained by determining the transmission of boron-containing samples. Neutron energies were determined by using the method of modulation of a cyclotron beam to obtain the time of flight of the neutrons over a 7.6-meter path between the neutron moderator and a BF_3 neutron detector. This method is similar to that described by Baker and Bacher[5] and by Bacher, Baker, and McDaniel.[6] The equipment used was constructed in the Physics Department at Cornell University by B. D. McDaniel and C. P. Baker; a description will appear in the literature shortly. Neutron pulses in twelve time-of-flight intervals could be recorded simultaneously.

In order to cover the range of neutron energies four samples, each of different boron content, were used. The one containing least boron was a BF_3 gas cell; the others were B_4C. Of the three B_4C samples the thickest and thinnest consisted of cells containing B_4C powder; the third was composed of a mixture of B_4C and lead borate which was hot-pressed to form a compact disk.

The curve of total cross section σ_T *vs.* time-of-flight τ for each absorber was found to vary in the following manner

$$\sigma_T = \alpha\tau + \beta,$$

where α and β are constants. It was assumed that the constant β corresponded to the scattering cross section of the various elements present, and the term $\alpha\tau$ corresponded to the absorption cross section of boron. The scattering cross section, β, was obtained by taking the extrapolated value of σ at $\tau=0$. The scattering cross section for boron was found by correcting β for the cross sections of the other elements present. Values used were for fluorine, 4.1×10^{-24} cm², for carbon, 4.85×10^{-24} cm², for oxygen, 4.2×10^{-24} cm², and for lead 9.6×10^{-24} cm². The value obtained for the boron scattering cross section was 4.2×10^{-24} cm². The total contribution of the other elements in the B_4C samples was 2.2×10^{-24} cm² per B atom. The capture cross section of boron was obtained from

$$\sigma_a = \sigma_T - \beta = \alpha\tau$$

by assuming that all the capture cross section was represented by $\alpha\tau$ and none was included in β. In Fig. 1 the values of the product of the capture cross section by neutron velocity are plotted as a function of neutron energy. The instrumental resolution function is triangular. The resolution used depended on the energy region under investigation; in Fig. 1 the base of the triangle is equal in length to the separation of the points.

The value of $\sigma_a v$ determined from the weighted average of the points on the curve is $1.61\pm.02\times10^{-24}$ cm² meter/μ sec. It can be seen from the curve that systematic deviations occur between different absorbers. This is probably owing to errors in the determination of the boron content of the absorbers. The value of $\sigma_a v$ determined from the BF_3 gas alone is 1.58×10^{-24} cm² meter/μ sec. which may be a better value than the one given above, since the boron content of the BF_3 was probably better known. Both these values are lower than the figure of $118\times10^{-24}E^{-\frac{1}{2}}$ cm² (or 1.63×10^{-24} cm² meter/μ sec.) recently given by Rainwater and Havens,[7] but are higher than the value of 1.55×10^{-24} cm² meter/μ sec. obtained by Bacher, Baker and McDaniel.[6] All agree within the uncertainties given. The figure also indicates that $\sigma_a v$ is essentially constant (to ±10 percent) up to 1000 ev, if the assumption is correct that β contains only components of scattering cross section.

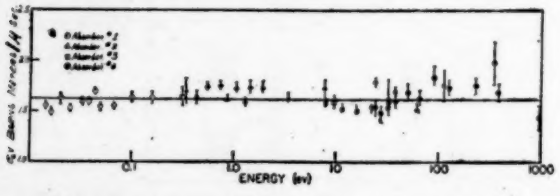

FIG. 1. The product ($\sigma_a v$) between boron absorption cross section and neutron velocity plotted against the logarithm of the neutron energy.

* This work was carried out under contract between the University of California and the Manhattan District, Corps of Engineers, War Department.
[1] Now at Carnegie Institute of Technology, Pittsburgh, Pennsylvania.
[2] Now at Cornell University, Ithaca, New York.
[3] Now at Milwaukee-Downer College, Milwaukee, Wisconsin.
[4] Now at Harvard University, Cambridge, Massachusetts.
[5] C. P. Baker and R. F. Bacher, Phys. Rev. 59, 332 (1941).
[6] R. F. Bacher, C. P. Baker, and B. D. McDaniel, Phys. Rev. 69, 443 (1946).
[7] J. Rainwater and W. W. Havens, Jr., Phys. Rev. 70, 136 (1946).

Remarks on Dr. Bhabha's Note "On the Expansibility of Solutions in Powers of the Interaction Constants"

Niels Arley
Institute of Theoretical Physics, Copenhagen, and Palmer Physical Laboratory, Princeton, New Jersey
January 13, 1947

IN a recent note Bhabha[1] has pointed out that the difference between the physical and the non-physical solutions in the classical electron theory proposed by Dirac[2] may be characterized by the fact that the former is

continuous in the interaction constant e at the point $e=0$, whereas the latter is not, and that consequently the former may be expanded into a power series in e, but the latter may not. Since the usual perturbation methods of solving problems in any quantum field theory which is the quantization of a classical field theory just consists in expanding into a power series of the relevant interaction constant, λ, Bhabha, therefore, lays down, not as a property to be proved, but as a general postulate that we have to demand all physical solutions to vary continuously for $\lambda \to 0$ in order that they be expansible into a power series of λ from the point $\lambda=0$.

Firstly, continuity is, however, not a sufficient condition for expansibility into a power series. For example the function $\lambda^2 \ln\lambda$ is both continuous and has a continuous derivative at the point $\lambda=0$, but is, nevertheless, not expansible into a power series of λ from $\lambda=0$, this point being an essential singularity since the function has here an infinite branch point in the complex λ-plane. The correct condition for expansibility is the much more severe condition that the solutions be analytic in λ at $\lambda=0$.

Secondly, in the quantum perturbation method used for calculating transition probabilities, the equations to be solved are infinite systems of simultaneous linear differential equations. It is true that the usual perturbation method consists in expanding into a power series of λ, thus tacitly assuming the solutions to be analytic in λ. This assumption need, however, by no means be true even in the simplest case in which all the coefficients are constant throughout the complex plane. In a previous paper[3] we have given a general mathematical theory of such differential equations and have shown that all forms of 'pathologies' may occur, such as, for instance, equations having no solutions at all, equations having infinitely many solutions for the same initial condition, equations with solutions which have a continuous derivative which is not differentiable for *any* value of the variable, and so on. In particular, there exist equations with constant coefficients which have a uniquely determined solution which may be found explicitly, but for which the usual perturbation procedure gives a divergent result even in the second approximation. (In this example the explicit expression shows that the solution contains just a term of the form $\lambda^2 \ln\lambda$ mentioned above.[4] Now it is in fact possible to develop other methods of perturbation, such as expansion in series which are only partly power series in λ, the coefficients containing also λ, which at any rate converge in this specific example. We are investigating these expansions more closely and the results will be published elsewhere.

Notwithstanding the fact that some of the divergence difficulties of the present quantum field theories, especially those connected with the self-energy problem, are certainly of a deeper nature which will require a quite new theory, presumably consisting in introducing Heisenberg's fundamental length l_0 in a suitable way,[5] it is, however, likely that some of them, especially those connected with transition probability problems, may be removed within the present mathematical formalism by better perturbation methods, as is indicated by the damping theory of Heitler and his co-workers, for instance. To insist in principle, as proposed by Bhabha, on the present special form of perturbation method is, therefore, neither justified nor desirable, and to do so may even be a hindrance for further progress.

[1] H. J. Bhabha, Phys. Rev. **70**, 759 (1946).
[2] P. A. M. Dirac, Proc. Roy. Soc. **A167**, 148 (1938).
[3] Arley and Borchsenius, Acta Math. **76**, 261 (1945).
[4] Cf. reference 3, p. 300.
[5] W. Heisenberg, Ann. d. Physik **32**, 20 (1938).

Erratum: Expanding Universe and the Origin of Elements

[Phys. Rev. 70, 572–573 (1946)]

G. GAMOW
The George Washington University, Washington, D. C.

THE value of the space curvature entering into the formulae (1) and (3) must be considered to be expressed not in centimeters but in the units of the selected length l. Thus estimating the radius of curvature from the expression (3) we get the value of $1.7\times10^{-17}(-1)^{\frac{1}{2}}\times l = 1.7\times10^{-7}(-1)^{\frac{1}{2}}$ cm, or about two billion imaginary light years, instead of 0.2 imaginary light year as given in the Letter to the Editor. This does not change, however, the further arguments.

Proceedings of the American Physical Society

MINUTES OF THE MEETING AT LOS ANGELES, CALIFORNIA, JANUARY 3–4, 1947

THE 276th meeting of the American Physical Society was held on Friday and Saturday, January third and fourth, 1947, at Los Angeles in Harris Hall of the University of Southern California. This was our first meeting at that University, which furnished excellent accommodations and management for our sessions. Our thanks are due particularly to R. E. Vollrath and G. L. Weissler. The attendance at the most populous session amounted to some 200. The four invited papers were admirable in content and presentation. The vice president of the Society was prevented by the grounding of his plane from presiding at the session of invited papers, and was replaced as Chairman by C. S. Van Atta. The other Chairmen were R. E. Vollrath and J. Kaplan.

J. KAPLAN
Local Secretary for the Pacific Coast
University of California
Los Angeles, California

Invited Papers

Interferometry. W. E. WILLIAMS, *Pasadena.*
Design of a Small Nuclear Reactor. ROBERT CHRISTY, *California Institute of Technology.*
Recent Progress in Applied Absorption Spectroscopy. R. R. BRATTAIN, *Shell Development Company.*
Recent Progress in Applied Mass Spectrometry. D. P. STEVENSON, *Shell Development Company.*

Contributed Papers

A1. The Atmospheric Bands of Oxygen. JOSEPH KAPLAN, *University of California, Los Angeles.*—A remarkable new afterglow has been discovered in which the well-known atmospheric bands of O_2 are emitted. This is the first time that these bands have been observed in emission. The bands of the system which were most readily photographed are the 0,0 band at λ7594 and the 0,1 band at approximately λ8650. The latter band has not been previously reported in either absorption or emission. Using small dispersion and Eastman IN plates, it was possible to obtain a good picture of the 7594 band in a one-hour exposure of the afterglow. Several other bands of the system and several apparently new bands of oxygen were obtained by using longer exposures. The new bands have not yet been identified. The exposure times were short compared with those needed to obtain comparable spectra of the auroral afterglow in nitrogen. The source of this new afterglow was a tube in which the auroral afterglow in nitrogen had been excited, and in which most of the nitrogen had been cleaned up. The addition of oxygen yielded this new glow. Considerable further study of this glow is planned because of its probable importance for the understanding of excitation processes in the upper atmosphere.

A2. Spectrophotometric Study of Reflectance Color Changes in Foods. E. J. EASTMOND, *Western Regional Research Laboratory.*—The influence of reflectance color on acceptability of foods has led to an investigation of the applicability of spectrophotometric methods to objective studies of color changes caused by processing conditions. Measurements have been made on a Hardy recording spectrophotometer and on a Hunter multipurpose reflectometer. Various methods of sample preparation have been investigated and the precision of results compared. Measurements can be made on samples in the original form, but in many cases homogenization is necessary for precision. In certain dehydrated foods chromaticity has been found to be essentially constant over fairly wide ranges of particle size and moisture content even though the brightness may vary considerably. In other cases careful standardization of particle size would be necessary to measure small color differences. Attention has been given to tristimulus specification and the precision of determination of trichromatic coefficients. These coefficients are useful as indices of reflectance color changes with time, temperature, and storage conditions. Luminous reflectance has also been found useful as a color variable. Changes in color are being correlated with quality and acceptability of food products.

A3. Possibility of Altering the Decay Rate of a Radioactive Substance. EMILIO SEGRÈ, *University of California, Berkeley.*—The radioactive decay constant of a substance decaying by orbital electron capture is proportional to $|\psi(0)|^2$ of the electrons. In the case of a light element like Be^7 it may be possible to alter this quantity by an appreciable amount by putting the Be in different chemical compounds. We would then have a slight change of the radioactive half-life of the Be in different compounds. The magnitude of the effect may be in the neighborhood of one percent, but it is practically impossible to give a quantita-

tive estimate because the total change of $\psi(0)$ is affected by certain factors such as the density of the crystal, nature of the chemical bond, etc. They are both positive and negative, and have comparable magnitudes. To obtain a reliable estimate of the effect we require a more detailed knowledge of the wave functions for various compounds than is at present available. Experiments are in progress to detect the effect by comparing the half-life of Be^7 in Be metal with that in BeO or BeF_2.

A4. Angular Distribution of α-Particles from Li^7+p. R. F. CHRISTY AND S. RUBIN, *California Institute of Technology.*—One of us has measured the angular distribution of α-particles resulting from the bombardment of a thin target of Li by protons of from 0.4 to 1.4 Mev. The same experiments gave some information on the variation of the total cross section for the reaction in the same energy range. The angular distribution is well represented by $1+A(E)\cos^2\theta$. A increases with energy up to 0.9 Mev where it has a maximum value of 2.1 and then decreases slightly to a value of 1.8 at 1.4 Mev. An attempt has been made to understand in terms of the dispersion theory the angular distribution in conjunction with the magnitude and energy dependence of the total cross section. Although the cross section above 0.4 Mev is not well known, it seems to show no pronounced indication of resonance from 0 to 1.4 Mev. A reasonable fit of the data is obtained with two resonances with $\Gamma\approx 1$ Mev at 0 and 1.8 Mev roughly. The latter is taken to have $J=2$ but the former may be $J=0$ or $J=2$. The proton width agrees well with that derived from the γ-ray resonance at 0.44 Mev only if the 0 energy resonance has also $J=2$.

A5. Angular Distribution of Long-Range Alpha-Particles from Excited Ne^{20}. SYLVAN RUBIN, *California Institute of Technology.*—Some preliminary measurements have been made of the angular distribution of the 5.9-cm alpha-particles from the reaction: $F^{19}(p,\alpha)O^{16}$. Measurements were made with a thin BeF_2 target at proton energies of 1.14, 1.20, 1.33 Mev, corresponding to the two highest resonance peaks and the minimum between them on the excitation curve.[1] The angular distribution was measured from 25° to 155° to the proton beam. The distributions were markedly asymmetric, with much stronger yield backward than forward. Previous measurements near 400 kev[2] showed strong asymmetry also, but with greater yield forward. Fitting of trial analytical angular distribution functions showed all powers of $\cos\theta$, at least up to $\cos^4\theta$, are needed to fit the data. The $\cos^3\theta$ and $\cos^4\theta$ terms indicate an appreciable effect from d-wave incident protons. A large $\cos^3\theta$ term at 1.14 Mev, and large $\cos\theta$ terms at 1.20 and 1.33 Mev, indicate strong interference among adjacent long range alpha-emitting states of Ne^{20}.

[1] J. F. Streib, W. A. Fowler, and C. C. Lauritsen, Phys. Rev. **59**, 253 (1941).
[2] W. B. McLean, A. Ellet, and J. A. Jacobs, Phys. Rev. **58**, 500 (1940).

A6. Device for Introducing Short-lived Radioactive Samples into a Cloud Chamber. T. LAURITSEN, W. A. FOWLER, AND C. C. LAURITSEN, *California Institute of Technology.*—In connection with the study of the radioactive products of Li^8 (0.88 sec.) a mechanism has been developed for automatically moving the activated target from the bombarding tube (at high vacuum) into the cloud chamber on a repeated cycle. The target is mounted at the end of a $\frac{1}{16}''$ stainless steel rod which, with an interlocking extension rod, passes through a series of locks connecting the bombardment position and the cloud chamber. Immediately after bombardment of the target, an air cylinder advances the rod, pushing the target into a socket in the end of the extension rod and passing the assembly successively through a rough vacuum region, a region at cloud chamber pressure, and into the cloud chamber. Once the target is in the cloud chamber, a second air cylinder retracts the extension rod, exposing the target. The reverse motion consists in covering the target, passing through the locks and uncovering in the bombardment position. Seals between the pressure locks are provided by Koroseal sleeves lubricated with high vacuum oil. A slight rotation of the rod facilitates passage through the seals. The elapsed time for a 10″ motion of the target into the chamber is about 1.5 sec. A somewhat longer interval is allowed on the return stroke to permit pumping out in the rough vacuum lock. This work was carried on under contract with the Office of Naval Research.

A7. Auger Showers. M. M. MILLS AND R. F. CHRISTY, *California Institute of Technology.*—Under the current assumptions of proton primaries in cosmic rays, the Auger showers (previously explained by primary electrons) demand a secondary source of energetic electrons or photons. A fast decaying mesotron ($\tau\sim 10^{-9}$ sec.) has already been proposed to account for the bulk of the soft component and β-decay lifetimes. The object of the present calculation is to determine whether this mesotron is also sufficient to account for Auger showers and bursts in unshielded ionization chambers. The coincident burst data of Lewis, which disagreed violently with the primary electron hypothesis,[1] has been examined in a preliminary way. If this experiment is to be explained at all in terms of ionization due to electrons, it will probably require initiating electrons of energy $>10^{14}$ ev produced predominately near the top of the atmosphere and with several electrons having considerable angular spread associated in one event. In terms of decay this would mean $\tau\leq 10^{-12}$ sec. An alternative possibility that the bursts are due to nuclear disintegrations is being examined. An experiment with three colinear chambers is suggested. The center would not necessarily fire simultaneously with the extremes according to these possibilities.

[1] L. Wolfenstein, Phys. Rev. **67**, 238 (1945).

A8. The Interpretation of the East-West Effect. ROBERT A. MILLIKAN, *California Institute of Technology.*—T. H. Johnson's equatorial measurements of the East-West effect indicate that the East-West dissymmetry is less at very high altitudes than at sea level. Suggestions are herewith presented which would limit the unbalance between positives and negatives to a region relatively near the earth in comparison with its radius and thus avoid the assumption of any electrical unbalance throughout space. Such an un-

balance has been generally recognized for fifty years as a valid objection to any theory which requires the earth to be bombarded by high speed particles of one sign only rather than of both signs, or else of no sign. If the validity of the principle is accepted all interpretation of the East-West effect must in some way or other conform with this principle of electrical balance throughout interstellar space. The suggestions necessary to produce such conformity are here discussed.

A9. Cosmic Ray Directional Counter for the Determination of the Azimuthal Variation of Primary Cosmic Radiation at Fixed Zenith Angles. ALFREDO BAÑOS, JR. AND M. L. PERUSQUÍA, *University of California, Los Angeles, and National University of Mexico, Mexico City.*—At the 1939 Symposium on Cosmic Rays held at the University of Chicago, M. S. Vallarta[1] suggested that the knowledge of the azimuthal variation of cosmic radiation could be used for the purpose of determining the sign and the energy spectrum of primary cosmic rays. In following this suggestion the writers designed, constructed, and operated, at the Institute of Physics of the National University of Mexico, an instrument consisting of four triple coincidence Geiger-Müller telescopes mounted at zenith angles of 0°, 20°, 40°, and 60°, and so arranged that, by rotation around a vertical axis, the directional intensity or counting rate could be measured at 16 equally spaced azimuths. The rotation and photographic recording were made fully automatic. Several novel features of the apparatus are here discussed. Most important of all is the feature that, in contradistinction to the usual parallel connection of the three counters, as used in the standard Rossi[2] circuit and necessitating an amplifier tube for each Geiger-Müller counter, a decided simplification in the circuits and a corresponding ease of operation were obtained by connecting the three counters in series feeding a single stage of amplification. Extensive statistical tests of the counting rate observed with the series connection were made by one of us[3] showing that the series connection was at least as reliable as the conventional parallel circuit. The results of two experiments, covering in excess of 100-days for each continuous run, have been reported by M. S. Vallarta.[4]

[1] M. S. Vallarta, Rev. Mod. Phys. 11, 239 (1939).
[2] B. Rossi, Nature 125, 636 (1930).
[3] Alfredo Baños, Jr., Rev. Mex. de Ing. y Arq. 19, 121–147 (1941).
[4] M. S. Vallarta, M. L. Perusquía and J. de Oyarzábal, Bull. Am. Phys. Soc. 21, Cl (September, 1946).

A10. On the Meson Theory of Nuclear Forces. LESLIE L. FOLDY, *Department of Physics and Radiation Laboratory, University of California, Berkeley, California.*—The failure of the Møller-Rosenfeld-Schwinger mixture to yield quantitative agreement with the observed properties of the deuteron has suggested the possibility that this agreement might be obtained with other mixtures in which tensor-force singularities are cancelled. Several such possibilities exist involving vector, pseudovector, and pseudoscalar mesons, some of which possess the interesting characteristic that they yield a finite tensor and central interaction in the limit where the meson masses approach equality and the square of the coupling constant increases indefinitely inversely as the difference in masses. In the symmetrical theories the resulting interaction is of the form

$$V_{12}=\frac{\tau_1\cdot\tau_2}{3}\left\{G^2S_{12}\left(\frac{1}{kr}+1\right)e^{-kr}+2F^2\sigma_1\cdot\sigma_2\left(\frac{2}{kr}-1\right)e^{-kr}\right\} \quad (1)$$

which is the same as would be obtained by differentiating the interaction with respect to the meson mass in the simple theories. The radial dependence of the central interaction is attractive at short ranges but repulsive at long ranges and thus would presumably lead to preferential forward scattering of high energy neutrons scattered by protons. In spite of the admitted conceptual difficulties concerning the limiting process by which (1) was obtained and the field-theoretic significance of the result, the simplicity of the result was sufficiently provoking to induce an attempt to compare the consequences of (1) with experiment. Preliminary results appear to indicate that agreement with the properties of both the proton-neutron and proton-proton system cannot be obtained if one employs in (1) the mass of cosmic-ray mesons.

A11. Possible Use of Thermal Noise for Low Temperature Thermometry. EDWARD GERJUOY AND A. THEODORE FORRESTER, *University of Southern California.*—The suggestion has recently been made that the Brownian motion of a quartz crystal be used to establish a low temperature thermodynamic scale.[1] The mean square noise voltage generated in any passive electrical network is $4kTR(f)df$, where $R(f)$ is the real part of the complex impedance. The noise voltage of a piezoelectric crystal, as well as that of ordinary resistors, must satisfy this relationship. The high impedance of a parallel resonant circuit at resonance suggests its use as a source of thermal noise. Subject to the condition that the output noise be representative of the low temperature to within 1 percent, a calculation was made which indicated that the lowest temperature measurable in this manner is certainly greater than 0.5°K. This limitation arises from the fact that the input impedance of the first tube must be much larger than the impedance of the resonant circuit. As a result there is an upper limit to the impedance at resonance which does not permit the noise in the tube to be exceeded at very low temperatures. This consideration applies equally well to piezoelectric crystals as to ordinary circuits.

[1] A. W. Lawson and E. A. Long, Phys. Rev. 70, 220 (1946).

A12. A Sensitive High Speed Radiation Thermocouple. HOWARD CARY* AND K. P. GEORGE, *National Technical Laboratories.*—The case of a thermocouple receiving modulated radiation is analyzed to determine the conditions yielding the maximum signal to noise ratio. It is concluded that: (*a*) vacuum operation is best, although the advantage is small at high modulation frequencies; (*b*) the optimum electrical resistance decreases with increasing frequency; (*c*) the thermal capacity of the thermoelectric leads must be made negligible by making the lead length less than a limiting value which varies inversely as the square root of the modulation frequency. A vacuum thermocouple designed for optimum performance at 10 c.p.s. is described.

The receiver is of gold foil 2.0 mm by 0.3 mm by 0.2μ thick, blackened with the equivalent of 0.2μ of gold. Taylor process bismuth and bismuth-tin thermocouple leads 0.2 mm long are used. To minimize thermal resistance of the receiver, four leads are soldered to the receiver at different points and connected to form two parallel thermojunctions with a combined resistance of one ohm. In agreement with theory, steady radiation of approximately 2×10^{-10} watt chopped at 10 c.p.s. and falling on the receiver produces an output signal equal to the r.m.s. noise of the thermocouple in a 1 c.p.s. band width.

* Now at Applied Physics Corporation, Pasadena, California.

A13. A Proposed Experiment on the Ponderomotive Forces Exerted by Microwaves on Dielectric Media. OTTO HALPERN, *Los Alamos Laboratory.*—Some formulations[1] of relativistic electrodynamics lead to the result that an electromagnetic wave propagating itself in a dielectric medium exerts a force density given by the self-explanatory formula

$$\mathbf{f}=\frac{\epsilon\mu-1}{c^2}\frac{\partial \mathbf{S}}{\partial t}$$

The smallness of $\mathbf{f}$ has so far been considered to prevent experimental verification. The author proposes an experiment in which the force of a standing microwave in a $\lambda/4$ layer be measured preferably with a static magnetic field superimposed in the direction of the r. f. magnetic field. A (resonant) quartz-plate may be used as a piezoelectric indicator. This experiment if successful would permit for the first time to measure the actual time dependent of Poynting's vector.

[1] Cf., e.g., W. Pauli, *Relativitaets-Theorie.*

B1. An Intense Positive Ion Source for Solids. A. E. SHAW, *Argonne National Laboratory.*—A positive ion source for solids has been developed. A tungsten crucible containing the solid material and heated by electron bombardment produced intense beams of singly charged ions. Pt-Ir (15 percent) yielded 120μA, for 100 watts of electron power, La_2O_3 yielded 212μA, for 105 watts, and Sm_2O_3 yielded 40μA for 150 watts. A mass spectrographic analysis of the positive ions from a tungsten crucible containing La_2O_3 and UN revealed the presence of La^+, LaO^+, W^+, WO^+, U^+, UN^+, UO^+ and possibly UO_2^+. A similar analysis of the ions from Pt-Ir (15 percent) revealed the presence of all the singly charged isotopes of W, Pt, and Ir. It is anticipated that this source will find application in the mass deposition of isotopes. For example, in 10 minutes a deposit of 0.50 microgram of the completely resolved isotopes of samarium has been obtained.

B2. The Determination of Particle Size by the Low Angle Scattering of X-Rays. A. E. SMITH, *Shell Development Company.*—The particle sizes of samples of pure γ-Al_2O_3 heated at various temperatures from 650°C to 1000°C were determined by the low angle scattering of x-rays by using a Philips Geiger counter x-ray spectrometer. The mean crystallite sizes of the same materials were also determined by measurement of line broadening. The particle size and crystallite size, as measured by the above methods respectively, agree within the limit of experimental error. The surface calculated from the particle size distribution and mean crystallite size is in reasonable agreement with the surface measured by the Brunauer, Emmet, Teller method. The results are summarized in Table I.

TABLE I.

Heat Treatment	Line Broadening Mean a_0	Line Broadening Calculated Specific Surface, m^2/g	Low Angle Scattering Mean D	Low Angle Scattering Calculated Specific Surface, m^2/g	E.B.T. Measured Specific Surface, m^2/g
650°C— 6 hr.	86A	194	97A	198	172
900°C—36 hr.	—	—	143	156	93.5
1000°C—12 hr.	129	129	142	132	78

B3. Temperature Coefficient of Electrical Resistivity for Crystalline Selenium Containing Various Percentages of Bromine. WAYNE E. BLACKBURN, *Westinghouse Research Laboratories and University of Pittsburgh.*—The temperature coefficient of electrical resistance of brominated selenium over the temperature range, −30°C to 100°C, was found to be negative and variable. The electrical resistivities of the selenium samples varied by factors of three to twelve for the temperature range mentioned depending upon the bromine content. A reproducible hysteresis loop was obtained on the plot of resistivity *versus* temperature. A minimum in the plot of electrical resistivity *versus* bromine content was found with 0.007 percent bromine in selenium. Activation energies for freeing electrons obtained from the slopes of conductivity *versus* temperature plots indicate a dependence upon bromine content in the selenium.

B4. Viscous and Thermal Absorption of Sound as Relaxation Phenomena. CARL ECKART, *Marine Physical Laboratory.**—In discussing the absorption of sound, reference is often made to relaxation phenomena, as distinguished from the "classical" viscous and thermal dissipative processes. While this may be convenient, it is not a basic distinction. By using known formulae, it is shown that viscous dissipation of sound can be considered as a relaxation phenomenon, with relaxation time $\tau_\nu=4(\nu+\nu')/3\rho c^2$, where ν,ν' = ordinary and dilational coefficients of viscosity, ρ = density of fluid, and c = velocity of sound. Similarly, the relaxation time for thermal dissipation is $\tau_\kappa=\kappa/\rho c^2 S$, where κ = thermal conductivity, and S = specific heat at constant volume. In the case of an ideal monatomic gas, the ratio $s=\tau_\nu/\tau_\kappa$ has the value 1.05 and both τ_ν and τ_κ are of the order of magnitude of one mean free time. For actual gases, s ranges from 0.57 for argon to 7.2 for air. In the case of liquids, a normal value of s appears to be 10, but it ranges from 0.032 for mercury to 9700 for glycerol. For liquids, there seems to be no simple picture of the two relaxation times, and there is no adequate theory of the ratio s for either gases as liquids.

* This work represents one of the results of research carried out under contract with the Bureau of Ships and Office of Naval Research, Navy Department.

B5. Ionization Currents in Cylindrical Electrode Systems. G. W. JOHNSON, *University of California, Berkeley.*—Ionization currents were measured in pure hydrogen between concentric cylinders for pressures from 0.01 mm to 740 mm. Above 1 mm $1/p \log i/i_0$ is a function of X/p. At lower pressures it depends also on the pressure. Auxiliary anodes permitted estimates of the location of ionization in the field which confirmed the spatial distribution predicted by Morton.[1] Electrons released in the low and collected in the high field region resulted in about 10 percent less ionization than in the reverse case. In both cases the ionization was greater than given by Townsend's equation, as noted also at high pressures by Fisher and Weissler[2] for confocal paraboloids. The peaks of Morton's i/i_0 *vs.* p curves are identified with the pressure corresponding to the minimum sparking potential. Application of the back diffusion equation of Rice[3] in the form $i=AV/(V+B/p)$, where A and B are constants, permitted the evaluation of i_0 at higher pressures than hitherto has been possible. The present work makes possible the delineation of tables and curves to predict the electron multiplication in highly divergent fields.

[1] P. L. Morton, Phys. Rev. 70, 358 (1946).
[2] L. H. Fisher and G. L. Weissler, Phys. Rev. 66, 95 (1944).
[3] C. W. Rice, Phys. Rev. 70, 228 (1946).

B6. Negative Corona in Freon-Air Mixtures at N.T.P. G. L. WEISSLER, *University of Southern California.*—In a point-to-plane corona gap of 3.1 cm, the onset potentials of the intermittent corona region were observed to be approximately constant, 6–7000 volts ($X/p \sim 100$) for all freon air mixtures, whereas in pure freon this value changed abruptly to 12,650 volts ($X/p \sim 200$). It is suggested that this is mainly due to a marked decrease in the first Townsend coefficient alpha, similar to the findings of Kruithoff and Penning[1] in A-Ne mixtures. Concentrations of freon of 10^{-4} to one percent were very similar to the known behavior of air,[2] mixtures from one to twenty percent showed in the intermittent corona region Trichel bursts, that indicated a very rapid decay in the amplitude of individual pulses. This is due to the formation of negative ions of freon decomposition products, such as chlorine and fluorine, which must be more stable at higher values of X/p (about 200) than those of oxygen (about 90). Also their probability of electron attachment is greater, since higher energy electrons can dissipate their excess in numerous vibrational states of freon, and in dissociation. Thus negative space charges must be stable much closer to the point and therefore be more efficient in choking off the discharge (decaying pulse size). Still higher concentrations inhibit proper avalanche formation such that Trichel bursts are barely observable. Current *vs.* potential curves show rapidly decreasing slopes with increasing freon content.

[1] Kruithoff and Penning, Physica 3, 515 (1936); 4, 430 (1937).
[2] Loeb, Kip, Hudson, and Bennett, Phys. Rev. 60, 714 (1941).

B7. Positive Corona in Freon Air Mixture at N.T.P. E. I. MOHR, *University of Southern California (introduced by G. L. Weissler).*—In order to further our understanding of positive corona and thereby of spark breakdown, space charge phenomena and current *vs.* potential characteristics were studied in a 3.1-cm point-to-plane gap (point diameter = ½ mm) in freon air mixtures. Streamer activity and strength increased going from pure air to 1 percent freon. Here the visual appearance of the corona changed markedly indicating that the discharge maintained itself solely by the streamer mechanism.[1] This seems due to a large increase in efficiency of photo-ionization in the gas without any appreciable change in the first Townsend coefficient α. As the freon content was increased to higher and higher values, the streamers became successively more degenerate until they could not be distinguished from burst pulses. This is compared to similar observations in air using needle points; here only incipient streamers can develop because of the rapid decrease of the field near the point resulting in too small values of $\int_{x_0}^{0} \alpha\, dx$. In our case the same was true because of the increased stability of negative freon decomposition product ions at higher values of X/p than those of O_2. The onset potentials of all observed phenomena were shifted to higher values and the current *vs.* potential curves showed decreasing slopes with increasing freon content. The changes in visual corona characteristics can be correlated to the space charge phenomena. The action of freon in suppressing discharge is ascribed to a gas mechanism, in contrast to the action of alcohol in A-counters,[2] which occurs at the cathode.

[1] L. B. Loeb and A. F. Kip, J. App. Phys. 10, 142 (1939).
[2] C. G. and D. D. Montgomery, J. Frank. Inst. 231, 447 (1941).

B8. A New Derivation of the Method of Characteristics for Axially Symmetrical Supersonic Flow. A. VAZSONYI, *North American Aviation, Inc. (introduced by S. H. Browne).*—Two-dimensional supersonic flow in nozzles and around airfoils and other bodies can be treated by the "method of characteristics." Recently this method has been extended to axially symmetrical flows. The differential equations using characteristic coordinates can be derived from the theory of hyperbolic partial differential equations. The derivation is laborious and does not clarify the basic physical principles involved. The alternative procedure proposed by the writer does not require an extensive knowledge of the theory of partial differential equations. Bernoulli's equation, the continuity equation, and the kinematical expression for the rotation are written down using intrinsic coordinates (coordinates along streamlines and normal to streamlines). The differential change in velocity can be expressed as a function of the differential distance, the local value of the rotation, Mach number, distance from the axis of the flow, differential change in flow direction, and the tangential and normal derivatives of the velocity. The last two quantities drop out when changes along a Mach line are considered, and the basic equation of the method of characteristics is obtained. It is believed that this new derivation gives a better physical understanding of the method.

B9. Atomization of Liquids. J. M. SCHMIDT, *California Institute of Technology.*—Various theories of the formation of droplets in pressure injection and air stream atomization of liquids are discussed. A number of experimental methods are described for the measurement of mean droplet sizes

as well as droplet size distributions in atomized liquids. Some of the methods used are high speed photography, impingement of the droplets on smoked plates, and photometric measurements of light absorption by sprays. Droplet size distributions are given for various liquids atomized under various conditions. In sprays of hydrocarbon fuels, injected under a pressure of 50 lb. per in.^{2} through hollow cone injectors into air streams moving with velocities of 20 ft. per sec., mean droplet diameters as small as 45 microns have been measured.

B10. Escape from the Earth by Multiple-Step Rockets. MARTIN SUMMERFIELD, *California Institute of Technology.*—Recent achievements in rocket vehicle performance as exemplified by the "V-2" rocket and the "WAC Corporal" rocket have focused attention on the physical factors limiting the velocities attainable in this manner. This paper deals with the question of escape from the surface of the earth, with special reference to four missions: (1) an earth-satellite revolving around the earth just above the atmosphere, (2) a "stationary" earth-satellite whose angular velocity equals that of the earth, (3) a vehicle that completely escapes the earth, (4) a vehicle that escapes the solar system. General performance equations are presented that bring out the effects of the following important parameters: jet exhaust velocity, ratio of propellant mass to gross mass, time of burning, and a drag factor. It is shown that, if exhaust velocities are limited by the energies produced by chemical reactions, it is doubtful that a single rocket can be constructed that is capable of leaving the earth. By means of multiple-step rockets much greater velocities can be imparted to the vehicle. Several cases of multiple-step escape rockets are calculated, and their characteristics discussed. Special emphasis is placed on the importance of determining the optimum number of steps.

B11. Problems in the Application of Nuclear Energy to Rocket Propulsion. H. S. SEIFERT AND M. M. MILLS, *California Institute of Technology.*—Consideration is given to the basic physical limitations involved in the application of nuclear energy sources to the propulsion of rockets. Quantitative estimates are made of the performance parameter *specific impulse* (impulse transmitted to the rocket per unit mass of expelled propellant) for the cases where propulsion is accomplished by: (a) photons, (b) fission fragments, and (c) an inert working fluid. Because of the fundamental difference between chemical rockets, in which the propellant is used both as a source of energy and as the mass to be ejected in obtaining thrust, and a "nuclear" rocket of type (c) above, in which these two functions may be separated, there exists an optimum ratio of payload or nonexpendable mass to working fluid or expendable mass, which differs for the two types of rockets. This was first pointed out by Ackeret.*

* J. Ackeret, Helv. Phys. Acta **19**, 103 (1946).

B12. Gamma-Radiation from Be^9+H^1. C. C. LAURITSEN, T. LAURITSEN, AND W. A. FOWLER, *California Institute of Technology.*—Further investigations have been made of the gamma-radiation from Be^9 bombarded by protons[1] particularly in the region of the resonances in the thin target excitation curve near 0.975 and 1.06 Mev. The first resonance has been found to have a width of 100 Kev. The thick target yield is 2×10^{-8} quanta per proton, so that $\omega\Gamma_\gamma\Gamma_p/\Gamma$ equals 20 volts. The second resonance width is less than 10 Kev, higher resolution in proton energies and thinner targets being necessary to complete this determination. The thick target yield is 2×10^{-9} quanta per proton so that $\omega\Gamma_\gamma\Gamma_p/\Gamma$ equals 2 volts. Measurements of the secondary pairs from a thick target bombarded at 1.1 Mev indicate radiation of energy 7.2 ± 0.2 Mev. Absorption measurements indicate no soft radiation. Thus the radiation from the strong wide resonance, at least, arises from a single transition from the compound nucleus B^{10} to its ground state. The width in this case must be due to competition with the re-emission of s-wave protons and probably with the emission of deuterons and alpha-particles. The narrow resonance must arise from p-wave capture with alpha and deuteron emission relatively improbable or forbidden. This work was carried on under contract with the Office of Naval Research.

[1] W. J. Hushley, Phys. Rev. **67**, 34 (1945).